ALTERED METABOTROPIC GLUTAMATE RECEPTOR FUNCTION IN THE NEOCORTEX OF A FRAGILE X MOUSE

By

Jacqueline Ann Fenn

A DISSERTATION

Submitted to
Michigan State University
in partial fulfillment of the requirements
for the degree of

Neuroscience-Doctor of Philosophy

2017

ABSTRACT

ALTERED METABOTROPIC GLUTAMATE RECEPTOR FUNCTION IN THE NEOCORTEX OF A FRAGILE X MOUSE

By

Jacqueline Ann Fenn

Fragile X Syndrome (FXS) is the leading cause of inherited intellectual disability. It is characterized by a wide array of symptoms, including cognitive impairments, attention deficit and hyperactivity disorder (ADHD), hypersensitivity to sensory stimuli, autistic features, mood lability, and seizures. Since the creation of the *Fmr1* KO mouse more than 20 years ago, a wealth of studies have uncovered a role for group I metabotropic glutamate receptors (mGluRs) in mediating many FXS phenotypes, leading to development of "The mGluR Theory of Fragile X". However, studies supporting this theory have focused on impairments in the hippocampus, amygdala, and other structures of the allocortex. The isocortex remains largely uninvestigated, despite its major role in sensory integration, attentional processes, and executive function.

MgluRs are also highly expressed in the neocortex, where they can modulate neuronal excitability and synaptic transmission. Using electrophysiological methods, I investigated the role of group I and group II mGluRs in modulating neocortical circuits in primary visual cortex. Humans with FXS show severe visual-motor deficits, and perform poorly on global motion tasks. Autopsy studies also reveal abnormal dendritic spine morphologies in layer 5/6 of the visual neocortex, and this is substantiated in the *Fmr1* KO mouse. Using whole cell patch clamp recordings of different neuron subtypes in layer 5/6 of primary visual cortex, I found that *Fmr1* KO layer 5/6 somatostatin expressing neurons (SST+) have a significant decrease in input resistance compared to wild type (WT), indicating that they are less intrinsically excitable than WT SST+ neurons. Further, I show that activation of group II mGluRs leads to disinhibition of

excitatory pyramidal neurons. I also discover that suppression of GABAergic transmission by group II mGluRs is normal in the *Fmr1* KO, leading to my hypothesis that increased disinhibition of pyramidal neurons by group II mGluRs is due to their altered modulation of fast glutamatergic transmission onto layer 5/6 interneurons in the *Fmr1* KO mouse.

Using recordings from fluorescently labeled interneurons in layer 5/6 visual neocortex, I discover that group II mGluR-mediated suppression of fast excitatory glutamatergic transmission onto inhibitory neurons is exaggerated in the *Fmr1* KO mouse. I show that this effect is cell specific, as it only occurs in SST+ interneurons and not parvalbumin expressing interneurons. Finally, I show that this deficit in excitatory drive onto SST+ interneurons is mediated by presynaptic mGluRs, and that these defects are specific to layer 5/6 visual neocortex. Both the decreased excitability of SST+ interneurons and exaggerated group II-mGluR mediated suppression of excitatory drive onto these cells would lead to neocortical circuit hyperexcitability in the *Fmr1* KO mouse. A hyperexcitable neocortical circuit would be anticipated to negatively impact sensory integration, a requirement for both stimulus encoding and attentional processes. Lastly, a hyperexcitable neocortical network could give rise to epileptiform activity.

The results of these studies are fascinating, as group II mGluRs have not previously been implicated in studies of the neocortical pathogenesis in the *Fmr1* KO mouse. This investigation also showed that group I mGluR-mediated modulation of membrane excitability and fast synaptic transmission is unaltered in the *Fmr1* KO mouse, suggesting that "The mGluR theory of Fragile X" may in fact be more or less valid contingent on the brain region under investigation. It is my hope that these circuit studies will inform scientific investigations on autism spectrum disorders and epilepsy syndromes, as both show high comorbidity in individuals with FXS.

This work is dedicated to my mother, who continues to work relentlessly to help me achieve my goals. Thank you for your endless love and for pushing me to never give up.

ACKNOWLEDGEMENTS

I would first like to recognize my advisor, Dr. Charles "Lee" Cox, for allowing me to complete my degree in his lab and for his financial support throughout my graduate career. Lee has taught me to troubleshoot, think independently, and to never accept published science as fact without first asking questions. He has instilled in me that conducting research means being wrong, and that's okay. Still, he's taught me to treasure the moments when my data confirms my hypothesis and adds to the body of scientific knowledge. This experience has helped me appreciate the endless complexities of the brain. I am continuously perplexed and amazed by the nuances of neural circuits. I owe this to my advisor, who remains as impassioned by electrophysiology today as I can presume he was during his earlier career. I would like to thank him for his patience whilst teaching me to be a scientist.

I would also like to thank Dr. Joseph Beatty, who is an extremely qualified electrophysiologist that seldom says no when asked for help. Since his arrival in the lab, my research technique has exponentially improved and I attribute this to the countless number of times he has assisted me in troubleshooting my equipment and reviewing fundamentals. I deeply value the input he has given me regarding my research technique and theory.

I want to thank all of the members of my research committee, Dr. Hongbing Wang, Dr. James Galligan, and Dr. Peter Cobbett, who have advised me since my first committee meeting at Michigan State University. Not only have they been generous with their time, but they have continued to sharpen my scientific acumen in our meetings. I greatly appreciate their perspectives on my research, as it has helped bring to my attention both the gaps in my knowledge and my data so that I may continue to develop my scientific competency.

I would like to thank my colleagues in Cox Lab, past and present, who have all helped with my research. I would like to thank Dr. Paul, who helped me navigate my initial patch-clamp learning curve and also taught me how to do histology post hoc. I would be remiss not to thank Dawn Autio. She maintains all the mouse colonies, performs histology, maintains lab materials, and still manages to conduct her own research. She is a phenomenal technician and my mom away from home. Finally, Kathleen Louis, who became one of my best friends during our shared lab experiences. I thank her for commiserating with me during this journey.

I would like to thank the Neuroscience Program for their continued support of me during my educational endeavors. The staff is remarkably knowledgeable about the logistical components of grad school, and have always been readily available to me when I needed help.

Lastly, I would like to thank my family and friends who have consistently helped me throughout my journey. I want to thank Rachael White, who finds the time to call me every week. She is the closest thing I have ever had to a sister, and for her I am grateful. I would like to thank Dr. James Anderson for being my teacher and spiritual advisor since high school. I would like to thank Dr. Erica Wehrwein for being an astonishing and strong female role model for me in academia and life. I would also like to thank my mother Sylvia Maldonado. I am not me without her, and there are literally no words to describe her importance to me. I would like to thank Jeremy Otero, who would travel day or night to do whatever I asked of him without complaint. Since he came into my life I have never lacked the presence of a father figure. I also want to thank Jimmy, who has loved me during some of the most trying times of my degree program. He has never stopped believing in me or pushing me to work. Most importantly, I would like to thank God for the hands, head, and heart he has given me. Hands to collect the data, a head to understand it, and a heart to keep the faith!

TABLE OF CONTENTS

LIST OF TABLES

LIST OF FIGURES

KEY TO ABBREVIATIONS

ACPD	(1S,3R)-1-Aminocyclopentane-1,3-dicarboxylic acid
AHP	after-hyperpolarizing potential
AMPA	α-amino-3-hydroxy-5-methyl-4-isoxazole-propionic acid
APDC	(2R,4R)-4-aminopyrrolidine-2,4-dicarboxylate
ASD	autism spectrum disorder
cAMP	cyconucleotide aminophosphate
CHR2	channelrhodopsin 2
DAP	depolarizing afterpotential
DHPG	(RS)-3,5-dihydroxyphenylglycine
DNQX	6,7-dinitroquinoxaline-2,3-dione
EPSC	excitatory postsynaptic current
ERK	extracellular signal regulated kinase
FMRP	fragile x mental retardation protein
FS	fast spiking
FXS	fragile x syndrome
GABA	γ-aminobutyric acid
GFP	green fluorescent protein
GPCR	g-protein coupled receptor
IB	intrinsic bursting
IPSC	inhibitory postsynaptic current
LGN	lateral geniculate nucleus
LTD	long term depression

LTP	long term potentiation
MAP1B	microtubule associated protein 1B
MAPK	mitogen activated protein kinase
mGluR	metabotropic glutamate receptor
mEPSC	miniature excitatory postsynaptic current
mIPSC	minitature inhibitory postsynaptic current
mTOR	mammalian target of rapamycin
NFS	non-fast-spiking
NMDA	N-methyl-D-aspartate
pI3K	Phosphatidylinositol-4,5-bisphosphate 3-kinase
PPR	paired pulse ratio
PV+	parvalbumin
RGC	retinal ganglion cells
RS	regular spiking
sIPSC	spontaneous inhibitory postsynaptic current
SNARE	Soluble N-ethylmaleimide-sensitive factor activating protein receptor
SST+	somatostatin positive
STEP	striatal-enriched protein tyrosine phosphotase
Tsc ½	tuberous sclerosis ½
V1	primary visual neocortex
WT	wild type

CHAPTER I: INTRODUCTION

In 1943, Martin and Bell, described a group of patients characterized by a common set of features including intellectual disability and social withdrawal (Bhakar, Dolen, & Bear, 2012). These individuals carried a fragile site on the X chromosome, giving rise to the name Fragile X Syndrome (FXS). The features of FXS are both physical and neurological, but the mechanisms underlying these abnormalities were completely speculative until the development of a murine animal model that recapitulated several of the human phenotypes (Dutch Belgium Consortium, 1994). Since the development of the *Fmr1* KO mouse, scientists have been fortunate enough to uncover several cellular changes in the brains of these mice attributable to the loss of the fragile X mental retardation protein (FMRP). Absent FMRP leads to defects in cell signaling pathways and altered mRNA/protein expression of a variety of critical receptors, ion channels, and proteins involved in different synaptic processes. Changes in synaptic events presumably lead to anatomical and behavioral changes, which are also observed in *Fmr1* KO mice. What are these synaptic changes? This is a question that continues to plague the field, although remarkable progress has been made. Several brain regions show changes in synaptic transmission and/or plasticity, and in many instances this is instigated by altered signaling downstream of group I metabotropic glutamate receptors (mGluRs). Armed with this knowledge, my dissertation studies are aimed at investigating the role that mGluRs play in cellular excitability and synaptic transmission in the primary visual neocortex, a region that has been documented to exhibit both anatomical and electrophysiological alterations in the *Fmr1* KO mouse. In the following pages, I first provide an overview of the nonhuman primate model of the visual system. I spend a disproportionate amount of time discussing the region under my investigation, the primary visual cortex (V1). Additionally, I will then compare the visual system of the mouse to the nonhuman

primate model. With this foundation of the visual system, I next provide an overview of the structure and function of the three groups of mGluRs, one of which has been in the spotlight of Fragile X research since the advent of the *Fmr1* KO mouse and was a logical choice to investigate in my dissertation research. Finally, I provide an overview of FXS in humans, including how it occurs, what the clinical manifestations are, and what human studies have revealed about the FXS brain. I then discuss the *Fmr1* KO animal model, including what we have learned regarding alterations in glutamatergic and GABAergic transmission. Finally, I discuss findings from the limited functional studies that have been done in the neocortex of the *Fmr1* KO mouse. Armed with this introductory material, I can make broader speculations about my research findings and how they fit into what we already know about the visual system and the pathogenesis of FXS.

1.1 Organization of the Visual System

The visual system is highly structured. Similar to other sensory systems, it is functionally organized such that neurons having similar response properties are located in close proximity. However, this topographical arrangement becomes less defined as information moves from the retina to the visual cortex and each successive level of information processing leads to increased integration of visual stimuli. Your visual world can be divided into a left and right visual field. Information from the left visual field is transferred to the right side of each retina, and subsequently to the right hemisphere of your brain. The opposite is true for the right half of your visual field, which is detected on the left side of each retina and transferred to the left hemisphere of your brain. In this way, both hemispheres of the brain process visual information from both eyes.

Extraction of the features of your external environment begins at the level of the eye. Visual information is integrated by retinal ganglion cells (RGCs). Smaller RGCs located predominantly in the central region (fovea) of the retina have smaller receptive fields and are color sensitive, making them good for detecting fine details of the visual environment as well as color contrast (Callaway 1998). However, these cells are also slowly adapting and have axons with slower conduction velocities, making it difficult for these neurons to detect rapid movement. For these reasons, these RGCs give rise to a visual pathway that carries information specific to the "what" details of the visual environment. This pathway, known as the parvocellular (P) pathway, carries its information more ventrally through the brain and is otherwise known as the ventral or temporal stream. In contrast, another subset of RGCs reside disproportionately in more peripheral locations on the retina and possess some qualities that are diametrically opposed to those of the P Pathway. These RGCs have larger receptive fields, are color insensitive, rapidly adapting, and have larger diameter axons with faster conduction velocities. They are also extremely sensitive to luminance contrast, making them optimally suited for detecting the form and movement of objects. These RGCs give rise to the M pathway of the visual system. The M pathway is also known as the dorsal or parietal stream because it carries visual information dorsally from the retina to higher order visual areas in the parietal lobe. It is commonly known as the "where" pathway because it carries information specific to the location of objects. A third subset of RGCs, giving rise to the koniocellular (K) pathway, have the smallest diameter axons of the three RGC subtypes and have been suggested to play a role in modulating the information received through the M and P pathways (Casagrande 1994). The features of these different RGCs are preserved in their respective recipient neurons throughout the visual system. For example, the primary visual cortex (V1) has specific neurons that are recipients of P pathway

information. These neurons are smaller in size and have smaller receptive fields, while V1 neurons that are recipients of M pathway information are typically larger and have larger receptive fields.

Almost all RGC axons travel through the optic nerve to the visual thalamus, or lateral geniculate nucleus (LGN). Once these fibers reach the LGN, they disperse to synapse onto six different layers of the thalamus. The four most dorsal layers are termed the parvocellular layers while the two most ventral layers are termed the magnocellular layers, and these layers receive and deliver visual information specific to the P pathway and M pathway respectively. The K pathway thalamic neurons are intercalated between the P and M layers of the LGN. Each layer of the LGN responds to information from either the left or right eye, so at the level of the thalamus we can say that cells exhibit ocular dominance. Axons from the six layers of the LGN will travel together along the optic radiations to ascend to V1.

V1 is one of the most extensively studied and anatomically understood neocortical brain regions. Also known as the striate cortex, V1 contains approximately 200 million neurons, and has six layers that are intralaminarly subdivided in humans and other primates (Lund 1988, Callaway 1998, Balaram and Kaas 2014). The first two layers have no subdivisions. Layers 3 and 5 are divided into sublayers 3A/3B and 5A/5B respectively. Layer 4 is divided into three sublayers 4A, 4B, and 4C. Finally, layer 6 is traditionally referred to as a single layer (Lund 1988, Callaway, 1998), although some scientists prefer to divide it into sublayer 6A and 6B based on cell density (Balaram and Kaas, 2014). This delineation, however, is less obvious due to the heterogeneity of cell types and sizes. For this reason, I will refer to it as one layer. The architecture of V1 is highly systematic, with its cells residing in what are known as ocular dominance columns. These columns run vertically through the visual neocortex. If you imagine

a recording electrode penetrating the neocortical surface perpendicularly such that it crosses through all six layers, you would expect the cells in that column to respond strongly to visual information from either the right or left eye. All of these cells would also respond most strongly to a visual stimulus of one particular orientation. Thus visual neocortical cells also exhibit orientation columns, with the exception of layer 4 where cells have no orientation preference. Within a V1 layer, every 50 μM the orientation of a cells receptive field shifts 10 degrees in either a counterclockwise or clockwise direction. Thus, intralaminar organization is also highly structured. As previously mentioned, the journey of information processing through V1 begins at Layer 4C, where the majority of axons leaving the LGN synapse will synapse. Generally speaking, V1 cells that are closest to Layer 4C exhibit less complicated behavior then cells in the superficial and deep neocortical layers. For this reason, the majority of Layer 4C cells are known as "simple" cells. These cells are similar to LGN cells in that they exhibit ocular dominance and have on-off center-surround receptive fields. However, some of these simple cells will also respond more strongly to stimuli of a particular orientation and are thus said to be orientation selective. Outside of Layer 4C, simple cells will synapse onto cells that exhibit more complex receptive field properties. These cells, known as complex cells, comprise the majority of V1 cells. Complex cells exhibit orientation selectivity like simple cells, but they lack positional selectivity. This means that complex cells can respond to a properly oriented line no matter where it resides in the receptive field. Thus, as the line moves complex cells have a sustained response and are considered to be movement selective. Depending on the layer, these complex cells can respond to additional characteristics of visual stimuli. For example, 10 to 20 percent of complex cells in layer 2/3 show direction selectivity (Hubel, 1988), preferring the oriented stimulus to move in one direction over its opposing direction. Some complex cells also

respond strongly to specific line lengths and curvatures. Now that I have covered some general features of V1, I will provide a review of the feed-forward and feed-back circuitry of the visual neocortex, as well as a discussion of the different neuron subtypes distributed throughout V1. For a schematic of the V1 circuitry, please see the appendix at the end of this chapter (**Figure 1.1**).

A. Feed-forward visual neocortical circuitry

The beginning of neocortical feed-forward processing begins in Layer 4C, where the majority of thalamic afferents of the lateral geniculate nucleus (LGN) synapse onto both excitatory spiny stellate neurons and inhibitory interneurons of V1 (Hubel and Wiesel 1972, Callaway 1998, Balaram and Kaas 2014). As previously stated, the cells of layer 4C maintain ocular dominance but may or may not also possess orientation selectivity. The magnocellular and parvocellular LGN afferents selectively target different divisions of Layer 4C, although they also weakly innervate layer 6. Koniocellular afferents synapse onto neurons in layer 1-3. Thus, it has been determined that LGN afferents synapse in almost every layer of V1, excluding Layer 4B and Layer 5.

Magnocellular afferents synapse onto cells in Layer 4Cα (Callaway 1998). These cells can, but do not always, exhibit orientation selectivity. Layer 4Cα spiny stellate cells send their axonal projections either to excitatory spiny stellate and pyramidal neurons of layer 4B or to pyramidal neurons in the lower third of layer 2/3 (3B) (Martin 2002). Magnocellular afferents from 4B then synapse onto "blob" regions in layers 2-3A, and 3B. Thus it can be said that the magnocellular information in layer 4Cα is inevitably carried to the blob regions of layers 2 and 3, where information about spatial relationships and object location is processed (Callaway 1998). Although monocular dominance columns are prevalent throughout the cortical layers, in layer

2/3 we see the first signs of binocularity in the visual cortex, with over half of all cells being influenced by both the eyes. Thus it can be said that V1 architecture becomes less structured as information moves out of layer 4 and the receptive fields of neurons begin to overlap and integrate more complicated stimuli. From layer 2/3, cells that received M pathway information travel to layer 4 of higher order visual cortical areas outside of V1. These areas include V2, medial temporal area (V5), and medial superior temporal area (MST). Axons from layer 2/3 that do not leave V1, will synapse onto layer 5 and 6 excitatory neurons. Axons from Layer 5 cells will then leave V1 through the white matter to synapse onto subcortical structures important in visual processing. Axons from layer 6 will predominantly synapse onto thalamic neurons.

Parvocellular LGN afferents take a different path through V1. These afferents synapse onto excitatory spiny stellate neurons in Layer 4Cß and to a lesser extent in layer 4A. Cells in Layer4Cß also exhibit center-surround receptive fields and ocular dominance, but they lack orientation selectivity. From Layer 4Cß, axonal projections travel to layer 3B. Pyramidal neurons in layers 2/3 are selective to orientation, but can exhibit binocularity. These neurons are also clustered together in regions known as blob and interblob areas. Cells in the blob area are not selective for orientation, but may be selective for color. Inputs from layer 2/3 leave V1 and synapse in layer 4 of the following higher order areas: V2, V3, V4, and the inferotemporal (IT) areas. These regions are located ventrally, and code information about the shape of an object.

In summary, studies looking at the density of axonal arborizations in the different cortical layers have determined that layer 4 spiny stellate cells project predominantly to layer 2/3, with a small subset of inputs synapsing in layer 5. Upon receiving layer 4 inputs, layer2/3 excitatory neurons then project to layer 5 and 6 neurons in V1, and send inputs outside of V1 to accessory cortical regions. Layer 5 neurons project to layer 6 and back to layer 2/3. Layer 6 neurons will

then send projections back to layer 2/3 and layer 4C V1. Thus, layer 5/6, which I will discuss in detail in the next section, is traditionally referred to as the feedback layer, although it also sends axonal projections outside of V1.

B. Feed-back visual neocortical circuitry

Layer 5/6 is composed of layers 5 and 6. Layer 5 neurons receive inputs from layers 2-4B and they project inputs back to these layers with no specificity for blob or interblob regions (Callway 1998). This is a characteristic feature of feedback projections, which typically exhibit more generically distributed axonal arborizations. Layer 5 of the visual neocortex contains at least three types of pyramidal neurons, each with distinct patterns of axonal arborization (Wiser & Callaway, 1996). The most common are type A, which account for 2/3rds of the population. Their basal and apical dendrites are confined almost exclusively to layer 5, and they receive the majority of their input from layers 2-4B. The axons of these pyramidal neurons have a plethora of arborizations in layers 2-4B. Another set of pyramidal neurons, have an apical dendrite extending to layer 1-3, but an axon that remains predominantly localized to layer 5. These cells receive inputs from layer 2-4B, but modulate mostly other layer 5 cells, with the exception of a subset whose axons project through the white matter. It is speculated that due to the size of these projecting axons, that they predominantly synapse onto the pulvinar nucleus of the thalamus. However, this has not been definitively shown.

The third class of excitatory neurons have extremely large cell bodies relative to the other pyramidal cells in layer 5, and these pyramids have an apical dendrite that extends to layer 1. They receive input from both layer 2/3 and potentially from K pathway cells in layer one. Due to their size, it is likely that they project to the superior colliculus, a region in the brain that controls saccadic eye movements (Lund et al., 1988).

Layer 6 excitatory neurons are the most diverse of all the cell layers. There are 2 classes of excitatory neurons in this layer and they each comprise about half of all layer 6 pyramidal neurons. Class I excitatory neurons have very few dendritic branches in layer 5 and they predominantly send dense feedback axonal projections to layer 4C. Class II neurons have abundant dendritic arbor throughout layer 5, but their axonal destination varies based on whether they are in Class IIA or Class IIB excitatory neurons. Class IIA neurons, receive the majority of their input from layers 2-4B. Their axons stay predominantly in layer 5 and 6 and are speculated to thus predominantly mediate intralaminar excitation. Class IIB neurons keep their axons in V1, but have dendrites in both layer 5 and layer 6. Thus, they receive input from thalamic afferents and layer 2-4B. They predominantly send feedback projections to layer 2-4B. The discussion of feedback and top-down circuits included explicit detail about excitatory neurons, so I will now discuss the role that the various interneuron subtypes play in V1.

C. Murine model of the visual system

Although the murine model of the visual system is in many ways remarkably similar to nonhuman primates, it retains some key distinctions. Visual integration also begins at the level of the retinal ganglion cells in mice, however they have a smaller central zone dedicated to binocular vision (Priebe and McGee, 2014). Also different than primates, RGCs with receptive fields in the binocular zone only send minor projections to the LGN, while the contralateral eye provides the majority of input to mouse LGN. The mouse thalamic neurons that receive ipsilateral inputs differentially project their axons to binocular regions of V1 (Priebe and McGee, 2014). The mouse LGN also has a disproportionate number of relay neurons that are orientation and direction selective, and these cells are speculated to be homologous to monkey koniocellular cells (Cheong et al., 2013). Once in V1, mouse neurons share remarkable similarity to primate

neurons, exhibiting orientation-selectivity as well as the presence of both simple and complex cells (Niell and Stryker, 2008). Also similar to primates, as information moves to the deep layers of V1 cells exhibit broader orientation tuning compared to more superficial layers (Kashube, 2014). One large difference, however, lies in the spatial resolution of V1 cells, which is significantly lower in mice. Thus they prefer stimuli that have lower spatial frequencies. They also exhibit a higher proportion of simple cells relative to complex cells, while the majority of primate V1 is composed of complex cells (Niell, 2015). While the architecture of V1 in the mouse is less structured than primates, there also exists ocular dominance columns (Dolen et al., 2007). Also similar to primates, there is ample evidence in support of separate parallel processing streams in the visual neocortex of the mouse. Once information leaves V1, it gets processed in one of 9 extrastriate regions (Katzner et al. 2013) that form topically organized representations of the contralateral eye. Information specific to the ventral stream is processed in the following areas: lateralintermediate (LI), posterior (P), postrhinal (POR). The dorsal stream is processed by the following areas: rostrolateral (RL), anteriorlateral (A), posteromedial (PM) and anteromedial (AM) (Wang et al., 2011,2012; Glickfeld et al., 2013; Laramee and Borie, 2015). Furthermore, the feedforward and feedback circuitry is also extremely comparable to the aforementioned circuits I described above in nonhuman primates. However, one key difference is that inputs into V1 not only target layer 4, but also target both layers 2/3 and 5/6. Nevertheless, the majority of layer 2/3 neurons project to layer 5 pyramidal neurons, and layer 5 pyramidal neurons also project to the thalamic nuclei and superior colliculus, as well as to specific neurons in layers 2-4. In vivo recordings on V1 putative interneurons have also discovered properties of these neurons that are similar to primates, including their broader tuning (Metin et al., 1988). In the subsequent paragraphs, I discuss some properties of the varies mouse

interneuron subtypes in V1.

D. Interneuron contributions to local microcircuits

Inhibition is a critical element of proper circuit function in the brain. Interneurons are abundant throughout all of the neocortical layers, where they play a pivotal role in modifying the aforementioned excitatory circuits of the visual cortex as they integrate visual information. There are several different subtypes of interneurons in the visual neocortex that synthesize γ-aminobutyric acid (GABA), the most abundant inhibitory neurotransmitter in the CNS. These interneuron subtypes are composed of different biochemical, morphological, and synaptic properties dependent on their location in the CNS. The three major neocortical interneuron subtypes include 1) fast-spiking interneurons expressing the Ca+ binding protein parvalbumin (PV), 2) non fast-spiking interneurons expressing the neuropeptide somatostatin, and 3) interneurons expressing the serotonin receptor 5HT3a (Rudy et al., 2011). These three subtypes, together, comprise 20-30% of all neocortical neurons (Markram et al., 2004).

D1. Fast-spiking interneurons

Fast-spiking interneurons (FS) comprise the most abundant interneuron subtype in the CNS, make up 40% of all inhibitory neocortical neurons (Rudy, B. et al., 2011, Markram, H et al., 2004; Ascoli, et al., 2008). These interneurons express the calcium-binding protein parvalbumin (PV+), and are thus also commonly referred to as PV+ interneurons. Typically, FS interneurons exhibit a basket cell morphology with aspiny, multipolar dendrites (Rudy et al., 2011). This morphology comes from the fact that these cells preferentially target the somata and proximal dendrites in such a way that the convergent inputs of several FS cells give the appearance of a "basket" around pyramidal cell somata. A second common morphology adopted by FS cells is that of the chandelier shape (Rudy et al., 2011). Chandelier cells most commonly

target the axon initial segment (AIS) of pyramidal neurons (Kawaguchi and Kubota, 1997; Markram, H. et al 2004). FS interneuron axonal arborizations are typically restricted to the layer in which their soma resides, although a small subset of FS cells have been shown to extend their axons translaminarly (Rudy, B. et al 2011). FS cells exhibit fast-spiking electrophysiological properties which include the ability to fire sustained high-frequency trains of action potentials (APs) with both large and fast afterhyperpolarizations (AHPs) and very little spike frequency adaptation (Kawaguchi and Kubota., 1997; Beierlein and Connors, 2000). They can be observed to "stutter", or fire abrupt episodes of intermittent, nonadapting, repetitive discharges. Of all the neocortical interneurons they have the lowest input resistance and the fastest membrane time constant (Rudy et al., 2011; Markram et al., 2004). FS interneurons provide significant lateral inhibition across neocortical columns, and receive the majority of thalamocortical afferents in the input layer of the neocortex (Beierlein and Connors, 2003). Neocortical pyramidal neurons synapse predominantly on the dendrites of these interneurons. Research suggests that 90% of local glutamatergic inputs synapse onto the dendrites, while the other 10% of inputs synapse on the soma (Markram, H. et al., 2004). Although FS cells reside in most of the neocortical layers, their greatest numbers lie in layer 4 where they comprise the largest distribution of the three interneuron subtypes (Rudy et al., 2011). They also comprise the second largest distribution of interneurons in layers 2/3 and layers 5/6, while they are absent in layer 1 of the neocortex. Thus, the distribution of FS interneurons exhibits an inside-out laminar gradient. In vivo optogenetic studies of the role of FS interneurons in the neocortical circuitry, indicate that they are the major participants in the generation of γ oscillations (30-80Hz) in the neocortical microcircuit (Sohal, V. et al 2009), as well as active participants in neocortical UP-DOWN states.

D2. Non-fast-spiking interneurons

The second largest group of neocortical interneurons are the non-fast-spiking (NFS) interneurons, expressing somatostatin (SST+) neuropeptide (Rudy et al., 2011; Markram et al., 2004). NFS interneurons comprise 30% of neocortical interneurons (Rudy et al., 2011). The most commonly discussed NFS interneurons are those of the martinotti cell morphology (Palusckiewicz et al., 2011; Oliva et al., 2000). Martinotti cells are present throughout layers 2-6 of the neocortex, and their axons ascend vertically through the cortical layers, arborizing onto the dendritic tufts of pyramidal neurons (Kawaguchi and Kubota, 1997; Rudy et al., 2011). Unlike FS interneurons, NFS interneurons make their synaptic contacts onto the dendritic shafts and spines of both basal and apical dendrites of excitatory pyramidal neurons (Markram et al., 2004). The electrophysiological properties of these interneurons also differ greatly in comparison to FS cells. Martinotti cells have a regular adapting firing pattern, and as such have frequently been termed regular spiking non-pyramidal (RSNP) cells (Rudy et al., 2011; Kawaguchi and Kubota, 1997; Beierlein and Connors, 2000; Markram et al., 2004). They have higher input resistances than other interneuron subtypes, and in layer 5/6 are frequently seen firing bursts of action potentials when they are depolarized from hyperpolarized membrane potentials (Beirlein and Connors 2000; Beierlein and Connors 2003). Local glutamatergic inputs from pyramidal neurons onto Martinotti cells are facilitating, unlike those of FS interneurons which are depressing. This facilitating capability, allows Martinotti cells to increase their feedback inhibition as the rate and duration of presynaptic discharge increases (Tai et al., 2014). It is speculated that this unique feature, makes Martinotti cells most likely to be activated during periods of high network activity. Of mention, although Martinotti cells are the most well documented NFS interneuron in the neocortex, NFS interneurons are a heterogeneous population

of neurons with a variety of morphologies and biochemical profiles (Rudy et al., 2011). The advent of transgenic mouse lines, allowed scientists to investigate the heterogeneity of this population for the first time. In the X94 mouse, a unique NFS interneuron was discovered that exhibited many of the electrophysiological properties of a FS interneuron, with the exception that these cells did have significant spike adaptation (Ma et al., 2015). Similar to Martinotti cells, these neurons also received facilitating inputs from local glutamatergic cells. They have axonal arborizations that synapse in layer 4 of the neocortex rather than layer 1. Only time will tell whether other NFS interneurons are present in the neocortex, however given the diversity of molecular marker expression and connectivity of this population of interneurons studied thus far (Gonchar et al., 2007; McGarry et al., 2010), it is highly likely that other NFS interneuron subtypes exist. Most recently, it was shown that NFS interneurons that co-express calretinin Ca^{2+} binding protein, preferentially reside in layer 2/3 while those NFS interneurons without calretinin expression target infragranular layers preferentially (Rudy et al., 2011). These cell types received varying inputs from the cortical layers, with NFS/ calretinin + cells receiving excitatory inputs mainly from layers 2/3, while the deeper layer NFS/calretinin - neurons received strong excitation from both layers 2/3 and layer 4. Interestingly, both of these subtypes share a similar electrophysiological profile to the widely studied Martinotti cell. NFS neurons are most abundant in layers 5 and 6, while they are the second largest population of interneurons in layer 4. They are the least abundant of the three cell types in layers 2 and 3, and have almost no occupants in layer 1.

D3. 5HT3a receptor-expressing interneurons

Interneurons expressing the 5HT3a serotonin receptor (5HT3aR) comprise the remaining 30% of neocortical interneurons (Rudy et al., 2011). Of all the interneuron subtypes, these

interneurons are the most heterogeneous population (Rudy et al., 2011, Markram et al., 2004). It is because of this, that 5HT3aR interneurons are the least understood of the three neocortical subtypes. One biochemical finding in this subtype of interneurons, showed that some 5HT3aR expressing interneurons also express vasoactive intestinal peptide (VIP), while neither NFS or FS interneurons express this neuropeptide (Rudy et al., 2011). Using a transgenic mouse that expresses GFP in interneurons expressing the 5HT receptor, it was shown that the VIP+ interneurons account for up to 40% of all interneurons expressing the 5HT receptor (Rudy et al., 2011; Kawaguchi and Kubota, 1997). Another difference between this cell population and both NFS and FS cells is their developmental origin. Unlike the other two subtypes, almost 90% of 5HT3aR interneurons have been shown to develop from the caudal ganglionic eminence (Rudy et al., 2011). One study (Myoshi et al., 2010), found 9 different electrophysiological subtypes of interneurons originating from the caudal ganglionic eminence. The majority of VIP+ neurons form synapses with dendrites, although a small subset synapse onto the soma of pyramidal neurons, similar to FS cells. Interestingly, this subset of neurons also shares the basket cell morphology of FS cells, but its morphologies are more heterogeneous than the neurons (Rudy et al., 2011). VIP+ neurons have the highest input resistance of all the cell types, and are thus the most excitable. They are the predominant interneuron subtype in layer 2/3, and comprise almost the entire interneuron population in layer 1.

The understanding of these different neocortical interneuron subtypes is imperative for making broader generalizations about the results of my dissertation studies, as it is highly likely that the differences I discussed above in the laminar distributions, electrophysiological properties, and biochemical profiles of these interneurons are likely to lead to very different modulation of the V1 excitatory neocortical circuitry. In the subsequent section, I will provide

an overview of the three major classes of mGluRs, as this will also be pivotal to understanding my research results.

1.2 Metabotropic Glutamate Receptors

A. General features of metabotropic glutamate receptors

L-Glutamate is the most abundant excitatory neurotransmitter in the nervous system. The majority of excitatory CNS synapses utilize glutamate transmission (Petralia et al., 1996) and express a unique composition of both ionotropic and metabotropic glutamate receptors. Fast excitatory neurotransmission is predominantly mediated by three ionotropic glutamate receptor types: N-methyl-D-aspartate (NMDA), α-amino-3-hydroxy-5-methyl-4-isoxazolepropionate (AMPA; GluR1-GluR4) and kainate (GluR5-GluR7, KA1, KA2) receptors. Metabotropic glutamate receptors (mGluRs) are the second type of glutamate receptors, comprising a heterogeneous family of G protein-coupled receptors (GPCRs). A GPCR is a membrane-bound protein that is activated by extracellular ligand binding, and interacts with G proteins to transduce intracellular signals leading to a variety of downstream effects (Niswender and Conn, 2010). Upon ligand binding, a conformational change in the GPCR leads to dissociation of the G-protein complex, consisting of α, ß, and γ subunits. The dissociated units continue on to exert the various mGluR effects. The mGluRs belong to family C GPCRs, and these receptors are constitutive dimers. Each dimer has 7 transmembrane spanning domains. The mGluRs are divided into three distinct subtypes: group I mGluRs, group II mGluRs, and group III mGluRs. These receptors are coupled to a variety of intracellular second messenger signaling cascades. MGluRs are expressed throughout the nervous system, where they have been shown to modulate intrinsic excitability, synaptic plasticity, and neurotransmission, at a wide array of both excitatory and inhibitory synapses. While they most often function as neuromodulators of

synaptic activities, sometimes they are directly involved in neurotransmission (Nakanishi, 1994). The exact distribution of the various mGluR subtypes show regional, developmental, synaptic, and cell specificity. Activation of mGluR second messenger systems leads to a variety of downstream effects, including phosphoinositide hydrolysis, activation of phospholipase D, changes in cAMP formation, and changes in ion channel function (Schoepp and Conn, 1993). Modulation of the CNS by mGluRs has been implicated to have therapeutic potential in treating several pathological conditions including schizophrenia, major depression, anxiety, addiction, neurodegenerative disease, epilepsy, and FXS. A table summarizing the information provided below is located at the end of this chapter (**Table 1.1**).

B. Group I mGluRs

Group I mGluRs include mGluR1 and mGluR5. There are several splice variants of each of these receptors. Group I mGluRs have been shown to be highly expressed throughout the brain, with sub-type specific differences in the location of expression. For example, mGluR1 has been observed at high levels in hippocampus, globus pallidus, substantia nigra, thalamus, cerebellum, and the olfactory bulb (Hovelso, et al., 2012; Bhattacharyya, 2016, Martin et al., 1992). MGluR1 has also been found in the striatum, neocortex, and hypothalamus, albeit the expression is less than that in the aforementioned structures (Hovelso et al 2012). The second group I mGluR receptor, mGluR5, has high expression in hippocampus and olfactory bulb, as well as in the neocortex, striatum, caudate nucleus, and nucleus acumbens (Hovelso et al., 2012). Compared to mGluR1, mGluR5 has lower expression levels in the cerebellum (Bordi and Ugolini, 1999) and thalamus (Hovelso 2012). Group I mGluRs are also expressed in astrocytes. In particular, astrocytic mGluR5 has been shown to affect neurotransmission of adjacent synapses (Hovelso et al., 2012). The distribution of these mGluR receptors changes throughout

the course of development, indicating that mGluRs may be crucial for early circuit maturation. The expression of mGluR1 continues to increase throughout development in both neocortex and hippocampus (Shigemoto et al.,1992; Catania et al., 1994). However, expression of splice variant mGluR5a has some developmental time limitations. In particular, mGluR5a expression reaches its peak in the second postnatal week, and then decreases further on in development (Reid et al., 1995). MGlur5b expression continues to increase postnatally and becomes the predominant form of mGluR5 in the adult brain. It is suggested that the differential expression of these mGluRs throughout development is important for synaptogenesis and/or neurogenesis of the neocortex (Munoz et al., 1999; Martinez-Galan et al., 2001). Electron microscopy has demonstrated that group I mGluRs are located mostly perisynaptically on the postsynaptic side of the synapse (Tamaru et al., 2001). Binding of glutamate to group I mGluR receptors occurs on the extracellular domain while allosteric modulators bind group I mGluRs along the seven transmembrane spanning domain. Group I mGluRs are associated with the G_q/G_{11} G-protein, and this protein positively couples group I mGluRs to phospholipase $C_ß$ ($PLC_ß$). $PLC_ß$ activation leads to hydrolysis of phosphoinositides which forms both inositol 1,4,5-triphosphate (IP_3) and diacyl-glycerol (DAG). IP_3 mobilizes intracellular calcium and this in conjunct with DAG is sufficient to activate protein kinase C (PKC). Activation of protein kinase C leads to the production of new protein synthesis. Group I mGluRs activate several downstream effectors, including phospholipase D, protein kinase pathways (casein kinase 1, cyclin-dependent protein kinase 5, Jun kinase, and components of the mitogen-activated protein kinase/extracellular receptor kinase (MAPK/ERK) pathway, and the mammalian target of rapamycin pathway (MTOR/p70 S6 kinase pathway). The latter two pathways have both been implicated in Fragile X pathology. The MAPK pathway can be activated by group I mGluRs in both hippocampal and

neocortical cells, and is involved in group I mGluR-mediated long term depression (LTD) in hippocampal excitatory neurons. This mGluR-LTD is exaggerated in Fragile X Syndrome. For more details about MAP kinase and MTOR signaling, see section 1.3 **("The MgluR Theory of Fragile X")**. Furthermore, group I mGluRs have been shown to alter neurotransmitter release through regulation of K^+ and Ca^{2+} channels. Inhibition of presynaptic K^+ channels by group I mGluRs delays repolarization to increase neurotransmitter release whereas bidirectional regulation of presynaptic Ca^{2+} channels leads to either increases or decreases in release. Further, they have been shown to decrease neurotransmitter release through postsynaptic stimulation of endocannabinoids, which are retrograde neurotransmitters that bind to CB1 receptors presynaptically. Finally, group I mGluR-mediated LTD has been reported in many different brains regions (Huber et al., 2002; Anwyl, 1999; Citri and Malenka, 2008), although group I mGluRs have also been shown to modulate NMDA-dependent long term potentiation (LTP). Upon activation of their second messenger systems, group I mGluRs undergo desensitization via phosphorylation. A similar process is observed for the other mGluR groups. This desensitization is important for preventing chronic overstimulation of the signaling pathway.

C. Group II mGluRs

Similar to group I mGluRs, group II mGluRs are widely expressed in the CNS. Group II mGluRs consist of mGlur2 and mGluR3. Although splice variants have not been identified for mGluR2, mGluR3 RNA is alternatively spliced into at least 4 variants (Niswender and Conn, 2010). Group II mGluRs are highly expressed in several brain regions including hippocampus, neocortex, nucleus acumbens, striatum, and amygdala (Holvelso et al., 2012; Petralia et al., 1996). mGluR2 is also highly expressed in olfactory bulb, cerebellum, caudate nucleus, and thalamic reticular nucleus, while mGluR3 is particularly abundant in septum, and substantia

nigra (Tamaru et al., 2001). MGluR3 is also the predominant group II mGluR receptor expressed in microglial cells (Petralia et al., 1996), where it has been shown to induce an apoptotic pathway (Taylor et al., 2005). The expression of group II mGluRs is also developmentally regulated. The location of group II mGluRs varies depending on the region of investigation. In the hippocampus, presynaptic mGluRs are predominantly type 2, while postsynaptic receptors are most often mGluR3 (Shigemoto, et al 1997; Tamaru et al., 2001; Petralia et al., 1996). However, this is not always the case as brain structures including neocortex, hippocampus, and striatum may have both mGluR2 and mGluR3 receptors located pre- and post- synaptically (Hovelso et al., 2012). Presynaptic mGluR2s are typically located extrasynaptically at axons and pre-terminal regions, while postsynaptic mGluR2s are concentrated at the soma and dendritic shafts. In contrast, postsynaptic mGluR3s are abundant on dendritic spines, where they are located perisynaptically. This is similar to the distribution of group I mGluRs (Tamaru et al., 2001; Zou, Jiang & Yang, 2017). Both group II mGluR subtypes are coupled to $G_{i/o}$ G-proteins. Dissociation of $G_{i/o}$ leads to inhibition of adenylate cyclase (AC) and reduction of cyclic AMP (cAMP) production. Decreased cAMP leads to subsequent decreases in protein kinase A (PKA) activity and a decrease in protein translation. Additionally, these receptors can also directly regulate ion channels when the ßγ subunit dissociates from the mGluR and directly binds the ion channel (Chavis, et al 1994). Through this mechanism, group II mGluRs have been shown to inhibit P/Q-type Ca^{2+} channels, effectively decreasing neurotransmitter release (O'Connor et al., 1999). They have also been shown to regulate the neurotransmitter release machinery downstream of Ca^{2+} entry (Hovelso, et al. 2012). Furthermore, the ßγ subunits can directly interact with the SNARE complex (Hovelso et al., 2012). Thus, group II mGluR activation can lead to a reduction in the number of active release

sites. Group II mGluRs also play a role in synaptic plasticity, mediating both long term depression and long term potentiation, although group II mGluR LTP has not been widely documented (Hovelso, et al., 2012). Group II mGluRs are present at both glutamatergic an GABAergic synapses, where they have been shown to inhibit neurotransmission (Doi et al., 2002; Flavin et al., 2000, Wan, et al., 2007).

D. Group III mGluRs

Although my dissertation studies focus solely on the role of group I and II mGluRs in Fragile X pathology, for the purpose of completeness I will briefly discuss some features of group III mGluRs. Group III mGluRs consist of mGluR4, mGluR6, mGluR7, and mGluR8. There are several splice variants of mGluR6, mGluR8, and mGluR7, although not all studies agree on whether variants exist for mGluR4 (Niswender and Conn, 2010). Expression of group III mGluRs varies depending on brain region and receptor subtype. While mGluR4 has a wide expression in the CNS, it is only highly expressed in hippocampus and cerebellum. MGluR7 is the most highly expressed group III mGluR overall, being located in large quantities in the following brain structures: hippocampus, neocortex, globus pallidus, amygdala, colliculi, and olfactory bulb (Hovelso et al., 2012). It is also located in striatum, substantia nigra, caudate nucleus, and nucleus acumbens, albeit to a lesser extent. Group III mGluRs are also present in microglia, where they have been shown to activate a neuroprotective pathway (Taylor et al., 2005). All of the group III mGluRs are linked to the $G_{i/o}$ subunit and decrease cAMP through the same pathway as group II mGluRs. Group III mGluRs are mainly localized within the presynaptic active zone of glutamatergic synapses where they act as autoreceptors (Kinoshita et al., 1998; Shigemoto et al., 1997, Hovelso et al., 2012). Presynaptic group III mGluRs are similar to presynaptic group II mGluRs with regard to their effects on hippocampal synaptic

plasticity. In particular, these receptors have been shown to activate a form of long term depression at synapses between hippocampal mossy fibers and stratum lucidum interneurons (Hovelso et al. 2012). They have also been shown to have an indirect effect on LTP at these synapses mediated by mGluR7. Current literature suggests that group II and group III mGluRs can also activate both the MAPK pathway as well as the phosphotidyl inositol 3-kinase (PI3) pathway (Niswender and Conn, 2010), making the understanding of the role of these receptors in modulating synaptic transmission increasingly complicated.

E. Distribution and functional role of mGluRs in the visual neocortex

MGluRs are located in all layers of the visual neocortex and are known to play a role in the developmental maturation of the visual circuitry, while also maintaining a role in the modulation of synaptic events in mature vertebrate circuits. Although there is some layer variation, generally speaking, the critical period for plasticity in the visual cortex starts in the third week, peaks during weeks 4-6, and ends by one year after birth (Daw et al. 1992). During this time, mGluRs play a very important role in the formation of eye-specific connections in the visual neocortex. Immunohistochemical studies indicate that the quantity of group I mGluRs diminishes over time during development (Reid et al., 1997), however, changes in the laminar distribution of group I mGluRs is subtype specific. Postnatal expression of both group I mGluRs is predominant in layers 1 and 5/6 immediately after birth (Reid et al., 1997). While this distribution remains unchanged for mGluR1a, by the peak of the critical period for ocular dominance plasticity, mGluR5 changes its major laminar distribution to layer 4, where it remains abundant for the rest of the lifespan (Reid et al., 1997). Sensory deprivation during the critical period postpones the laminar change in mGluR5 and produces increased levels of mGluR5 up to 6 weeks postnatally, without affecting mGluR1 expression and laminar distribution. Thus it is

evident that mGluR5 is especially critical for normal sensory-dependent maturation of the visual neocortex. Group I mGluRs also mediate synaptic plasticity during circuit maturation and after the critical period ends.

Group II mGluRs show a unique laminar distribution throughout the course of development. Immunohistochemical studies show that by 3-4 weeks, group II receptors are present in all layers (Reid et al. 1995). However, over the next 3-5 weeks the distribution changes such that group II mGluRs disappear from layer 4 in the adult brain (Reid et al., 1995). Sensory-deprivation during this time postpones the disappearance of group II mGluRs from layer 4. These findings are validated with functional studies observing the response of neocortical neurons to visual stimulation in vivo (Beaver, Ji, & Daw, 1999). Iontophoretic application of group II mGluR agonist, APDC, at three weeks led to suppression of visually evoked responses as well as spontaneous activity in individual neurons from all layers. This effect was absent from layer 4 past 6 weeks of age. Furthermore, over the course of the lifespan group II mGluR expression decreases, similar to what is seen with group I mGluRs (Beaver, Ji, & Daw, 1999). The time course of the disappearance of group II mGluRs coincides with the development of ocular dominance columns, and subsequent studies have shown that group II mGluRs are involved in ocular dominance plasticity.

Group I and group II mGluRs affect mature visual neocortical circuits in a variety of ways, including modulation of intrinsic properties, synaptic transmission, and synaptic plasticity. Visual cortical neuron excitatory postsynaptic currents from adolescent mice (p14-p20), are reversibly suppressed by a general mGluR I/II agonist in layers 4-6 (Sladeczek et al., 1993). This effect can be blocked by potassium channel blocker 4-aminopyridine (4-AP), indicating that mGluRs can act to open presynaptic potassium channels and effectively decrease transmitter

decrease. A later study looking at a specific group II mGluR agonist, APDC, showed that group II mGluRs were responsible for attenuating excitatory postsynaptic currents in pyramidal neurons of all cortical layers (Flavin et al., 2000). This function of group II mGluRs was present throughout development, as these changes were observed in both young (17-31) and old (53-67) rats. Additionally, group II mGluRs have been shown to suppress GABAergic transmission in layer 4 of the visual neocortex (Liu, Petrof & Sherman, 2014). From these studies, it appears that the major role of group II mGluRs in mature circuits is to limit neurotransmitter release.

Due to the variation in group I and group II mGluR expression in V1 throughout development, it is likely that alterations in signaling of either of these receptor subtypes in individuals with FXS, will affect both the developmental maturation of the V1 circuitry as well as the functionality of the circuits thereafter. For example, in the *Fmr1* KO changes in group I mGluR signaling have a significant effect on development of ocular dominance plasticity during earlier V1 circuit maturation (Dolen et al., 2007), while altered signaling in adult mice leads to absent plasticity in layer 5/6 of V1 (Wilson and Cox, 2007). These changes, and others, will be discussed in the following paragraphs about Fragile X Syndrome.

1.3 Fragile X Syndrome

FXS is a heritable disorder of intellectual disability. Current consensus places the prevalence of FXS at 1 in 4,000 males and 1 in 8,000 females (Hagerman, 2008). In the United States alone, it is estimated that 1 million Americans carry the Fragile X mutation, and 100,000 of those individuals have a full FXS diagnosis (National Fragile X Foundation, 2017). The mutation leading to FXS is located on the X chromosome in a region coding for the FMR1 gene. Translation of this gene leads to production of FMRP protein, an mRNA binding protein present in a variety of human tissues including brain, testes, ovaries, lung, and kidney (Hinds et al.,

1993). In the 5' untranslated region of the FMR1 gene, there is a CGG sequence with a variable number of repeats located in the first exon of the FMR1 gene. It resides 250 base pairs downstream of the CpG island that serves as the promotor region of the gene. In healthy individuals, this CGG sequence is <55 repeats. Individuals with a repeat number between 55-200 are considered premutation carriers, and can exhibit unique phenotypes including Fragile X Associated Tremor Ataxia Syndrome (FXTAS) and Fragile X Associated Primary Ovarian Insufficiency (FXPOI). When the repeat number exceeds 200, the CpG island of the FMR1 gene becomes hypermethylated, effectively silencing gene transcription. Subsequent production of FMRP protein is almost nonexistent, leading to the development of a full FXS phenotype (**Figure 1.2**). Severity of this phenotype is directly correlated to the expression level of FMRP, which can vary in individuals that exhibit germline mosaicism and in females that undergo X inactivation of the mutated chromosome with compensation by the second X-chromosome (De Boulle et al., 1993). These individuals will typically have less severe symptoms than those with a fully hypermethylated gene.

A. Physical and behavioral phenotype

The Fragile X phenotype includes a wide array of physical abnormalities in addition to behavioral disturbances. Physical features of FXS vary throughout the lifespan and include wide and protruding ears, long narrow faces with a prominent jaw and forehead, long and narrow eye openings, excessively large head relative to body size, epicanthal folds, and strabismus. Growth patterns in FXS children are also altered, with FXS children more commonly exhibiting precocious puberty and thus being larger in size until adulthood, at which point these individuals are smaller in stature than healthy adults (Loesch and Hay, 1988). This disrupted growth pattern is believed to be secondary to endocrine dysfunction as is the exhibition of macroorchidism in

more than 80% of FXS adult males (Merenstein et al 1996). Further, although less is known about how loss of FMRP protein leads to connective tissue dysplasia, additional clinical manifestations suggestive of connective tissue disorder in FXS include hyperextensible finger joints, velvet-like skin, a high-arched palate, flat feet, recurrent otitis media, and increased incidence of mitral-valve prolapse and other cardiac involvement. Unlike other developmental disorders where the physical features are highly fixed and thus easily distinguished, the remarkable variability of the physical features in FXS leads to a diagnosis made most frequently by observation of neurological and/or behavioral manifestations.

The neurological symptoms of FXS include learning impairments, hypersensitivity to sensory stimuli, hyperactivity and attention deficit, impulsivity, aggressiveness, anxiety, sleep disturbances, epilepsy, and autistic features (D'Hulst 2007; Hagerman 2000). FXS always includes some degree of cognitive impairment, with as many as 85% of males and 25% of females having an intelligence quotient less than 70 (Stafstrom, 2009). This intelligence quotient does not indicate a general handicap of intellect, as FXS children show cognitive strength in vocabulary, long-term memory for meaningful and learned information, and face emotion perception (Kogan et al., 2004). They do, however, have relative weaknesses in attentional control, working memory, linguistic processing, and visual spatial cognition (Kogan et al., 2004). However, the intellectual and behavioral disturbances typically vary in both type and severity. Male children with FXS most commonly exhibit attention deficit hyperactivity disorder and aggressive behaviors, while females with FXS most commonly show social avoidance and shyness (Hagerman and Stafstrom, 2009). However, two other relatively common neurological disturbances in FXS include epilepsy and autistic behaviors. It is estimated that up to 25% of children with FXS full mutation will have seizures (Stafstrom, 2009), and as many as 50% of

pre-pubertal fragile X children exhibit atypical electroencephalographic (EEG) patterns. Thus, hyperexcitability of the CNS is a hallmark feature in humans with FXS. The seizures most frequently resemble benign focal epilepsy of childhood (BFEC) (Berry-Kravis, 2002). EEG patterns for BFEC commonly show abnormal centrotemporal spike patterns. BFEC typically resolves before adulthood, making the observation of centrotemporal spike patterns on the EEG of children with FXS a positive prognostic indicator (Hagerman & Hagerman, 2002). Of the variable types of seizure patterns, complex partial seizures are most common in FXS, although some children with FXS will have generalized tonic-clonic seizures (Wisniewski et al 1991; Berry-Kravis, 2002). It is currently unknown how loss of FMRP leads to epilepsy in FXS, however several potential mechanisms have been speculated based on animal studies **(see 1D and 1F**). Autistic features, including gaze aversion, hand flapping or biting, shyness, and social avoidance, are extremely common in FXS. As many as 30% of children with FXS will also receive a full autism diagnosis (Gibson et al. 2008; Hagerman et al. 2005). Additionally, 2-5% of autistic children have FXS, making it the leading genetic cause of autism (Kaufman et al. 2004). It is hypothesized that hyperexcitable cortical circuitry underlies the pathology of autism, as inundation of the neocortical circuitry with sensory information that cannot be inhibited properly may lead to impaired sensory integration and subsequent alterations in physical and/or behavioral responses. Finally, hypersensitivity to sensory stimuli is another key feature of neurological pathology in FXS and is believed to be due to impaired sensory integration. Impaired performance on tasks requiring sensory processing is suggestive of impaired sensory integration. Impaired performance has been observed in males with FXS performing a global motion task that probes the M pathway (Kogan et al., 2004). As previously mentioned, the magnocellular pathway is specialized for extrapolating information about object motion. When

FXS males where presented with visual stimuli that probe the magnocellular pathway (low spatial frequency, high temporal frequency), they performed significantly worse than mental-age matched and chronological-age matched controls in their ability to detect contrast (Kogan et al., 2004). While it could be argued that attentional deficits led to the impaired performance, scientists also probed for the ability to detect stimuli that probe the parvocellular pathway (color stimuli, motionless gratings). Individuals with FXS had no trouble with these tasks. Additionally, immunohistochemical studies confirmed that FMRP expression is elevated in areas of the thalamus that carry magnocellular pathway visual information, providing an anatomical correlate to suggest that the magnocellular pathway is more susceptible to pathology in the absence of FMRP. Other studies have also observed deficits in processing magnocellular pathway information (Kogan et al., 2004b; Cornish et al. 1998). Furthermore, individuals with FXS are also hypersensitive to somatosensory stimuli, suggesting potentially impaired integration of somatosensory information. Presumably, this hypersensitivity has neocortical origins, as higher integration of sensory stimuli occurs in the neocortex. However, the specific mechanisms have yet to be determined, although animal studies are beginning to uncover answers **(See 1F "Neocortical Pathogenesis in FXS").**

B. Neuroanatomical findings in FXS individuals

Neuroimaging studies in humans have documented a brain that is grossly normal in FXS. A handful of studies have shown increases in hippocampal volume (Kates et al., 1997b; Reiss et al 1994), as well as an enlarged caudate nucleus and thalamus (Reiss et al., 1995), although these changes may be age dependent as they are not always observed. One structural finding that has been shown more consistently is a decrease in posterior cerebellar vermis size (Mazzocco et al., 1997; Mostofsky et al., 1998; Reiss et al., 1994). The vermis has a role in modulating sensory

input to the auditory and visual cortices, as well as modulating higher executive functions through its connections with the frontal lobe (Ivry, 1993). Additional neuroanatomical studies using Golgi impregnation of individual neurons have also revealed changes in the dendritic morphology of both neocortical and hippocampal neurons in FXS (Hinton et al., 1991; Irwin, Galvez, & Greenough, 2000; Irwin et al., 2001; Rudelli et al., 1985). Specifically, these studies have shown an increase in immature dendritic morphologies in layers 3-5 of temporal and visual cortices (Hinton et al., 1991; Irwin et al., 2001; Rudelli et al., 1985), and the pyramidal layer of allocortex (Rudelli et al., 1985; Wisniewski et al., 1991). One study also documented an increased spine density (Irwin et al., 2001), although this finding has not been documented in the majority of human studies. These changes in spine maturation have also been documented in the mouse model of FXS (Comery et al., 1997; Irwin et al., 2002), and are discussed below **(see Section 1F "Neocortical Pathogenesis in FXS").**

C. FMRP function and sub-cellular localization

FMRP is a cytoplasmic RNA-binding protein expressed in most neurons and glia, although there is some regional specificity in expression level within the CNS. In particular, higher FMRP expression levels are observed in the granular cell layers of the hippocampus and cerebellum, habenula, and cerebral cortex (Hinds et al., 1993). FMRP is highly expressed cytoplasmically, where it serves to regulate protein translation in the cell body, dendrites, and synapses. However, dimerized FMRP can also shuttle into the nucleus through a nuclear localization signal. It has three RNA-binding domains, two of which can bind RNAs with "kissing-complex" tertiary motifs (Bhakar et al., 2012), and the third of which preferentially binds RNAs with a G-quartet structure (Bassell and Warren, 2008). Inside the nucleus, FMRP can be found bound to nuclear mRNAs, pre-mRNAs while they are being transcribed, and a

nuclear exporter protein (Bhakar et al 2012). Together, these components comprise a ribonucleoprotein complex (mRNP). This complex contains a nuclear export signal that allows it to be translocated out of the nucleus, where it can be packaged into RNA granules. The granules are shuttled to synapses, and release their contents upon stimulation. This allows the translation of several different proteins including those implicated in spine morphogenesis and synaptic plasticity. FMRP is estimated to bind 4% of total brain mRNA (Ashley et al., 1993; Darnell et al., 2011), and has been shown to regulate the translation of 4-8% of synaptic proteins (Bassell and Warren, 2008). The vast majority of rodent work to-date has focused on the role of FMRP in regulating postsynaptic processes including protein translation (Pfeiffer and Huber, 2009). However, FMRP also targets mRNAs that comprise one-third of the presynaptic proteome (Darnell et. al 2011) and is expressed presynaptically in granules (Antar et al., 2006; Christie et al., 2009; Till et al., 2012, Akins et al., 2009; Akins et al., 2012). Thus, it seems highly likely that loss of FMRP would lead to impaired presynaptic functions. Oddly, to-date very few functional studies have been published about the role of presynaptic mechanisms of FMRP regulation, so many questions remain about the pathology that results when FMRP is silenced presynaptically. Nevertheless, postsynaptic studies have provided a wealth of information about the general functions of FMRP. When FMRP is bound to its mRNA target, protein translation does not occur. Thus it is considered to negatively regulate protein translation, potentially through blockade of both the initiation (Centonze et al 2008, Lacoux et al 2012) and the elongation phase of translation (Ceman et al 2003, Darnell et al. 2011). Evidence in support of negative regulation by FMRP includes FMRP dose-dependent suppression of mRNA that is removed when FMRP is not allowed to bind its mRNA targets (Li et al., 2001), as well as increased levels of protein synthesis occurring in the absence of FMRP (Huber et al.,

2002). Deletion of FMRP impacts the expression of several different types of mRNAs and proteins, including those responsible for a variety of cation channels, adhesion molecules, neurotransmitter receptors, and components of the vesicular transport and release machinery (Brown et al. 2001; Qiu et al 2008, Schutt et al 2009, Paluszkiewicz 2011).

D. The Fmr1 KO as an animal model of FXS

The murine homolog of FMRP has a 97% identical amino acid sequence with human FMRP (Ashley et al., 1993), which makes it an optimal animal model for studying the pathology of FXS. In 1994, the Dutch Belgium Consortium implanted embryonic stem cells containing a viral vector with a disrupted *Fmr1* DNA sequence into pseudo-pregnant C57BL/6J (B6) female mice (Dutch Belgium Consortium, 1994). Offspring were crossed again with B6 mice resulting in the first mouse model of FXS. These mice did not produce FMRP protein but did contain detectable levels of *Fmr1* mRNA, setting up an animal model that would hopefully resemble human FXS phenotypes. While the gross physical features of *Fmr1* KO mice were normal relative to control mice (Bakkar et al., 1994), these investigators found enlarged testes in *Fmr1* KO mice that has been corroborated in later studies (Slegtenhorst-Eegdeman et al., 1998). Several studies also detected morphological changes in neocortical dendritic spines resembling the observations made in the neocortex of human autopsy brains (Svoboda, K et al., 2001; Irwin et al., 2002; Galvez and Greenough, 2005). Abnormal hippocampal spine morphologies, albeit different than neocortical immature spines, were also observed in the *Fmr1* KO mouse (Grossman et al., 2006), and are discussed below **(See 1D "The MGluR Theory of Fragile X")**. The Dutch Belgium Consortium (1994) conducted the first behavioral studies in the *Fmr1* KO mouse, and found that these mice show normal behaviors during passive avoidance tasks, increased exploratory behavior and motor activity, and impaired acquisition of novel spatial

information during platform reversal trials in the Morris Water Maze task. Although the authors were uncertain about what increased motor activity and exploratory behaviors mean, they proposed that these changes could be the result of hyperactivity or less efficient learning of the environment, requiring a need to continue exploring (Dutch Belgium Consortium, 1994). They also suggested that impaired acquisition of novel spatial information during reversal trials may be due to deficits in hippocampal plasticity, a mechanism required for spatial learning. Nevertheless, these studies were the first to demonstrate that the *Fmr1* KO mouse did model some of the features of human FXS. A surplus of behavioral studies conducted since then, appear to have more or less conflicting results depending on the behavior under investigation. While not necessarily a "behavior", one of the most agreed upon features of the *Fmr1* KO is increased seizure susceptibility. Although spontaneous seizures have not been documented, the *Fmr1* KO has increased susceptibility to audiogenic seizures, induced by a 120-125 decibel, high-intensity siren (Bakkar et al., 1994; Pacey et al., 2009, Yan et al., 2005; Ding, Sethna, & Wang, 2014; Musumeci et al., 2000). Interestingly, the degree to which *Fmr1* KO mice express audiogenic seizure sensitivity is dependent on a variety of factors, including developmental age and background strain (Pietropaolo s et al 2011, Veeraragavan et al., 2011; Goebel-Goody et al 2012). Another fairly consistent behavioral finding in the *Fmr1* KO mouse is hyperactivity. *Fmr1* KO mice placed in an open-field have increased locomotor activity and/or enter the center of the open field more often than wild type mice (Bakkar et al., 1994; Ding et al., 2014, Pietropaolo et al., 2011; Kazdoba et al., 2014). Some behaviors observed in humans that have also been observed in *Fmr1* KO mice are repetitive behaviors (Pietropaolo et al., 2011; Spencer et al., 2011), impaired sociability (Dahlhaus et al., 2010; McNaughton et al., 2008), and delayed language development (Mineur et al., 2002), but these observations are not reproducible across

all labs. For example, repetitive behaviors such as higher levels of self-grooming and excessive marble-burying have also been observed in the *Fmr1* KO mouse (McNaughton et al., 2008), although not all studies show significant differences (Veeraragavan et al., 2011; Thomas et al., 2011). The same can be said of behavioral assays for anxiety and cognitive deficits. Studies done in mice to look at anxiety behaviors have produced more conflicting results with animals showing reduced anxiety, measured as more time in open arms in an elevated plus-maze (Peier et al., 2000; Heulens et al., 2012). Alternatively, others show either no change or reduced time in open arms, indicative of increased anxiety (Bilousova et al., 2009; Mineur et al., 2002; Yan et al., 2004). While it may seem like the conflicting results of several of these assays would diminish the usefulness of the *Fmr1* KO mouse as an animal model for the human disease, it is important to keep in mind that behavioral assays are highly sensitive to several factors, including, but not limited to: testing conditions, animal housing, genetic strain and age (Kazdoba et al., 2014). Thus, it is possible that any one of these factors could be contributing to the variable results produced from some of these assays. Furthermore, scientists may interpret the behavior of these animals in different ways. For example, some scientists may consider more time spent entering the center of an open field as a measure of decreased anxiety, whereas others may consider it a measure of increased hyperactivity. However, extrapolating the reason for an observed behavior is extremely difficult, as many behaviors are not limited to the activation of a single brain region and some assessments may test several behaviors at once. Nevertheless, the consensus that *Fmr1* KO mice exhibit anatomical defects, hyperactivity, and increased seizure susceptibility, suggests that this mouse is indeed a valid model of human FXS. All of the aforementioned deficits have been rescued by an mGluR5 antagonist (Dolen et al., 2007), and this has helped develop broad support of "The mGluR Theory" of FXS, which I will next discuss

in detail.

E. Altered glutamate signaling and "The mGluR Theory"

Around the time that the *Fmr1* KO mouse was developed, it was shown that activation of group I mGluRs leads to increased protein synthesis (Weiler et al., 1993) and that FMRP is translated at synaptosomes in response to stimulation of group I mGluRs (Weiler et al., 1997). Additionally, it was determined that synaptic events such as long-term depression (LTD) and long-term potentiation (LTP) require local protein synthesis for their maintenance (Kang and Schuman, 1996). These studies provided a rationale to study mGluR-dependent LTD in the hippocampus of the *Fmr1* KO mouse, a form of plasticity that was known to depend on protein translation at the synapse (Huber, Roder & Bear, 2001; Huber and Bear, 2000). The results of this study determined that group I mGluR-mediated LTD in the CA1 region of the hippocampus was elevated in the *Fmr1* KO (Huber et al. 2002). This original study prompted the development of "The mGluR Theory of Fragile X" (**Figure 1.3**), which postulated that several of the neurological and psychiatric aspects of FXS are due to exaggerated responses downstream of group I mGluR activation (Bear, Huber, and Warren, 2004). This theory maintains that any processes requiring synaptic protein translation upon activation of group I mGluRs will be exaggerated in the absence of FMRP. Subsequent hippocampal studies built support for this theory. In particular, it was shown that activation of group I mGluRs in the CA3 region led to prolonged epileptiform discharges in the *Fmr1* KO mouse (Chuang et al., 2005), and that stimulation of endogenous glutamate was sufficient to activate these epileptiform discharges in the *Fmr1* KO. This was not the case for wild type animals, which required pharmacological activation of group I mGluRs before any epileptiform activity was observed. Exaggerated mGluR-LTD has also been observed in the cerebellum of the *Fmr1* KO mouse (Koekkoek et al.,

2005), while reduce mGluR LTD has been reported in the neocortex (Martin, Lasalle & Manzoni, 2016). Nevertheless, it appears that blocking mGluR5 signaling may be therapeutically advantageous in the *Fmr1* KO mouse. A pivotal study supporting the mGluR theory used genetic reduction of mGluR5 in the *Fmr1* KO mouse to rescue several of the observed defects in the *Fmr1* KO mouse, including increased seizure susceptibility, aberrant spine morphology, elevated hippocampal protein synthesis, exaggerated hippocampal mGluR-LTD, and aberrant experience-dependent plasticity in the visual neocortex (Dolen et al., 2007). Pharmacological administration of the mGluR5 antagonist was also able to rescue behavior on an open field test and increased susceptibility to audiogenic seizures (Yan et al., 2005), prolonged epileptiform discharges (Chuang et al., 2005), hypersensitive acoustic startle (De Vrij et al., 2008), and decreased mRNA granule expression (Aschrafi et al., 2005). In addition, other labs have been able to replicate the original study using group I mGluR antagonism to restore excess hippocampal protein synthesis (Osterweil et al., 2010) and hippocampal spine density (de Vrij et al., 2008). Restoration of plasticity deficits in the neocortex have also been reported (Martin, Lasalle & Manzoni, 2016). In addition to restoration of synaptic plasticity, another study in the amygdala showed that application of a group I mGluR antagonist MPEP, could rescue decreased frequency of fast ionotropic glutamate-receptor-mediated miniature excitatory postsynaptic currents (mEPSCs) in the *Fmr1* KO (Suvrathan et al., 2010). Therefore, although it appears that the changes in group I mGluR-mediated signaling vary regionally, in many cases blockade of these mGluRs is effective in restoring several of these defects.

At the time that the original hippocampal mGluR-LTD study was conducted in the *Fmr1* KO mouse, it was uncertain how FMRP was interacting with group I mGluR signaling to regulate synaptic protein translation. As I previously mentioned group I mGluRs not only

activate their canonical G_q mediated pathway, but they also activate multiple kinase pathways, all of which lead to local protein translation (Tang and Schuman, 2002). The PI3K-mTOR and ERK/MAPK signaling pathways, however, can both be activated in the dendrites by group I mGluR signaling, and have been shown to play a role in the exaggerated mGluR-LTD occurring due to loss of FMRP (Bhakar, Dolen & Bear, 2012). When group I mGluRs are stimulated in the WT mouse, PI3K-mToR pathway is activated via formation of a protein complex consisting of a scaffolding protein (homer), mGluR5, and PIKE. PIKE activates phosphoinositide 3-kinase (PI3K) resulting in phosphorylation of PIP2. Newly created PIP3, with the assistance of another kinase called phosphoinositide-dependent kinase (PDK) phosphorylates serine/threonine kinase (Akt). Akt directly phosphorylates mTOR, leading to translation of proteins at the synapse that are important for cell growth, proliferation, autophagy, and synaptic plasticity. FMRP normally functions to negatively repress mTOR signaling by binding PIKE and other effectors of mTOR. Upon stimulation of group I mGluRs, protein phosphatase 2A (PP2A) is activated, which leads to dephosphorylation of FMRP, freeing PIKE to initiate mTOR-mediated protein translation (Narayanan et al., 2007). mTOR signaling will eventually activate S6K, which will rephosphorylate FMRP to shutdown FMRP-dependent translation once again (Santor et al., 2011). In fact, blockade of mTOR signaling by rapamycin leads to loss of mGluR-LTD at CA1 synapses in the hippocampus of wild-type mice (Sharma et al., 2010). However, loss of FMRP in the *Fmr1* KO mouse leads to enhanced mTOR signaling at rest and exaggerated mGluR-LTD that becomes mTOR-pathway independent (Sharma et al., 2010).

The extracellular signal regulated kinase (ERK) pathway is also important for group I mGluR-mediated LTD. The ERK pathway is a mitogen-activated protein kinase signaling

cascade (MAPK), which means that it characteristically involves the following sequential steps: GTPase activation (Ras), activation of a MAPK kinase (Raf), phosphorylation of MAPK kinase (MEK), phosphorylation of ERK, and ERK-mediated protein translation. ERK activates protein translation directly via activation of ribosomal protein S6K (RSK) as well as indirectly through phosphorylation of MAPK interacting protein kinase (MNK ½), which leads to activation of eukaryotic elongation initiation factor (eIF4E). eIF4E binds the 5' mRNA cap and initiates translation of proteins involved in AMPA receptor internalization (Bhakar, Dolen & Bear, 2012). These include, but are not limited to, Arc/Arg3.1, oligophrenin-1 (OPHN1), microtubule-associated protein 1B (MAP1B), and STEP (Sanderson et al., 2016). AMPA receptor internalization is the main mechanism mediating mGluR-LTD. Several of these proteins are elevated in the *Fmr1* KO (Zalfa et al. 2003; Darnell et al. 2011), providing a potential explanation for exaggerated mGluR LTD in FXS. Furthermore, the internalization of AMPA receptors is also implicated in dendritic spine stability, which is aberrant in the *Fmr1* KO. AMPA receptor endocytosis is correlated with actin reorganization (Vanderklish et al., 2002; Eales et al., 2014), and it is this remodeling that changes the morphology of dendritic spines (Cingolani et al., 2008). Finally, ERK signaling has been shown to be responsible for the elevated protein synthesis in the *Fmr1* KO, as inhibition of ERK ½ pharmacologically leads to normalization of excessive protein levels (Osterweil et al., 2010). This is not observed by blocking the mTOR pathway.

In summary, Group I mGluRs have been implicated in the pathogenesis of FXS since the creation of the *Fmr1* KO mouse over 20 years ago. The pathogenic mechanisms downstream of group I mGluR activation occur due to loss of FMRP regulation downstream of two pathways connected to group I mGluR signaling, the pI3-mTOR and ERK/MAPK pathways. These

defects led to the development of "The mGluR theory of Fragile X" which postulates that any processes requiring protein translation downstream of group I mGluR signaling will be altered in FXS, and this may be the hallmark alteration implicated in the wide array of FXS phenotypes. Intriguingly, group II and III mGluRs have also been suggested to activate the pathways that are aberrantly regulated upon group I activation in the *Fmr1* KO (Niswender and Conn, 2010), so it is possible that signaling of these receptors is also dysregulated in FXS. This warrants their inclusion in our investigation of mGluR-mediated defects in the neocortex of the *Fmr1* KO mouse. Finally, it is worth mentioning that the wealth of basic science research implicating exaggerated group I mGluR signaling in the *Fmr1* KO led to the investigation of an mGluR antagonist for therapeutic usefulness in humans with FXS. Unfortunately, the clinical trials have published disappointing results (Davenport et al., 2016). Phase II clinical trials were conducted with the mGluR5 antagonists mavoglurant and basimglurant to assess their therapeutic potential on a variety of different outcome measures. However, in both cases individuals with FXS were comparable to placebo groups (Clapp, 2016; Santarelli, 2016), and the trials were subsequently discontinued. At the very least, these results suggest that alterations in group I mGluR signaling cannot alone explain the clinical manifestations of FXS. Clinical trials using agonists of GABAergic signaling, however, have shown some promise. In the next section, I will discuss several of the observed alterations in GABAergic signaling in the *Fmr1* KO.

F. GABAergic dysfunction in the Fmr1 KO

Proper brain function depends on a correct balance between excitatory and inhibitory signaling (Sabanov, 2016). While several of the aforementioned studies discovered changes in glutamatergic function, other studies have uncovered defects in GABAergic inhibitory signaling. GABA is the predominant inhibitory neurotransmitter in the CNS, and it binds to GABA

receptors, of which there are two types: fast ionotropic $GABA_A$ receptors and metabotropic $GABA_B$ receptors coupled to a G-protein signaling cascade. Both $GABA_A$ and $GABA_B$ receptors are capable of hyperpolarizing the cell membrane, albeit through different mechanisms. $GABA_A$ receptors are ion channels that permit influx of chloride into the cell upon GABA binding. $GABA_B$ receptors mediate hyperpolarization of the membrane through opening of inward rectifying K^+ channels linked to the G-protein signaling cascade. Furthermore, $GABA_A$ receptors mediate two types of inhibition: fast, phasic, inhibition that occurs upon release of a high concentration of neurotransmitter, and tonic inhibition which is a slow, persistent, $GABA_A$ current occurring when low concentrations of GABA reside in the extrasynaptic space. All interneuron subtypes release GABA into the synaptic cleft, leading to inhibition of the postsynaptic cell.

In the *Fmr1* KO mouse, both biochemical and electrophysiological studies have demonstrated defects in GABAergic function. Changes at GABAergic synapses have currently been reported in the hippocampus (Hong et al., 2012; Sabanov et al., 2016), subiculum (Curia et al., 2009), amygdala (Olmos-Serrano et al., 2010; Vislay et al., 2013), striatum (Centonze et al., 2008), and neocortex (El Idrissi et al., 2005; Adusei, et al., 2010). Some of the first studies to uncover deficits in inhibitory neurotransmission in Fragile X, found regional-specific changes in the expression of both mRNAs and proteins comprising several $GABA_A$ receptor subunits, as well as changes in expression of compounds important for the synthesis, transportation, and catabolism of GABA. *Fmr1* KO mice show decreased mRNA levels of $GABA_A$ δ and $ß_3$ subunits in the hippocampus and neocortex (Gantois, I. et al, 2006; Hong et al., 2012). Additionally, 8 out of 18 known subunits of the $GABA_A$ receptor have been shown to be underexpressed in the neocortex of Fragile X mice. This underexpression includes the subunits

comprising the most abundant GABA receptor in the CNS, namely α1, β2, and γ2. These GABA subunits comprise 60% of the GABAA receptors in the brain (D'Hulst et. al, 2006). Interestingly, these results are corroborated in a drosophila model of FXS, indicating that dysfunctional inhibition is an evolutionarily conserved pathology in Fragile X Syndrome. Protein expression of several of the aforementioned $GABA_A$ subunits have also been shown to be reduced in the neocortex, hippocampus, diencephalon, and brainstem of Fragile X mice (El Idrissi et al., 2005, Adusei, D. et al 2010). Deficits in the expression of these various subunits point to a potentially therapeutic intervention, as these subunits are sensitive to either and/or both benzodiazepines and neuroactive steroids like alphaxalone (D'Hulst et. al, 2006). Interestingly, there appears to be developmentally specific changes in the expression levels of these mRNAs and proteins. While many of the above mentioned mRNAs had correspondingly decreased protein expression at early time points in development, by adulthood (2-3months) the majority of these mRNAs show normal protein expression. The exception to this lies in the protein expression of $ß_2$ subunit, which remains decreased into adulthood, and has been linked to disrupted locomotor behavior in the mouse model of Fragile X (Adusei, D et al., 2010). Furthermore, not only has decreased $GABA_A$ subunit expression been extensively documented, but mRNA expression of Gad1, Gat1 and Gat4, and ssadh have been shown to be decreased in both the neocortex and cerebellum. These mRNAs create proteins important for GABA synthesis, transport, and degradation, respectively (D'Hulst, C. et al 2008). A protein responsible for the clustering of $GABA_A$ receptors to the postsynaptic membrane, gephyrin, also showed reduced expression in the neocortex (D'Hulst, C. et al 2008). Presynaptically, changes in the expression of GABA-synthesizing enzyme GAD have also been documented (Adusei et al., 2010, D'Hulst et al., 2009, El Idrissi et al. 2005, Olmos-Serrano et al 2010), and these

changes appear to be dependent on the brain region examined. Given that underexpression of several elements of the GABAergic system have been shown abundantly in the neocortex, it seems highly likely that inhibition, more so than excitation, is mediating regional specific changes in the neocortex (D'Hulst, 2009).

In addition to the extensive mRNA and protein expression studies, a growing body of electrophysiological evidence is building to confirm the functional defects in inhibitory neurotransmission in FXS. Not surprisingly, these changes show both increases and decreases in inhibitory transmission that are, to some degree, regional specific. Fragile X mice showed a marked increase in the frequency of spontaneous and miniature inhibitory currents, suggesting that phasic GABAergic transmission is elevated in the striatum due to the loss of FMRP (Centonze, et al. 2008). This study also shows decreased GABAergic synapse density in the subiculum, contrary to their electrophysiology results. It is plausible that increased GABAergic transmission is a compensatory mechanism induced by the reduction in synapse number, although this remains to be proven. Later studies, also show decreases in tonic inhibition in the subiculum (Curia, 2009), a region critical to spatial encoding and retrieval of short-term memories (D'Antuono, M. et al. 2003). Inhibitory deficits were later documented in the amygdala, a limbic area that processes emotionally salient information, especially those pertaining to fear. Both phasic and tonic inhibition, mediated by $GABA_A$ receptors, were reduced in the amygdala of the *Fmr1* KO mouse. Electron microscopy in the amygdala showed decreases in the number of inhibitory synapses in *Fmr1* KO mice, similar to what was observed in the subiculum (Olmos-Serrano, et al. 2010). The authors attribute the decrease in synapse number as well as a decrease in GABA production to the electrophysiological defects they observe. A recent study done in the hippocampus of the *Fmr1* KO also demonstrated decreased

amplitude in evoked inhibitory currents of CA1 pyramidal neurons, as well as decreased amplitude and frequency of sIPSCs and mIPSCs (Sabanov et al., 2016). Although the authors provide no mechanism to explain these changes, they show that there is decreased protein expression of several GABA subunits, indicating a potential decrease in the number of GABA receptors in CA1 pyramidal neurons, or a change in their composition and function. Although all of these studies implicate $GABA_A$ abnormalities, a selective few studies have also shown changes with $GABA_B$ in the *Fmr1* KO. Henderson et al. (2012), found that several disease-related pathologies in the *Fmr1* KO mouse could be reversed in slice preparations, cultured neurons, or in vivo, by activation of arbaclofen, an agonist at $GABA_B$ receptors. These pathologies include increased basal protein synthesis, elevated AMPA internalization, and abnormal dendritic spine morphology. Abnormal auditory EEG patterns as well as increased audiogenic seizures can also be corrected by arbaclofen (Pacey et al., 2009; Sinclair et al., 2017), in addition to rescue of behavioral performances on a T-maze task and anxiety behaviors (Sinclair et al, 2017). Finally, an electrophysiological study recording IPSPs in hippocampal pyramidal neurons, showed that application of arbaclofen could restore $GABA_B$ deficits in inhibition (Wahlstrom-Helgren & Klyachko, 2015). Unfortunately, just this month phase III trial results from an arbaclofen study have recently been published and have reported no improvement in symptoms (Berry-Kravis et al., 2017). It is evident from both this clinical trial as well as the failed clinical studies of mGluR5 antagonists, that several different receptor pathways converge on FMRP, such that any drug treatment targeting one receptor is unlikely to be enough to rescue abnormal physical and/or neuropsychiatric phenotypes.

G. Neocortical pathogenesis in FXS

Studies in the neocortex of the *Fmr1* KO provide evidence for changes in both spine

morphology and intrinsic excitability. Network level studies also show changes in neocortical excitability measured as differences in synaptic plasticity, spontaneous activity, and synchronicity of firing. Although single cell electrophysiological studies are limited, they too provide support for increased synaptic excitability, that appears to be contingent on the synapse under investigation. Furthermore, some of these changes can be rescued by glutamatergic receptors. In the following paragraphs, I will provide details about each of these investigated changes, and will conclude with a discussion about neocortical changes specific to development.

G1. Anatomical studies

Of all the investigations into neocortical pathology in FXS, perhaps the most widely identified disruption is with the spine morphology of excitatory pyramidal neurons. Dendritic spines in the neocortex are the major postsynaptic recipients of excitatory glutamatergic inputs (Pan et al.; 2010), and so it seems likely that aberrant spine morphology would affect the excitability of the neocortical circuitry as well as its ability to integrate sensory information. As previously discussed, Golgi-stain impregnations in autopsy brains of males and females with Fragile X have uncovered significant changes in the spine morphology of the human neocortex (Irwin et al, 2000). All of these studies have documented the presence of long, thin, immature spines on the apical dendrites of pyramidal neurons in layers 3 and 5 of the parieto-occipital cortex (Rudelli et al.,1985; Wisniewski et al., 1991; Hinton et al., 1991; Irwin et al., 2001). Immature neocortical spines typically exhibit longer lengths with irregular dilations and smaller spine head sizes relative to the shaft. These spines are presumed to be less functional than mature spines. These pathological findings have been extensively studied in the neocortex of the *Fmr1* KO. Layer 5 visual neocortical neurons from brains of both younger (p21) and older mice (p60-120) show an increased number of long spines relative to short spines as well as an

increased number of immature spine morphologies (Comery et al., 1997; Irwin et al., 2002; Su et al., 2011; Restivo et al., 2005). Some labs show an increase in spine density as well (Dolen et al., 2007; Comery et al.; 1997; Su et al., 2011), but this finding is more controversial as it is not always seen (Irwin et al.,2002) and is speculated by some to be dependent on developmental stage (Nimchinsky et al., 2001). Similar spine pathology has been documented in the somatosensory cortex of neonatal and adult mice (Pan et al.; 2010; Nimchinsky et al.; 2001). Several labs have seen partial restoration of morphological deficits with chronic application of antagonists of the group I mGlu5 receptor (Dolen et al.; 2007, Pan et al.; 2010), further implicating group I mGluRs in neocortical pathology.

G2. Intrinsic excitability of neocortical neurons

Changes in the intrinsic excitability of neocortical neurons in the *Fmr1* KO have not been widely documented, although a handful of studies have found some differences. Gibson and associates (2008) report that layer 4 excitatory neurons of the somatosensory cortex have elevated intrinsic membrane excitability. Specifically, these neurons show an increase in input resistance and a decrease in cell capacitance. These authors reported no changes in the intrinsic excitability and action potential (AP) properties of FS interneurons in this layer. Another study also showed that NFS interneurons of layer 2/3 somatosensory cortex (S1) have no change in their intrinsic properties (Paluskiewicz et al., 2011). No other studies have assessed the intrinsic properties of GABAergic neurons of the neocortex. Another study looking at the excitability of cortical pyramidal neurons in layer 5B of S1 found no change in resting membrane potential, input resistance, sag ratio, or membrane time constant in the *Fmr1* KO, as well as no change in the properties of single APs (Zhang et al., 2014). This same group did show increases in excitability of the dendritic compartments of these neurons, however, and they attributed this to a

change in Bk and HCN 1 (Ih) channels. Yet another study also determined that somatic measures of input resistance, membrane time constant, and firing threshold are normal in layer 5 pyramidal neurons (Desai et al., 2006), demonstrating more evidence in favor of normal intrinsic excitability of neocortical neurons. Whether changes in intrinsic excitability of other neocortical brain regions are present, remains to be determined.

G3. Synaptic plasticity defects and other network alterations

Given that group I mGluRs are implicated in altered hippocampal plasticity in the *Fmr1* KO, it seemed likely that they would play a role in neocortical synaptic plasticity as well. In support of this, several studies have shown defective neocortical synaptic plasticity. In the visual neocortex, loss of long-term potentiation was observed in layer 5/6 of the *Fmr1* KO (Wilson & Cox, 1997). This plasticity was partially mediated by group I mGluR5 receptor. Absent or diminished LTP, as well as increased threshold for long term potentiation has also been observed in the prefrontal neocortex (Meredith et al., 2007; Martin et al., 2016), somatosensory cortex (Li et al., 2002; Desai et al., 2006,) auditory cortex (Yang et al., 2014), and anterior cingulate cortex (Tao Chen et al., Zhao, et al., 2005; Koga et al., 2015). Group I mGluRs were either mediators of this potentiation or rescued plasticity defects in the *Fmr1* KO. These studies provide compelling evidence to support the idea that there are population level changes in the excitability of the neocortex. Additional network level studies in the neocortex have determined this to be the case.

Additional studies show that *Fmr1* KO mice exhibit a reduced threshold for audiogenic seizures (Chen and Toth, 2001; Musumeci et al., 2000; Yan et al., 2005; Ding, Sethna, & Wang, 2014). In slice preparations, scientists have further shown that both thalamically driven and spontaneous upstates show increased durations in layer 4 and layer 5 of the somatosensory cortex

of *Fmr1* KO mice (Gibson et al., 2008; Hays et al., 2011). These findings have also been validated in vivo (Hays et al., 2011). Authors of the Gibson et al. (2008) study, found that the duration of a layer 4 upstates in the *Fmr1* KO was almost two-fold longer than control animals. They further discovered that inhibitory network synchrony during upstates was significantly decreased. Increasing inhibition of network activity is suggested to terminate upstates (Brunel and Wang 2001), so loss of inhibitory synchrony would be expected to result in longer upstate duration. Further, it was shown that genetic reduction of mGluR 5 signaling could restore defects in upstate duration, and that this was not dependent on protein translation (Hays et al., 2011). What exactly are upstates? Upstates are periods of higher neuronal activity, where cells are more depolarized and more likely to fire action potentials. Upstates are frequently rhythmic, vacillating with downstates (periods where cells are more hyperpolarized and exhibit little to no firing) at a frequency of < 1Hz. While the exact function of upstates is unknown, it is speculated that they comprise the slow oscillatory rhythm seen during slow wave sleep and quiet wakefulness (Steriade et al., 1993). However, given that neuronal activity is heightened during upstates, it is logical to use the duration spent in an upstate as a measure of cortical excitability. Increased frequency of upstates in layer 2/3 of the somatosensory cortex of *Fmr1* KO mice, with normal upstate durations, has also been shown in vivo (Goncalves et al., 2013). These authors noted layer 2/3 neurons have 3-fold higher firing rates during states of sleep or quiet wakefulness, but this effect is not observed in awake behaving animals. Periods of rest are extremely critical for memory consolidation (Ji and Wilson, 2007), and individuals with FXS are known to struggle with memory tasks. Further, they are also known to exhibit sleep disturbances, including shorter sleep durations and frequent awakenings (Hagerman & Hagerman, 2002). Thus, the increased neuronal firing observed in the *Fmr1* KO mouse during

rest may be indicative of hyperarousal during sleep. Additionally, developmentally transient alterations in the neocortical network of *Fmr1* KO mice have also been reported (Bureau et al., 2008; Goncalves et al., 2013; Harlow et al., 2010). For example, as early as postnatal day 4, two photon Ca^{2+} imaging has shown that there is more frequent, synchronous firing of neuronal ensembles in the *Fmr1* KO that lasts until the 4th week of life (Goncalves et al., 2013). This is significant, as these defects are occurring during the critical period of mouse brain development (Anis, Vitaly, & Portera-Cailliau, 2015), and are likely to cause changes in circuit maturation. All of these studies suggest that the neocortex in FXS is hyperexcitable, and may be hyperresponsive to incoming sensory input. Not surprisingly, the somatosensory cortex of the *Fmr1* KO mouse, shows a faster spread of depolarization and increased sensory evoked activity in response to whisker stimulation and forepaw stimulation respectively (Zhang et al., 2014).

While the above network studies provided sufficient evidence in favor of a hyperexcitable cortical network, the individual synapses and cell types that are responsible for this cortical excitability remain mostly unknown. Are all neocortical synapses affected by loss of FMRP, or does this loss preferentially impact specific synapses, cell types, and/or layers? A handful of studies have begun to answer this question, although single cell electrophysiological investigations remain underrepresented in the neocortex. Paired recordings from layer 4 of the somatosensory cortex show both a reduction in connection frequency and strength of pyramidal neuron synapses onto FS interneurons, indicating a 51% reduced excitatory drive onto these cells (Gibson et al., 2008). Furthermore, there was also a decrease, albeit smaller, in excitatory drive onto pyramidal neurons of around 18%. The authors hypothesized that these changes should lead to a net imbalance of excitatory/inhibitory circuitry in favor of hyperexcitability, and this was confirmed with the upstate studies I discussed previously. A later study using transgenic

mice that selectively express FMRP in either GABAergic cells or excitatory cells, showed that deletion of *Fmr1* in excitatory neurons mimics the longer upstates seen in the *Fmr1* KO (Hays et al., 2011). This was not the case for deletion of Fmr1 in GABAergic cells, indicating that defective excitatory drive onto FS interneurons is the major contributor to neocortical circuit hyperexcitability. Fast-spiking interneurons are not the only inhibitory cells that have been implicated in neocortical FXS pathology. Specifically, another study showed that group I mGluR mediated activation of NFS interneuron firing in layer 2/3 was reduced, and that this diminished activation of NFS neurons led to impaired synchronization of spontaneous inhibitory currents (sIPSCs) in the *Fmr1* KO (Paluskiewicz et al., 2011). NFS interneurons receive facilitating inputs from excitatory neurons, and so their inhibitory output increases with increasing network activity (Paluszkiewicz et al., 2011; Rudy et al., 2011). Therefore, defective inhibition by SST interneurons would specifically be detrimental in situations where cortical activity was abnormally high, such as during epileptiform situations or conditions of unrelenting sensory input.

G4. Developmental changes in the neocortex of the Fmr1 KO mouse

Further, single cell electrophysiological studies have determined that loss of FMRP impacts the timing of the critical period for synaptic plasticity (Bureau et al., 2008; Harlow et al., 2010). Strontium experiments looking at isolated Sr^{2+}-AMPA mEPSCs and Sr^{2}- NMDA mEPSCs determined that quantal amplitude of both the AMPA and NMDA components at developing thalamocortical synapses was unaltered. However, looking at the ratio of NMDA to AMPA EPSC failures during minimal stimulation experiments at these synapses determined the NMDA/AMPA ratio was increased in the *Fmr1* KO due to a decrease in NMDA EPSC failures. They suggest this indicates an abundance of silent synapses during the critical period (P7) in

layer 4 of the somatosensory cortex in these animals. Further, they show that this leads to a shift in the critical period for synaptic plasticity. In normal animals, LTP is strongest at P3 and P4, and gradually decreases over the course of development (Barth and Malenka, 2001). However, in *Fmr1* KO mice LTP is significantly decreased at these ages and subsequently increases until a maximum is reached at P6-7, wherein it starts to decline again and resembles the control mice developmental time course. Interestingly, another study reported that during immediate postnatal development, there was a decrease in connection probability of layer 4 spiny stellate cell synapses onto layer 2/3 neurons in the *Fmr1* KO compared to WT, and this alteration was normalized by the third postnatal week (Bureau et al., 2008). Thus, these reports support the idea that the neocortical critical period is delayed in the *Fmr1* KO, and that FMRP plays a critical role in circuit maturation. These functional studies are supported with anatomical spine studies showing transient changes in spine morphologies during similar time frames (Nimchinsky et al., 2001; Galvez and Greenough et al., 2005). These results are especially intriguing in light of the fact that children with FXS experience developmental delays in motors skills (Kau et al., 2002). Similar changes in critical period plasticity have been observed for ocular dominance in the *Fmr1* KO mouse (Dolen et al., 2007), providing additional evidence that FMRP is required for the normal developmental progression of neocortical synaptic maturation.

In summary, the neocortical pathogenesis of the *Fmr1* KO mouse is diverse. The most widely accepted findings include those showing abnormal dendritic spine morphology and absent or diminished LTP. In contrast, the jury is out regarding whether intrinsic excitability is altered in neocortical neurons, although most studies suggest that it is not. Further, while several network level studies show alterations in the *Fmr1* KO leading to neocortical hyperexcitability, studies of the individual synapses contributing to these network defects are rare. Finally, in the

neocortex and potentially in other brain regions, FMRP is important during the early postnatal development of the neocortex, as several deficits are seen during this time frame that are transient but nonetheless important for the normal maturation of neocortical circuitry. Studies in older mice are almost nonexistent, so it is difficult to say at this point how changes during development affect adult animals.

1.4 Concluding Remarks

While the development of a murine model of FXS has provided us with invaluable insight into the pathogenic neural mechanisms leading to the neuropsychiatric profile of FXS, these studies have left us with more questions than answers, especially where it involves neocortical involvement. My dissertation studies were conducted in an attempt to bridge the gap between what we know about neocortical FXS pathology and what we still need to understand.

Three particularly interesting patterns have been observed in the neocortex of *Fmr1* KO mice. First, dendritic spine morphology is aberrant and includes immature spine morphologies that may be contributing to the defective long term synaptic dynamics that have been documented in the neocortex. Second, group I mGluRs have been implicated in the neocortical pathology of this syndrome. However, it appears that there is regional specificity in the role of FMRP downstream of group I mGluR signaling, as the plasticity defects seen in the neocortex in most cases are diametrically opposed to the plasticity changes seen in the hippocampus. Thus, more research assessing the role that group I mGluRs play in neocortical pathology is required so that we may better understand how mGluR signaling in the neocortex differs from other brain regions. Third, while electrophysiological investigations at the level of a single neocortical synapse are limited in the *Fmr1* KO (Gibson et al., 2008), it is suggested that excitation of interneurons, in particular, seems to be the source of neocortical deficits. Defective excitation of

interneurons has been shown in all layers of somatosensory cortex layer 1 (Gibson et al., 2008; Hays et al., 2013; Paluskiewicz et al., 2011), and affects both FS and NFS interneurons. Changes such as these have not been investigated in V1 of the *Fmr1* KO despite several lines of evidence suggesting that human patients suffer from significant visual-motor deficits, and >90% of males with FXS are gaze aversive (Merenstein et al., 1996). These findings indicate sensory hypersensitivity in response to eye contact (Cohen et al., 1989), and implicate V1 as a brain region that is functionally altered in humans. The major alterations that have been observed in V1 of the *Fmr1* KO mice are layer 5/6 abnormal dendritic spine morphology, absent layer 5/6 LTP, and altered ocular dominance plasticity (Wilson and Cox, 2007; Dolen et al., 2007). Group I mGluRs are involved in all of these processes, but no one knows how group I mGluRs are modulating the individual synapses in these layers. Armed with the knowledge that mGluRs have been shown to modulate both glutamatergic and GABAergic transmission in the visual neocortex (Liu, Petro & Sherman, 2014)), it was my goal to investigate the role of mGluRs in the local V1 circuitry of the *Fmr1* KO. I provide evidence showing that group I mGluRs do not modulate glutamatergic synaptic transmission in layers 2/3 and 5/6 of V1, while group II mGluRs strongly suppress excitatory glutamatergic transmission in these layers. I also show that group II mGluR-mediated modulation of glutamatergic synaptic transmission onto NFS interneurons in layer 5/6 is altered. These results are significant, as they implicate an additional mGluR subtypes in the pathology of FXS. Further, my research findings support previously published research suggesting that reduced excitatory drive onto interneurons is a major dysfunction in neocortical pathogenic mechanisms of FXS. I show that this defect is presynaptic implicating FMRP in processes occurring at the axonal active zone, also supporting a previous study showing that deletion of presynaptic FMR1 specifically replicates deficits in excitatory

drive onto interneurons in somatosensory cortex (Hays et al., 2013). Hopefully, with mounting electrophysiological support for the presynaptic role of FMRP, scientists will begin to uncover new processes that are regulated by FMRP intracellularly. Finally, I show that changes in the group II mGluR modulation of neurotransmission leads to disinhibition of the excitatory neurons in layer 5/6, indicating circuit hyperexcitability in V1. This hyperexcitability may also be due to the decreased intrinsic excitability I observe in layer 5/6 somatostatin interneurons. This finding is the first to demonstrate changes in the intrinsic excitability of neocortical interneurons in layer 5/6 of the visual neocortex.

APPENDIX

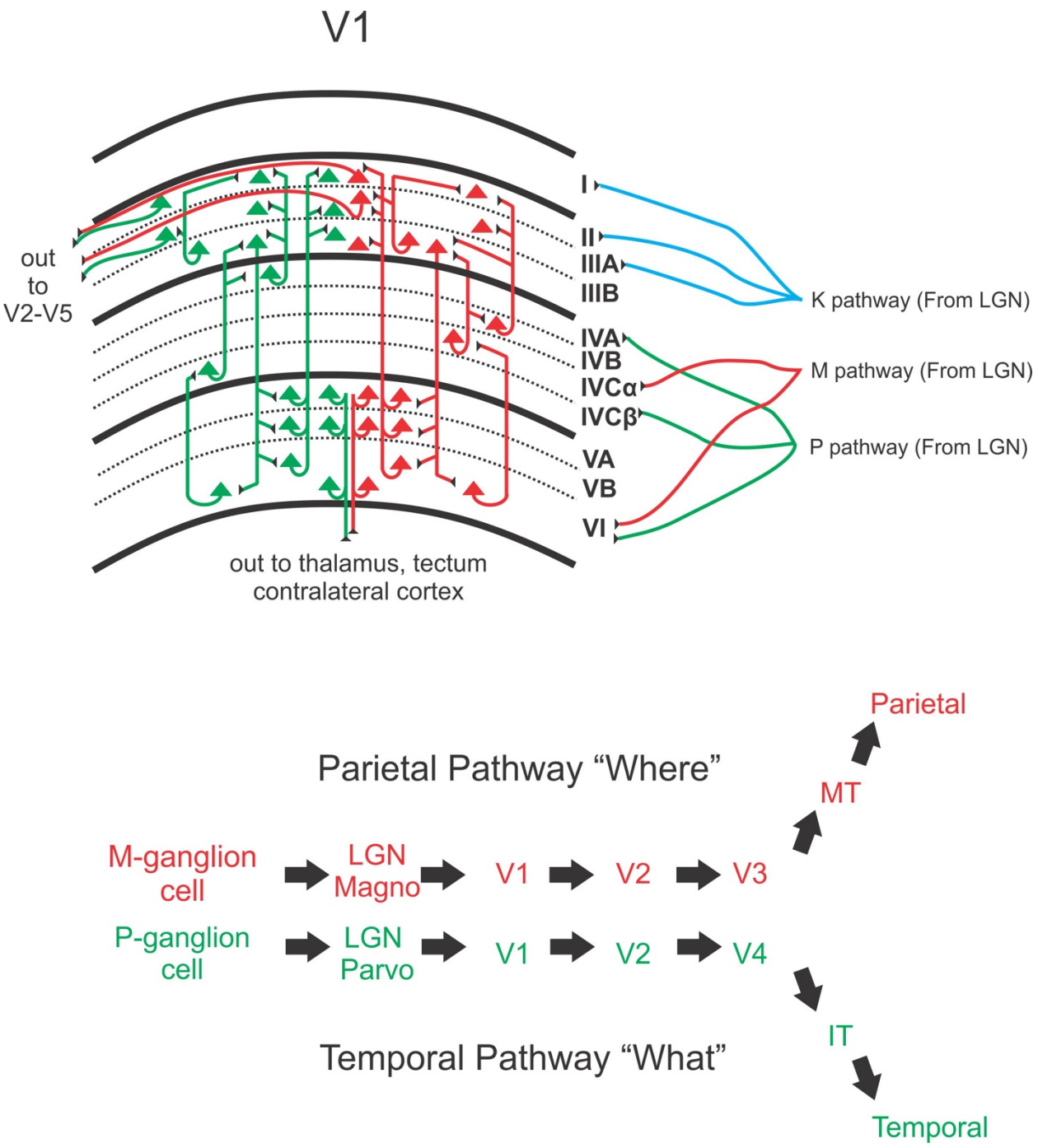

Figure 1.1. Primary visual neocortex circuitry and parallel visual pathways.
In the top half of the diagram is a schematic drawing of the microcircuits in V1. K pathway synapses modulate M (red) and P pathway (green), and are not shown for simplicity purposes. Below the diagram are flow charts depicting the sequential flow of information through the parallel pathways of the visual system.

Table 1.1. Three groups of metabotropic glutamate receptors.
Metabotropic glutamate receptors belong to class C GPCRs. Group I mGluRs include receptor subtypes 1 and 5, and are positively coupled to the G_q/G_{11} signaling pathway. Activation of the G_q pathway leads to PLC_β activation and hydrolysis of phosphoinositides. This leads to formation of IP_3 and DAG. IP_3 mobilizes intracellular calcium and this in conjunct with DAG is sufficient to activate PKC. Activation of PKC leads to the production of new protein synthesis. Group II and III mGluRs are negatively coupled to the $G_{i/o}$ signaling pathway. Dissociation of $G_{i/o}$ leads to inhibition of adenylate cyclase (AC) and reduction of cAMP production. Decreased cAMP leads to subsequent decreases in PKA activity and a decrease in protein translation. All of these receptors can also modulate ion channel activity directly, and have been shown to reside upstream from MAPK/ERK and PI3-mTOR signaling.

mGluR groups	Receptor subtypes	G-protein signaling pathway
Group I mGluRs	mGluR1, mGluR5	G_q/G_{11}
Group II mGluRs	mGluR2, mGluR3	$G_{i/o}$
Group III mGluRs	mGluR4, mGluR6-8	$G_{i/o}$

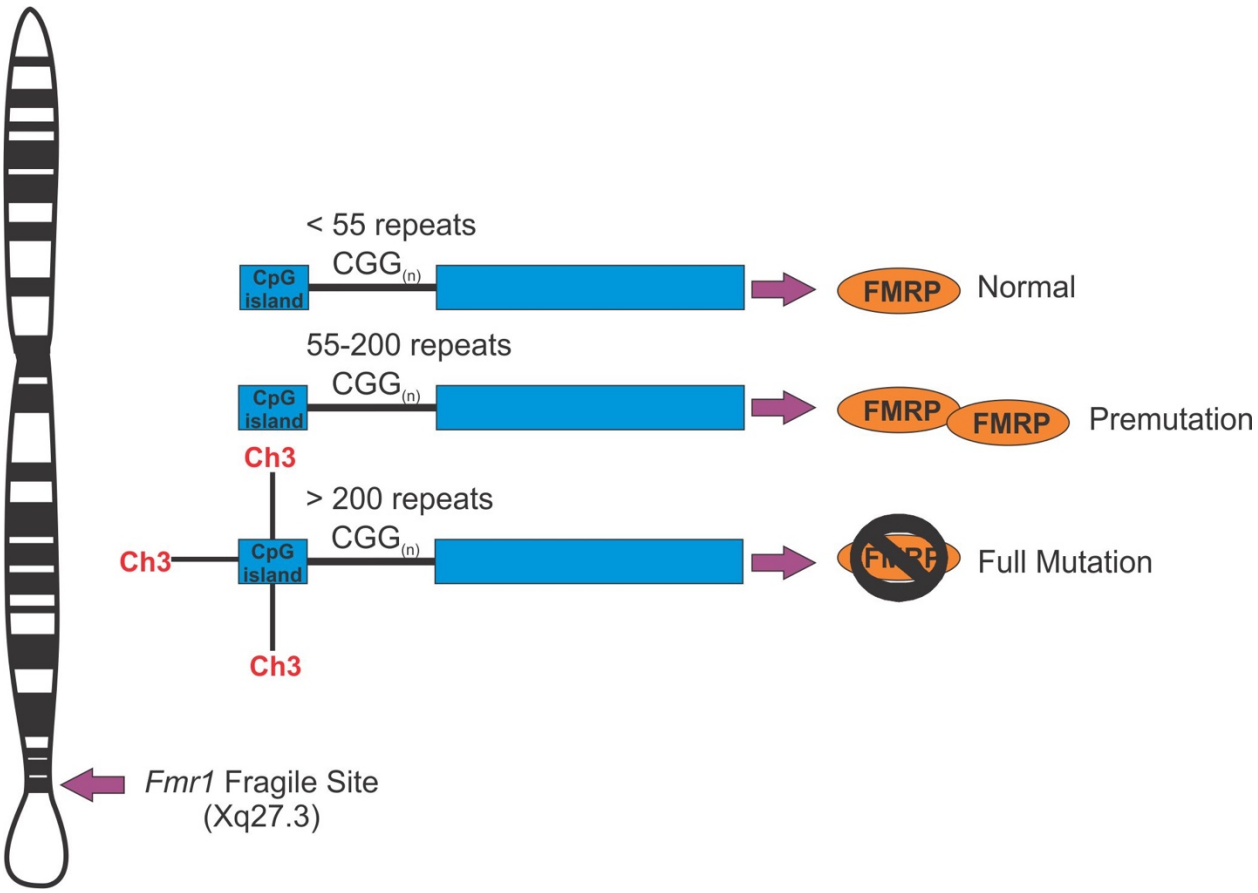

Figure 1.2. Development of FXS premutation and full mutation.
This diagram displays an X chromosome with a "fragile site" where the Fmr1 gene is located. In healthy individuals, a CGG repeat region downstream from the promotor CpG island is normal repeated no more than 55 times. In individuals with the permutation, CGG repeats vary from 55-200, and this leads to excess production of FMRP and gain-of-function phenotypes, including FXPOI and FXTAS. Individuals with a CGG repeat number > 200 will have hypermethylated promotor regions and subsequent loss of FMRP production. This leads to the full FXS phenotype.

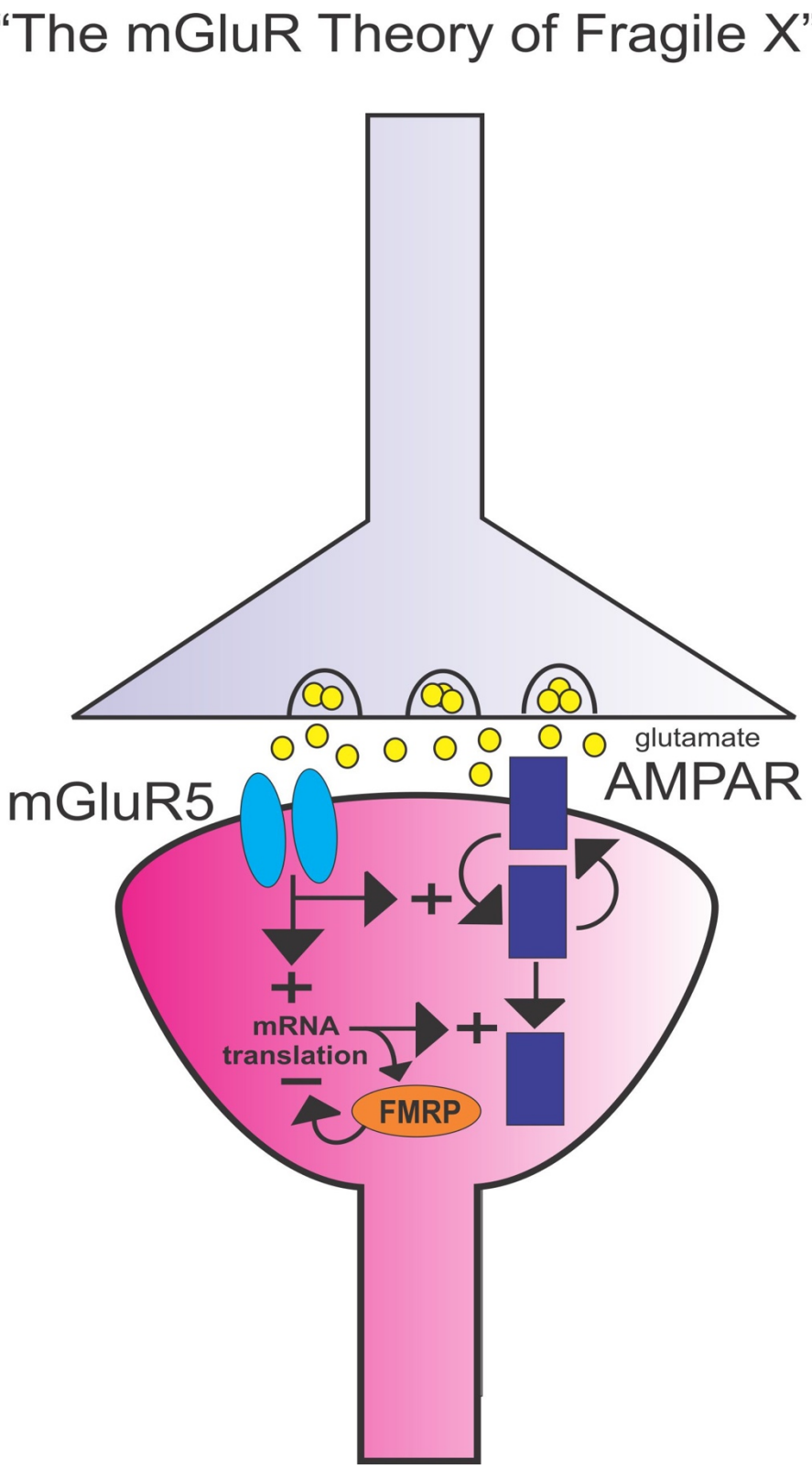

Figure 1.3. The mGluR Theory of Fragile X Syndrome.

Figure 1.3. (cont'd)

The mGluR theory of FXS proposes that loss of FMRP downstream of group I mGluR signaling, leads to increased translation of proteins implicated in synaptic plasticity, In the absence of negative regulation of mRNA translation, proteins that cause internalization of AMPA receptors are produced in excess, leading to the synaptic phenotype of exaggerated mGluR-LTD in the hippocampus of the *Fmr1* KO mouse. Loss of FMRP downstream of group I mGluR signaling also leads to increased translation of proteins important for normal spine development, leading to aberrant spine morphologies in the Fmr1 KO. Alterations in mGluR signaling have subsequently been found in other brain regions, implicating a role for mGluRs in Fragile X Syndrome pathogenic mechanisms.

REFERENCES

REFERENCES

Abrams, M. T., Reiss, A. L., Freund, L. S., Baumgardner, T. L., Chase, G. A., & Denckla, M. B. (1994). Molecular-neurobehavioral associations in females with the fragile X full mutation. *Am J Med Genet, 51*(4), 317-327. doi:10.1002/ajmg.1320510407

Adusei, D. C., Pacey, L. K., Chen, D., & Hampson, D. R. (2010). Early developmental alterations in GABAergic protein expression in fragile X knockout mice. *Neuropharmacology, 59*(3), 167-171. doi:10.1016/j.neuropharm.2010.05.002

Akins, M. R., Berk-Rauch, H. E., & Fallon, J. R. (2009). Presynaptic translation: stepping out of the postsynaptic shadow. *Front Neural Circuits, 3*, 17. doi:10.3389/neuro.04.017.2009

Akins, M. R., Leblanc, H. F., Stackpole, E. E., Chyung, E., & Fallon, J. R. (2012). Systematic mapping of fragile X granules in the mouse brain reveals a potential role for presynaptic FMRP in sensorimotor functions. *J Comp Neurol, 520*(16), 3687-3706. doi:10.1002/cne.23123

Antar, L. N., Li, C., Zhang, H., Carroll, R. C., & Bassell, G. J. (2006). Local functions for FMRP in axon growth cone motility and activity-dependent regulation of filopodia and spine synapses. *Mol Cell Neurosci, 32*(1-2), 37-48. doi:10.1016/j.mcn.2006.02.001

Anwyl, R. (1999). Metabotropic glutamate receptors: electrophysiological properties and role in plasticity. *Brain Res Brain Res Rev, 29*(1), 83-120.

Aschrafi, A., Cunningham, B. A., Edelman, G. M., & Vanderklish, P. W. (2005). The fragile X mental retardation protein and group I metabotropic glutamate receptors regulate levels of mRNA granules in brain. *Proc Natl Acad Sci U S A, 102*(6), 2180-2185. doi:10.1073/pnas.0409803102

Ashley, C. T., Jr., Wilkinson, K. D., Reines, D., & Warren, S. T. (1993). FMR1 protein: conserved RNP family domains and selective RNA binding. *Science, 262*(5133), 563-566.

Bassell, G. J., & Warren, S. T. (2008). Fragile X syndrome: loss of local mRNA regulation alters synaptic development and function. *Neuron, 60*(2), 201-214. doi:10.1016/j.neuron.2008.10.004

Baumgardner, T. L., Reiss, A. L., Freund, L. S., & Abrams, M. T. (1995). Specification of the neurobehavioral phenotype in males with fragile X syndrome. *Pediatrics, 95*(5), 744-752.

Beaver, C. J., Ji, Q., & Daw, N. W. (1999). Effect of the group II metabotropic glutamate agonist, 2R,4R-APDC, varies with age, layer, and visual experience in the visual cortex. *J Neurophysiol, 82*(1), 86-93.

Beierlein, M., Gibson, J. R., & Connors, B. W. (2000). A network of electrically coupled interneurons drives synchronized inhibition in neocortex. *Nat Neurosci, 3*(9), 904-910. doi:10.1038/78809

Beierlein, M., Gibson, J. R., & Connors, B. W. (2003). Two dynamically distinct inhibitory networks in layer 4 of the neocortex. *J Neurophysiol, 90*(5), 2987-3000. doi:10.1152/jn.00283.2003

Beltramo, R., D'Urso, G., Dal Maschio, M., Farisello, P., Bovetti, S., Clovis, Y., . . . Fellin, T. (2013). Layer-specific excitatory circuits differentially control recurrent network dynamics in the neocortex. *Nat Neurosci, 16*(2), 227-234. doi:10.1038/nn.3306

Berger, T. K., Perin, R., Silberberg, G., & Markram, H. (2009). Frequency-dependent disynaptic inhibition in the pyramidal network: a ubiquitous pathway in the developing rat neocortex. *J Physiol, 587*(Pt 22), 5411-5425. doi:10.1113/jphysiol.2009.176552

Berry-Kravis, E. (2002). Epilepsy in fragile X syndrome. *Dev Med Child Neurol, 44*(11), 724-728.

Berry-Kravis, E., Hagerman, R., Visootsak, J., Budimirovic, D., Kaufmann, W. E., Cherubini, M., . . . Carpenter, R. L. (2017). Arbaclofen in fragile X syndrome: results of phase 3 trials. *J Neurodev Disord, 9*, 3. doi:10.1186/s11689-016-9181-6

Bhakar, A. L., Dolen, G., & Bear, M. F. (2012). The pathophysiology of fragile X (and what it teaches us about synapses). *Annu Rev Neurosci, 35*, 417-443. doi:10.1146/annurev-neuro-060909-153138

Bhattacharyya, S. (2016). Inside story of Group I Metabotropic Glutamate Receptors (mGluRs). *Int J Biochem Cell Biol, 77*(Pt B), 205-212. doi:10.1016/j.biocel.2016.03.003

Bilousova, T. V., Dansie, L., Ngo, M., Aye, J., Charles, J. R., Ethell, D. W., & Ethell, I. M. (2009). Minocycline promotes dendritic spine maturation and improves behavioural performance in the fragile X mouse model. *J Med Genet, 46*(2), 94-102. doi:10.1136/jmg.2008.061796

Blackmer, T., Larsen, E. C., Takahashi, M., Martin, T. F., Alford, S., & Hamm, H. E. (2001). G protein betagamma subunit-mediated presynaptic inhibition: regulation of exocytotic fusion downstream of Ca2+ entry. *Science, 292*(5515), 293-297. doi:10.1126/science.1058803

Bordi, F., & Ugolini, A. (1999). Group I metabotropic glutamate receptors: implications for brain diseases. *Prog Neurobiol, 59*(1), 55-79.

Brager, D. H., & Johnston, D. (2014). Channelopathies and dendritic dysfunction in fragile X syndrome. *Brain Res Bull, 103*, 11-17. doi:10.1016/j.brainresbull.2014.01.002

Brown, V., Jin, P., Ceman, S., Darnell, J. C., O'Donnell, W. T., Tenenbaum, S. A., . . . Warren, S. T. (2001). Microarray identification of FMRP-associated brain mRNAs and altered mRNA translational profiles in fragile X syndrome. *Cell, 107*(4), 477-487.

Bureau, I., Shepherd, G. M., & Svoboda, K. (2008). Circuit and plasticity defects in the developing somatosensory cortex of FMR1 knock-out mice. *J Neurosci, 28*(20), 5178-5188. doi:10.1523/JNEUROSCI.1076-08.2008

Cahusac, P. M., & Wan, H. (2007). Group II metabotropic glutamate receptors reduce excitatory but not inhibitory neurotransmission in rat barrel cortex in vivo. *Neuroscience, 146*(1), 202-212. doi:10.1016/j.neuroscience.2007.01.049

Cartmell, J., & Schoepp, D. D. (2000). Regulation of neurotransmitter release by metabotropic glutamate receptors. *J Neurochem, 75*(3), 889-907.

Catania, M. V., De Socarraz, H., Penney, J. B., & Young, A. B. (1994). Metabotropic glutamate receptor heterogeneity in rat brain. *Mol Pharmacol, 45*(4), 626-636.

Catania, M. V., Landwehrmeyer, G. B., Testa, C. M., Standaert, D. G., Penney, J. B., Jr., & Young, A. B. (1994). Metabotropic glutamate receptors are differentially regulated during development. *Neuroscience, 61*(3), 481-495.

Cea-Del Rio, C. A., & Huntsman, M. M. (2014). The contribution of inhibitory interneurons to circuit dysfunction in Fragile X Syndrome. *Front Cell Neurosci, 8*, 245. doi:10.3389/fncel.2014.00245

Ceman, S., O'Donnell, W. T., Reed, M., Patton, S., Pohl, J., & Warren, S. T. (2003). Phosphorylation influences the translation state of FMRP-associated polyribosomes. *Hum Mol Genet, 12*(24), 3295-3305. doi:10.1093/hmg/ddg350

Centonze, D., Rossi, S., Mercaldo, V., Napoli, I., Ciotti, M. T., De Chiara, V., . . . Bagni, C. (2008). Abnormal striatal GABA transmission in the mouse model for the fragile X syndrome. *Biol Psychiatry, 63*(10), 963-973. doi:10.1016/j.biopsych.2007.09.008

Chang, Y. M., & Luebke, J. I. (2007). Electrophysiological diversity of layer 5 pyramidal cells in the prefrontal cortex of the rhesus monkey: in vitro slice studies. *J Neurophysiol, 98*(5), 2622-2632. doi:10.1152/jn.00585.2007

Chattopadhyaya, B., Di Cristo, G., Higashiyama, H., Knott, G. W., Kuhlman, S. J., Welker, E., & Huang, Z. J. (2004). Experience and activity-dependent maturation of perisomatic GABAergic innervation in primary visual cortex during a postnatal critical period. *J Neurosci, 24*(43), 9598-9611. doi:10.1523/JNEUROSCI.1851-04.2004

Chavis, P., Shinozaki, H., Bockaert, J., & Fagni, L. (1994). The metabotropic glutamate receptor types 2/3 inhibit L-type calcium channels via a pertussis toxin-sensitive G-protein in cultured cerebellar granule cells. *J Neurosci, 14*(11 Pt 2), 7067-7076.

Choi, C. H., Schoenfeld, B. P., Bell, A. J., Hinchey, P., Kollaros, M., Gertner, M. J., . . . McBride, S. M. (2011). Pharmacological reversal of synaptic plasticity deficits in the mouse model of fragile X syndrome by group II mGluR antagonist or lithium treatment. *Brain Res, 1380*, 106-119. doi:10.1016/j.brainres.2010.11.032

Christie, S. B., Akins, M. R., Schwob, J. E., & Fallon, J. R. (2009). The FXG: a presynaptic fragile X granule expressed in a subset of developing brain circuits. *J Neurosci, 29*(5), 1514-1524. doi:10.1523/JNEUROSCI.3937-08.2009

Chuang, S. C., Bianchi, R., & Wong, R. K. (2000). Group I mGluR activation turns on a voltage-gated inward current in hippocampal pyramidal cells. *J Neurophysiol, 83*(5), 2844-2853.

Chuang, S. C., Zhao, W., Bauchwitz, R., Yan, Q., Bianchi, R., & Wong, R. K. (2005). Prolonged epileptiform discharges induced by altered group I metabotropic glutamate receptor-mediated synaptic responses in hippocampal slices of a fragile X mouse model. *J Neurosci, 25*(35), 8048-8055. doi:10.1523/JNEUROSCI.1777-05.2005

Citri, A., & Malenka, R. C. (2008). Synaptic plasticity: multiple forms, functions, and mechanisms. *Neuropsychopharmacology, 33*(1), 18-41. doi:10.1038/sj.npp.1301559

Comery, T. A., Harris, J. B., Willems, P. J., Oostra, B. A., Irwin, S. A., Weiler, I. J., & Greenough, W. T. (1997). Abnormal dendritic spines in fragile X knockout mice: maturation and pruning deficits. *Proc Natl Acad Sci U S A, 94*(10), 5401-5404.

Conn, P. J., & Pin, J. P. (1997). Pharmacology and functions of metabotropic glutamate receptors. *Annu Rev Pharmacol Toxicol, 37*, 205-237. doi:10.1146/annurev.pharmtox.37.1.205

Cornish, K. M., Munir, F., & Cross, G. (1998). The nature of the spatial deficit in young females with Fragile-X syndrome: a neuropsychological and molecular perspective. *Neuropsychologia, 36*(11), 1239-1246.

Cox, C. L., & Sherman, S. M. (1999). Glutamate inhibits thalamic reticular neurons. *J Neurosci, 19*(15), 6694-6699.

Crandall, S. R., & Cox, C. L. (2013). Thalamic microcircuits: presynaptic dendrites form two feedforward inhibitory pathways in thalamus. *J Neurophysiol, 110*(2), 470-480. doi:10.1152/jn.00559.2012

Curia, G., Papouin, T., Seguela, P., & Avoli, M. (2009). Downregulation of tonic GABAergic inhibition in a mouse model of fragile X syndrome. *Cereb Cortex, 19*(7), 1515-1520. doi:10.1093/cercor/bhn159

D'Antuono, M., Merlo, D., & Avoli, M. (2003). Involvement of cholinergic and gabaergic systems in the fragile X knockout mice. *Neuroscience, 119*(1), 9-13.

D'Hulst, C., De Geest, N., Reeve, S. P., Van Dam, D., De Deyn, P. P., Hassan, B. A., & Kooy, R. F. (2006). Decreased expression of the GABAA receptor in fragile X syndrome. *Brain Res, 1121*(1), 238-245. doi:10.1016/j.brainres.2006.08.115

D'Hulst, C., Heulens, I., Brouwer, J. R., Willemsen, R., De Geest, N., Reeve, S. P., . . . Kooy, R. F. (2009). Expression of the GABAergic system in animal models for fragile X syndrome and fragile X associated tremor/ataxia syndrome (FXTAS). *Brain Res, 1253*, 176-183. doi:10.1016/j.brainres.2008.11.075

D'Hulst, C., & Kooy, R. F. (2007). The GABAA receptor: a novel target for treatment of fragile X? *Trends Neurosci, 30*(8), 425-431. doi:10.1016/j.tins.2007.06.003

Dahlhaus, R., & El-Husseini, A. (2010). Altered neuroligin expression is involved in social deficits in a mouse model of the fragile X syndrome. *Behav Brain Res, 208*(1), 96-105. doi:10.1016/j.bbr.2009.11.019

Darnell, J. C., Van Driesche, S. J., Zhang, C., Hung, K. Y., Mele, A., Fraser, C. E., . . . Darnell, R. B. (2011). FMRP stalls ribosomal translocation on mRNAs linked to synaptic function and autism. *Cell, 146*(2), 247-261. doi:10.1016/j.cell.2011.06.013

Daw, N. W., Fox, K., Sato, H., & Czepita, D. (1992). Critical period for monocular deprivation in the cat visual cortex. *J Neurophysiol, 67*(1), 197-202.

De Boulle, K., Verkerk, A. J., Reyniers, E., Vits, L., Hendrickx, J., Van Roy, B., . . . Willems, P. J. (1993). A point mutation in the FMR-1 gene associated with fragile X mental retardation. *Nat Genet, 3*(1), 31-35. doi:10.1038/ng0193-31

De Diego Otero, Y., Severijnen, L. A., van Cappellen, G., Schrier, M., Oostra, B., & Willemsen, R. (2002). Transport of fragile X mental retardation protein via granules in neurites of PC12 cells. *Mol Cell Biol, 22*(23), 8332-8341.

Desai, N. S., Casimiro, T. M., Gruber, S. M., & Vanderklish, P. W. (2006). Early postnatal plasticity in neocortex of Fmr1 knockout mice. *J Neurophysiol, 96*(4), 1734-1745. doi:10.1152/jn.00221.2006

Ding, Q., Sethna, F., & Wang, H. (2014). Behavioral analysis of male and female Fmr1 knockout mice on C57BL/6 background. *Behav Brain Res, 271*, 72-78. doi:10.1016/j.bbr.2014.05.046

Doi, A., Ishibashi, H., Jinno, S., Kosaka, T., & Akaike, N. (2002). Presynaptic inhibition of GABAergic miniature currents by metabotropic glutamate receptor in the rat CNS. *Neuroscience, 109*(2), 299-311.

Dolen, G., Osterweil, E., Rao, B. S., Smith, G. B., Auerbach, B. D., Chattarji, S., & Bear, M. F. (2007). Correction of fragile X syndrome in mice. *Neuron, 56*(6), 955-962. doi:10.1016/j.neuron.2007.12.001

Fanselow, E. E., & Connors, B. W. (2010). The roles of somatostatin-expressing (GIN) and fast-spiking inhibitory interneurons in UP-DOWN states of mouse neocortex. *J Neurophysiol, 104*(2), 596-606. doi:10.1152/jn.00206.2010

Ferron, L., Nieto-Rostro, M., Cassidy, J. S., & Dolphin, A. C. (2014). Fragile X mental retardation protein controls synaptic vesicle exocytosis by modulating N-type calcium channel density. *Nat Commun, 5*, 3628. doi:10.1038/ncomms4628

Flavin, H. J., Jin, X. T., & Daw, N. W. (2000). 2R,4R-4-Aminopyrrolidine-2,4-dicarboxylate (APDC) attenuates cortical EPSPs. *Brain Res, 873*(2), 212-217.

Funauchi, M., Haruta, H., & Tsumoto, T. (1994). Effects of an inhibitor for calcium/calmodulin-dependent protein phosphatase, calcineurin, on induction of long-term potentiation in rat visual cortex. *Neurosci Res, 19*(3), 269-278.

Gantois, I., Vandesompele, J., Speleman, F., Reyniers, E., D'Hooge, R., Severijnen, L. A., . . . Kooy, R. F. (2006). Expression profiling suggests underexpression of the GABA(A) receptor subunit delta in the fragile X knockout mouse model. *Neurobiol Dis, 21*(2), 346-357. doi:10.1016/j.nbd.2005.07.017

Gibson, J. R., Bartley, A. F., Hays, S. A., & Huber, K. M. (2008). Imbalance of neocortical excitation and inhibition and altered UP states reflect network hyperexcitability in the mouse model of fragile X syndrome. *J Neurophysiol, 100*(5), 2615-2626. doi:10.1152/jn.90752.2008

Glickfeld, L. L., Andermann, M. L., Bonin, V., & Reid, R. C. (2013). Cortico-cortical projections in mouse visual cortex are functionally target specific. *Nat Neurosci, 16*(2), 219-226. doi:10.1038/nn.3300

Glickfeld, L. L., Histed, M. H., & Maunsell, J. H. (2013). Mouse primary visual cortex is used to detect both orientation and contrast changes. *J Neurosci, 33*(50), 19416-19422. doi:10.1523/JNEUROSCI.3560-13.2013

Goebel-Goody, S. M., Wilson-Wallis, E. D., Royston, S., Tagliatela, S. M., Naegele, J. R., & Lombroso, P. J. (2012). Genetic manipulation of STEP reverses behavioral abnormalities in a fragile X syndrome mouse model. *Genes Brain Behav, 11*(5), 586-600. doi:10.1111/j.1601-183X.2012.00781.x

Goncalves, J. T., Anstey, J. E., Golshani, P., & Portera-Cailliau, C. (2013). Circuit level defects in the developing neocortex of Fragile X mice. *Nat Neurosci, 16*(7), 903-909. doi:10.1038/nn.3415

Govindaiah, G., & Cox, C. L. (2006). Metabotropic glutamate receptors differentially regulate GABAergic inhibition in thalamus. *J Neurosci, 26*(52), 13443-13453. doi:10.1523/JNEUROSCI.3578-06.2006

Grossman, A. W., Elisseou, N. M., McKinney, B. C., & Greenough, W. T. (2006). Hippocampal pyramidal cells in adult Fmr1 knockout mice exhibit an immature-appearing profile of dendritic spines. *Brain Res, 1084*(1), 158-164. doi:10.1016/j.brainres.2006.02.044

Hagerman, P. J. (2008). The fragile X prevalence paradox. *J Med Genet, 45*(8), 498-499. doi:10.1136/jmg.2008.059055

Hagerman, P. J., & Stafstrom, C. E. (2009). Origins of epilepsy in fragile X syndrome. *Epilepsy Curr, 9*(4), 108-112. doi:10.1111/j.1535-7511.2009.01309.x

Hagerman, R., Hoem, G., & Hagerman, P. (2010). Fragile X and autism: Intertwined at the molecular level leading to targeted treatments. *Mol Autism, 1*(1), 12. doi:10.1186/2040-2392-1-12

Hagerman, R. J., Ono, M. Y., & Hagerman, P. J. (2005). Recent advances in fragile X: a model for autism and neurodegeneration. *Curr Opin Psychiatry, 18*(5), 490-496. doi:10.1097/01.yco.0000179485.39520.b0

Harlow, E. G., Till, S. M., Russell, T. A., Wijetunge, L. S., Kind, P., & Contractor, A. (2010). Critical period plasticity is disrupted in the barrel cortex of FMR1 knockout mice. *Neuron, 65*(3), 385-398. doi:10.1016/j.neuron.2010.01.024

Hays, S. A., Huber, K. M., & Gibson, J. R. (2011). Altered neocortical rhythmic activity states in Fmr1 KO mice are due to enhanced mGluR5 signaling and involve changes in excitatory circuitry. *J Neurosci, 31*(40), 14223-14234. doi:10.1523/JNEUROSCI.3157-11.2011

Henderson, C., Wijetunge, L., Kinoshita, M. N., Shumway, M., Hammond, R. S., Postma, F. R., . . . Healy, A. M. (2012). Reversal of disease-related pathologies in the fragile X mouse model by selective activation of GABAB receptors with arbaclofen. *Sci Transl Med, 4*(152), 152ra128. doi:10.1126/scitranslmed.3004218

Hensch, T. K. (2005). Critical period plasticity in local cortical circuits. *Nat Rev Neurosci, 6*(11), 877-888. doi:10.1038/nrn1787

Heulens, I., D'Hulst, C., Van Dam, D., De Deyn, P. P., & Kooy, R. F. (2012). Pharmacological treatment of fragile X syndrome with GABAergic drugs in a knockout mouse model. *Behav Brain Res, 229*(1), 244-249. doi:10.1016/j.bbr.2012.01.031

Hinds, H. L., Ashley, C. T., Sutcliffe, J. S., Nelson, D. L., Warren, S. T., Housman, D. E., & Schalling, M. (1993). Tissue specific expression of FMR-1 provides evidence for a functional role in fragile X syndrome. *Nat Genet, 3*(1), 36-43. doi:10.1038/ng0193-36

Hinton, V. J., Brown, W. T., Wisniewski, K., & Rudelli, R. D. (1991). Analysis of neocortex in three males with the fragile X syndrome. *Am J Med Genet, 41*(3), 289-294. doi:10.1002/ajmg.1320410306

Hong, A., Zhang, A., Ke, Y., El Idrissi, A., & Shen, C. H. (2012). Downregulation of GABA(A) beta subunits is transcriptionally controlled by Fmr1p. *J Mol Neurosci, 46*(2), 272-275. doi:10.1007/s12031-011-9531-5

Hovelso, N., Sotty, F., Montezinho, L. P., Pinheiro, P. S., Herrik, K. F., & Mork, A. (2012). Therapeutic potential of metabotropic glutamate receptor modulators. *Curr Neuropharmacol, 10*(1), 12-48. doi:10.2174/157015912799362805

Huber, K. M., Gallagher, S. M., Warren, S. T., & Bear, M. F. (2002). Altered synaptic plasticity in a mouse model of fragile X mental retardation. *Proc Natl Acad Sci U S A, 99*(11), 7746-7750. doi:10.1073/pnas.122205699

Ivry, R. (1993). Cerebellar involvement in the explicit representation of temporal information. *Ann N Y Acad Sci, 682*, 214-230.

Kang, H., & Schuman, E. M. (1996). A requirement for local protein synthesis in neurotrophin-induced hippocampal synaptic plasticity. *Science, 273*(5280), 1402-1406.

Kasper, E. M., Larkman, A. U., Lubke, J., & Blakemore, C. (1994). Pyramidal neurons in layer 5 of the rat visual cortex. I. Correlation among cell morphology, intrinsic electrophysiological properties, and axon targets. *J Comp Neurol, 339*(4), 459-474. doi:10.1002/cne.903390402

Kates, W. R., Abrams, M. T., Kaufmann, W. E., Breiter, S. N., & Reiss, A. L. (1997). Reliability and validity of MRI measurement of the amygdala and hippocampus in children with fragile X syndrome. *Psychiatry Res, 75*(1), 31-48.

Kato, N. (1993). Dependence of long-term depression on postsynaptic metabotropic glutamate receptors in visual cortex. *Proc Natl Acad Sci U S A, 90*(8), 3650-3654.

Katz, L. C., & Shatz, C. J. (1996). Synaptic activity and the construction of cortical circuits. *Science, 274*(5290), 1133-1138.

Katzner, S., & Weigelt, S. (2013). Visual cortical networks: of mice and men. *Curr Opin Neurobiol, 23*(2), 202-206. doi:10.1016/j.conb.2013.01.019

Kaufmann, W. E., Cortell, R., Kau, A. S., Bukelis, I., Tierney, E., Gray, R. M., . . . Stanard, P. (2004). Autism spectrum disorder in fragile X syndrome: communication, social interaction, and specific behaviors. *Am J Med Genet A, 129A*(3), 225-234. doi:10.1002/ajmg.a.30229

Kawaguchi, Y., & Kubota, Y. (1997). GABAergic cell subtypes and their synaptic connections in rat frontal cortex. *Cereb Cortex, 7*(6), 476-486.

Kazdoba, T. M., Leach, P. T., Silverman, J. L., & Crawley, J. N. (2014). Modeling fragile X syndrome in the Fmr1 knockout mouse. *Intractable Rare Dis Res, 3*(4), 118-133. doi:10.5582/irdr.2014.01024

Kinoshita, A., Shigemoto, R., Ohishi, H., van der Putten, H., & Mizuno, N. (1998). Immunohistochemical localization of metabotropic glutamate receptors, mGluR7a and mGluR7b, in the central nervous system of the adult rat and mouse: a light and electron microscopic study. *J Comp Neurol, 393*(3), 332-352.

Koekkoek, S. K., Yamaguchi, K., Milojkovic, B. A., Dortland, B. R., Ruigrok, T. J., Maex, R., . . . De Zeeuw, C. I. (2005). Deletion of FMR1 in Purkinje cells enhances parallel fiber LTD, enlarges spines, and attenuates cerebellar eyelid conditioning in Fragile X syndrome. *Neuron, 47*(3), 339-352. doi:10.1016/j.neuron.2005.07.005

Kogan, C. S., Bertone, A., Cornish, K., Boutet, I., Der Kaloustian, V. M., Andermann, E., . . . Chaudhuri, A. (2004). Integrative cortical dysfunction and pervasive motion perception deficit in fragile X syndrome. *Neurology, 63*(9), 1634-1639.

Kogan, C. S., Boutet, I., Cornish, K., Zangenehpour, S., Mullen, K. T., Holden, J. J., . . . Chaudhuri, A. (2004). Differential impact of the FMR1 gene on visual processing in fragile X syndrome. *Brain, 127*(Pt 3), 591-601. doi:10.1093/brain/awh069

Lacoux, C., Di Marino, D., Boyl, P. P., Zalfa, F., Yan, B., Ciotti, M. T., . . . Bagni, C. (2012). BC1-FMRP interaction is modulated by 2'-O-methylation: RNA-binding activity of the tudor domain and translational regulation at synapses. *Nucleic Acids Res, 40*(9), 4086-4096. doi:10.1093/nar/gkr1254

Laramee, M. E., & Boire, D. (2014). Visual cortical areas of the mouse: comparison of parcellation and network structure with primates. *Front Neural Circuits, 8*, 149. doi:10.3389/fncir.2014.00149

Larkum, M. E., Nevian, T., Sandler, M., Polsky, A., & Schiller, J. (2009). Synaptic integration in tuft dendrites of layer 5 pyramidal neurons: a new unifying principle. *Science, 325*(5941), 756-760. doi:10.1126/science.1171958

Larson, J., Jessen, R. E., Kim, D., Fine, A. K., & du Hoffmann, J. (2005). Age-dependent and selective impairment of long-term potentiation in the anterior piriform cortex of mice lacking the fragile X mental retardation protein. *J Neurosci, 25*(41), 9460-9469. doi:10.1523/JNEUROSCI.2638-05.2005

Lee, C. C., & Sherman, S. M. (2009). Glutamatergic inhibition in sensory neocortex. *Cereb Cortex, 19*(10), 2281-2289. doi:10.1093/cercor/bhn246

Li, J., Pelletier, M. R., Perez Velazquez, J. L., & Carlen, P. L. (2002). Reduced cortical synaptic plasticity and GluR1 expression associated with fragile X mental retardation protein deficiency. *Mol Cell Neurosci, 19*(2), 138-151. doi:10.1006/mcne.2001.1085

Li, Z., Zhang, Y., Ku, L., Wilkinson, K. D., Warren, S. T., & Feng, Y. (2001). The fragile X mental retardation protein inhibits translation via interacting with mRNA. *Nucleic Acids Res, 29*(11), 2276-2283.

Liu, T., Petrof, I., & Sherman, S. M. (2014). Modulatory effects of activation of metabotropic glutamate receptors on GABAergic circuits in the mouse cortex. *J Neurophysiol, 111*(11), 2287-2297. doi:10.1152/jn.00730.2013

Loesch, D. Z., & Hay, D. A. (1988). Clinical features and reproductive patterns in fragile X female heterozygotes. *J Med Genet, 25*(6), 407-414.

Lozano, R., Hare, E. B., & Hagerman, R. J. (2014). Modulation of the GABAergic pathway for the treatment of fragile X syndrome. *Neuropsychiatr Dis Treat, 10*, 1769-1779. doi:10.2147/NDT.S42919

Mann, K., Kiefer, F., Spanagel, R., & Littleton, J. (2008). Acamprosate: recent findings and future research directions. *Alcohol Clin Exp Res, 32*(7), 1105-1110. doi:10.1111/j.1530-0277.2008.00690.x

Markram, H., Toledo-Rodriguez, M., Wang, Y., Gupta, A., Silberberg, G., & Wu, C. (2004). Interneurons of the neocortical inhibitory system. *Nat Rev Neurosci, 5*(10), 793-807. doi:10.1038/nrn1519

Martin, H. G., Lassalle, O., & Manzoni, O. J. (2016). Differential Adulthood Onset mGlu5 Signaling Saves Prefrontal Function in the Fragile X Mouse. *Cereb Cortex*. doi:10.1093/cercor/bhw328

Martin, H. G. S., Lassalle, O., Brown, J. T., & Manzoni, O. J. (2016). Age-Dependent Long-Term Potentiation Deficits in the Prefrontal Cortex of the Fmr1 Knockout Mouse Model of Fragile X Syndrome. *Cereb Cortex, 26*(5), 2084-2092. doi:10.1093/cercor/bhv031

Martin, L. J., Blackstone, C. D., Huganir, R. L., & Price, D. L. (1992). Cellular localization of a metabotropic glutamate receptor in rat brain. *Neuron, 9*(2), 259-270.

Martinez-Galan, J. R., Lopez-Bendito, G., Lujan, R., Shigemoto, R., Fairen, A., & Valdeolmillos, M. (2001). Cajal-Retzius cells in early postnatal mouse cortex selectively express functional metabotropic glutamate receptors. *Eur J Neurosci, 13*(6), 1147-1154.

Mason, A., & Larkman, A. (1990). Correlations between morphology and electrophysiology of pyramidal neurons in slices of rat visual cortex. II. Electrophysiology. *J Neurosci, 10*(5), 1415-1428.

Mateo, Z., & Porter, J. T. (2007). Group II metabotropic glutamate receptors inhibit glutamate release at thalamocortical synapses in the developing somatosensory cortex. *Neuroscience, 146*(3), 1062-1072. doi:10.1016/j.neuroscience.2007.02.053

Mazzocco, M. M., Kates, W. R., Baumgardner, T. L., Freund, L. S., & Reiss, A. L. (1997). Autistic behaviors among girls with fragile X syndrome. *J Autism Dev Disord, 27*(4), 415-435.

McNaughton, C. H., Moon, J., Strawderman, M. S., Maclean, K. N., Evans, J., & Strupp, B. J. (2008). Evidence for social anxiety and impaired social cognition in a mouse model of fragile X syndrome. *Behav Neurosci, 122*(2), 293-300. doi:10.1037/0735-7044.122.2.293

Meredith, R. M., Holmgren, C. D., Weidum, M., Burnashev, N., & Mansvelder, H. D. (2007). Increased threshold for spike-timing-dependent plasticity is caused by unreliable calcium signaling in mice lacking fragile X gene FMR1. *Neuron, 54*(4), 627-638. doi:10.1016/j.neuron.2007.04.028

Merenstein, S. A., Sobesky, W. E., Taylor, A. K., Riddle, J. E., Tran, H. X., & Hagerman, R. J. (1996). Molecular-clinical correlations in males with an expanded FMR1 mutation. *Am J Med Genet, 64*(2), 388-394. doi:10.1002/(SICI)1096-8628(19960809)64:2<388::AID-AJMG31>3.0.CO;2-9

Metin, C., Godement, P., & Imbert, M. (1988). The primary visual cortex in the mouse: receptive field properties and functional organization. *Exp Brain Res, 69*(3), 594-612.

Mineur, Y. S., & Crusio, W. E. (2002). Behavioral and neuroanatomical characterization of FVB/N inbred mice. *Brain Res Bull, 57*(1), 41-47.

Mineur, Y. S., Sluyter, F., de Wit, S., Oostra, B. A., & Crusio, W. E. (2002). Behavioral and neuroanatomical characterization of the Fmr1 knockout mouse. *Hippocampus, 12*(1), 39-46. doi:10.1002/hipo.10005

Mostofsky, S. H., Mazzocco, M. M., Aakalu, G., Warsofsky, I. S., Denckla, M. B., & Reiss, A. L. (1998). Decreased cerebellar posterior vermis size in fragile X syndrome: correlation with neurocognitive performance. *Neurology, 50*(1), 121-130.

Munoz, A., Liu, X. B., & Jones, E. G. (1999). Development of metabotropic glutamate receptors from trigeminal nuclei to barrel cortex in postnatal mouse. *J Comp Neurol, 409*(4), 549-566.

Musumeci, S. A., Bosco, P., Calabrese, G., Bakker, C., De Sarro, G. B., Elia, M., . . . Oostra, B. A. (2000). Audiogenic seizures susceptibility in transgenic mice with fragile X syndrome. *Epilepsia, 41*(1), 19-23.

Nakanishi, S. (1994). Metabotropic glutamate receptors: synaptic transmission, modulation, and plasticity. *Neuron, 13*(5), 1031-1037.

Niell, C. M. (2015). Cell types, circuits, and receptive fields in the mouse visual cortex. *Annu Rev Neurosci, 38*, 413-431. doi:10.1146/annurev-neuro-071714-033807

Niell, C. M., & Stryker, M. P. (2008). Highly selective receptive fields in mouse visual cortex. *J Neurosci, 28*(30), 7520-7536. doi:10.1523/JNEUROSCI.0623-08.2008

Nimchinsky, E. A., Oberlander, A. M., & Svoboda, K. (2001). Abnormal development of dendritic spines in FMR1 knock-out mice. *J Neurosci, 21*(14), 5139-5146.

Niswender, C. M., & Conn, P. J. (2010). Metabotropic glutamate receptors: physiology, pharmacology, and disease. *Annu Rev Pharmacol Toxicol, 50*, 295-322. doi:10.1146/annurev.pharmtox.011008.145533

Ohishi, H., Neki, A., & Mizuno, N. (1998). Distribution of a metabotropic glutamate receptor, mGluR2, in the central nervous system of the rat and mouse: an immunohistochemical study with a monoclonal antibody. *Neurosci Res, 30*(1), 65-82.

Oliva, A. A., Jr., Jiang, M., Lam, T., Smith, K. L., & Swann, J. W. (2000). Novel hippocampal interneuronal subtypes identified using transgenic mice that express green fluorescent protein in GABAergic interneurons. *J Neurosci, 20*(9), 3354-3368.

Olmos-Serrano, J. L., Paluszkiewicz, S. M., Martin, B. S., Kaufmann, W. E., Corbin, J. G., & Huntsman, M. M. (2010). Defective GABAergic neurotransmission and pharmacological rescue of neuronal hyperexcitability in the amygdala in a mouse model of fragile X syndrome. *J Neurosci, 30*(29), 9929-9938. doi:10.1523/JNEUROSCI.1714-10.2010

Osterweil, E. K., Chuang, S. C., Chubykin, A. A., Sidorov, M., Bianchi, R., Wong, R. K., & Bear, M. F. (2013). Lovastatin corrects excess protein synthesis and prevents epileptogenesis in a mouse model of fragile X syndrome. *Neuron, 77*(2), 243-250. doi:10.1016/j.neuron.2012.01.034

Osterweil, E. K., Krueger, D. D., Reinhold, K., & Bear, M. F. (2010). Hypersensitivity to mGluR5 and ERK1/2 leads to excessive protein synthesis in the hippocampus of a mouse model of fragile X syndrome. *J Neurosci, 30*(46), 15616-15627. doi:10.1523/JNEUROSCI.3888-10.2010

Pacey, L. K., Heximer, S. P., & Hampson, D. R. (2009). Increased GABA(B) receptor-mediated signaling reduces the susceptibility of fragile X knockout mice to audiogenic seizures. *Mol Pharmacol, 76*(1), 18-24. doi:10.1124/mol.109.056127

Paluszkiewicz, S. M., Olmos-Serrano, J. L., Corbin, J. G., & Huntsman, M. M. (2011). Impaired inhibitory control of cortical synchronization in fragile X syndrome. *J Neurophysiol, 106*(5), 2264-2272. doi:10.1152/jn.00421.2011

Pan, F., Aldridge, G. M., Greenough, W. T., & Gan, W. B. (2010). Dendritic spine instability and insensitivity to modulation by sensory experience in a mouse model of fragile X syndrome. *Proc Natl Acad Sci U S A, 107*(41), 17768-17773. doi:10.1073/pnas.1012496107

Patel, A. B., Hays, S. A., Bureau, I., Huber, K. M., & Gibson, J. R. (2013). A target cell-specific role for presynaptic Fmr1 in regulating glutamate release onto neocortical fast-spiking inhibitory neurons. *J Neurosci, 33*(6), 2593-2604. doi:10.1523/JNEUROSCI.2447-12.2013

Paul, K., Venkitaramani, D. V., & Cox, C. L. (2013). Dampened dopamine-mediated neuromodulation in prefrontal cortex of fragile X mice. *J Physiol, 591*(4), 1133-1143. doi:10.1113/jphysiol.2012.241067

Peier, A. M., McIlwain, K. L., Kenneson, A., Warren, S. T., Paylor, R., & Nelson, D. L. (2000). (Over)correction of FMR1 deficiency with YAC transgenics: behavioral and physical features. *Hum Mol Genet, 9*(8), 1145-1159.

Petilla Interneuron Nomenclature, G., Ascoli, G. A., Alonso-Nanclares, L., Anderson, S. A., Barrionuevo, G., Benavides-Piccione, R., . . . Yuste, R. (2008). Petilla terminology: nomenclature of features of GABAergic interneurons of the cerebral cortex. *Nat Rev Neurosci, 9*(7), 557-568. doi:10.1038/nrn2402

Petralia, R. S., Wang, Y. X., Niedzielski, A. S., & Wenthold, R. J. (1996). The metabotropic glutamate receptors, mGluR2 and mGluR3, show unique postsynaptic, presynaptic and glial localizations. *Neuroscience, 71*(4), 949-976.

Pfeiffer, B. E., & Huber, K. M. (2009). The state of synapses in fragile X syndrome. *Neuroscientist, 15*(5), 549-567. doi:10.1177/1073858409333075

Pietropaolo, S., Guilleminot, A., Martin, B., D'Amato, F. R., & Crusio, W. E. (2011). Genetic-background modulation of core and variable autistic-like symptoms in Fmr1 knock-out mice. *PLoS One, 6*(2), e17073. doi:10.1371/journal.pone.0017073

Pin, J. P., & Duvoisin, R. (1995). The metabotropic glutamate receptors: structure and functions. *Neuropharmacology, 34*(1), 1-26.

Priebe, N. J., & McGee, A. W. (2014). Mouse vision as a gateway for understanding how experience shapes neural circuits. *Front Neural Circuits, 8*, 123. doi:10.3389/fncir.2014.00123

Qiu, L. F., Hao, Y. H., Li, Q. Z., & Xiong, Z. Q. (2008). Fragile X syndrome and epilepsy. *Neurosci Bull, 24*(5), 338-344. doi:10.1007/s12264-008-1221-0

Reid, S. N., & Daw, N. W. (1997). Activation of metabotropic glutamate receptors has different effects in different layers of cat visual cortex. *Vis Neurosci, 14*(1), 83-88.

Reid, S. N., & Romano, C. (2001). Developmental and sensory-dependent changes of group II metabotropic glutamate receptors. *J Comp Neurol, 429*(2), 270-276.

Reid, S. N., Romano, C., Hughes, T., & Daw, N. W. (1995). Immunohistochemical study of two phosphoinositide-linked metabotropic glutamate receptors (mGluR1 alpha and mGluR5) in the cat visual cortex before, during, and after the peak of the critical period for eye-specific connections. *J Comp Neurol, 355*(3), 470-477. doi:10.1002/cne.903550311

Reid, S. N., Romano, C., Hughes, T., & Daw, N. W. (1997). Developmental and sensory-dependent changes of phosphoinositide-linked metabotropic glutamate receptors. *J Comp Neurol, 389*(4), 577-583.

Reiss, A. L., Lee, J., & Freund, L. (1994). Neuroanatomy of fragile X syndrome: the temporal lobe. *Neurology, 44*(7), 1317-1324.

Ronesi, J. A., & Huber, K. M. (2008). Homer interactions are necessary for metabotropic glutamate receptor-induced long-term depression and translational activation. *J Neurosci, 28*(2), 543-547. doi:10.1523/JNEUROSCI.5019-07.2008

Rudelli, R. D., Brown, W. T., Wisniewski, K., Jenkins, E. C., Laure-Kamionowska, M., Connell, F., & Wisniewski, H. M. (1985). Adult fragile X syndrome. Clinico-neuropathologic findings. *Acta Neuropathol, 67*(3-4), 289-295.

Rudy, B., Fishell, G., Lee, S., & Hjerling-Leffler, J. (2011). Three groups of interneurons account for nearly 100% of neocortical GABAergic neurons. *Dev Neurobiol, 71*(1), 45-61. doi:10.1002/dneu.20853

Sabanov, V., Braat, S., D'Andrea, L., Willemsen, R., Zeidler, S., Rooms, L., . . . Balschun, D. (2017). Impaired GABAergic inhibition in the hippocampus of Fmr1 knockout mice. *Neuropharmacology, 116*, 71-81. doi:10.1016/j.neuropharm.2016.12.010

Sabatini, B. L., Maravall, M., & Svoboda, K. (2001). Ca(2+) signaling in dendritic spines. *Curr Opin Neurobiol, 11*(3), 349-356.

Sanderson, T. M., Hogg, E. L., Collingridge, G. L., & Correa, S. A. (2016). Hippocampal metabotropic glutamate receptor long-term depression in health and disease: focus on mitogen-activated protein kinase pathways. *J Neurochem, 139 Suppl 2*, 200-214. doi:10.1111/jnc.13592

Santoro, M. R., Bray, S. M., & Warren, S. T. (2012). Molecular mechanisms of fragile X syndrome: a twenty-year perspective. *Annu Rev Pathol, 7*, 219-245. doi:10.1146/annurev-pathol-011811-132457

Scanziani, M., Salin, P. A., Vogt, K. E., Malenka, R. C., & Nicoll, R. A. (1997). Use-dependent increases in glutamate concentration activate presynaptic metabotropic glutamate receptors. *Nature, 385*(6617), 630-634. doi:10.1038/385630a0

Schoepp, D. D., & Conn, P. J. (1993). Metabotropic glutamate receptors in brain function and pathology. *Trends Pharmacol Sci, 14*(1), 13-20.

Schutt, J., Falley, K., Richter, D., Kreienkamp, H. J., & Kindler, S. (2009). Fragile X mental retardation protein regulates the levels of scaffold proteins and glutamate receptors in postsynaptic densities. *J Biol Chem, 284*(38), 25479-25487. doi:10.1074/jbc.M109.042663

Selby, L., Zhang, C., & Sun, Q. Q. (2007). Major defects in neocortical GABAergic inhibitory circuits in mice lacking the fragile X mental retardation protein. *Neurosci Lett, 412*(3), 227-232. doi:10.1016/j.neulet.2006.11.062

Sherman, S. M. (2014). The function of metabotropic glutamate receptors in thalamus and cortex. *Neuroscientist, 20*(2), 136-149. doi:10.1177/1073858413478490

Shigemoto, R., Kinoshita, A., Wada, E., Nomura, S., Ohishi, H., Takada, M., . . . Mizuno, N. (1997). Differential presynaptic localization of metabotropic glutamate receptor subtypes in the rat hippocampus. *J Neurosci, 17*(19), 7503-7522.

Shigemoto, R., Nakanishi, S., & Mizuno, N. (1992). Distribution of the mRNA for a metabotropic glutamate receptor (mGluR1) in the central nervous system: an in situ hybridization study in adult and developing rat. *J Comp Neurol, 322*(1), 121-135. doi:10.1002/cne.903220110

Silberberg, G., & Markram, H. (2007). Disynaptic inhibition between neocortical pyramidal cells mediated by Martinotti cells. *Neuron, 53*(5), 735-746. doi:10.1016/j.neuron.2007.02.012

Silverman, J. L., Pride, M. C., Hayes, J. E., Puhger, K. R., Butler-Struben, H. M., Baker, S., & Crawley, J. N. (2015). GABAB Receptor Agonist R-Baclofen Reverses Social Deficits and Reduces Repetitive Behavior in Two Mouse Models of Autism. *Neuropsychopharmacology, 40*(9), 2228-2239. doi:10.1038/npp.2015.66

Sinclair, D., Featherstone, R., Naschek, M., Nam, J., Du, A., Wright, S., . . . Siegel, S. J. (2017). GABA-B Agonist Baclofen Normalizes Auditory-Evoked Neural Oscillations and Behavioral Deficits in the Fmr1 Knockout Mouse Model of Fragile X Syndrome. *eNeuro, 4*(1). doi:10.1523/ENEURO.0380-16.2017

Sladeczek, F., Momiyama, A., & Takahashi, T. (1993). Presynaptic inhibitory action of a metabotropic glutamate receptor agonist on excitatory transmission in visual cortical neurons. *Proc Biol Sci, 253*(1338), 297-303. doi:10.1098/rspb.1993.0117

Slegtenhorst-Eegdeman, K. E., de Rooij, D. G., Verhoef-Post, M., van de Kant, H. J., Bakker, C. E., Oostra, B. A., . . . Themmen, A. P. (1998). Macroorchidism in FMR1 knockout mice is caused by increased Sertoli cell proliferation during testicular development. *Endocrinology, 139*(1), 156-162. doi:10.1210/endo.139.1.5706

Stafstrom, C. E. (2009). Severe epilepsy syndromes of early childhood: the link between genetics and pathophysiology with a focus on SCN1A mutations. *J Child Neurol, 24*(8 Suppl), 15S-23S. doi:10.1177/0883073809338152

Stern, E. A., Maravall, M., & Svoboda, K. (2001). Rapid development and plasticity of layer 2/3 maps in rat barrel cortex in vivo. *Neuron, 31*(2), 305-315.

Su, T., Fan, H. X., Jiang, T., Sun, W. W., Den, W. Y., Gao, M. M., . . . Yi, Y. H. (2011). Early continuous inhibition of group 1 mGlu signaling partially rescues dendritic spine abnormalities in the Fmr1 knockout mouse model for fragile X syndrome. *Psychopharmacology (Berl), 215*(2), 291-300. doi:10.1007/s00213-010-2130-2

Szabadics, J., Lorincz, A., & Tamas, G. (2001). Beta and gamma frequency synchronization by dendritic gabaergic synapses and gap junctions in a network of cortical interneurons. *J Neurosci, 21*(15), 5824-5831.

Tahvildari, B., Wolfel, M., Duque, A., & McCormick, D. A. (2012). Selective functional interactions between excitatory and inhibitory cortical neurons and differential contribution to persistent activity of the slow oscillation. *J Neurosci, 32*(35), 12165-12179. doi:10.1523/JNEUROSCI.1181-12.2012

Tai, C., Abe, Y., Westenbroek, R. E., Scheuer, T., & Catterall, W. A. (2014). Impaired excitability of somatostatin- and parvalbumin-expressing cortical interneurons in a mouse model of Dravet syndrome. *Proc Natl Acad Sci U S A, 111*(30), E3139-3148. doi:10.1073/pnas.1411131111

Tamaru, Y., Nomura, S., Mizuno, N., & Shigemoto, R. (2001). Distribution of metabotropic glutamate receptor mGluR3 in the mouse CNS: differential location relative to pre- and postsynaptic sites. *Neuroscience, 106*(3), 481-503.

Tanabe, Y., Masu, M., Ishii, T., Shigemoto, R., & Nakanishi, S. (1992). A family of metabotropic glutamate receptors. *Neuron, 8*(1), 169-179.

Tassone, F., Hagerman, R. J., Loesch, D. Z., Lachiewicz, A., Taylor, A. K., & Hagerman, P. J. (2000). Fragile X males with unmethylated, full mutation trinucleotide repeat expansions have elevated levels of FMR1 messenger RNA. *Am J Med Genet, 94*(3), 232-236.

Taylor, D. L., Jones, F., Kubota, E. S., & Pocock, J. M. (2005). Stimulation of microglial metabotropic glutamate receptor mGlu2 triggers tumor necrosis factor alpha-induced neurotoxicity in concert with microglial-derived Fas ligand. *J Neurosci, 25*(11), 2952-2964. doi:10.1523/JNEUROSCI.4456-04.2005

Thomas, A. M., Bui, N., Graham, D., Perkins, J. R., Yuva-Paylor, L. A., & Paylor, R. (2011). Genetic reduction of group 1 metabotropic glutamate receptors alters select behaviors in a mouse model for fragile X syndrome. *Behav Brain Res, 223*(2), 310-321. doi:10.1016/j.bbr.2011.04.049

Thomas, A. M., Bui, N., Perkins, J. R., Yuva-Paylor, L. A., & Paylor, R. (2012). Group I metabotropic glutamate receptor antagonists alter select behaviors in a mouse model for

fragile X syndrome. *Psychopharmacology (Berl), 219*(1), 47-58. doi:10.1007/s00213-011-2375-4

Till, S. M., Wijetunge, L. S., Seidel, V. G., Harlow, E., Wright, A. K., Bagni, C., . . . Kind, P. C. (2012). Altered maturation of the primary somatosensory cortex in a mouse model of fragile X syndrome. *Hum Mol Genet, 21*(10), 2143-2156. doi:10.1093/hmg/dds030

Turk, J., & Cornish, K. (1998). Face recognition and emotion perception in boys with fragile-X syndrome. *J Intellect Disabil Res, 42 (Pt 6)*, 490-499.

Veeraragavan, S., Bui, N., Perkins, J. R., Yuva-Paylor, L. A., Carpenter, R. L., & Paylor, R. (2011). Modulation of behavioral phenotypes by a muscarinic M1 antagonist in a mouse model of fragile X syndrome. *Psychopharmacology (Berl), 217*(1), 143-151. doi:10.1007/s00213-011-2276-6

Vislay, R. L., Martin, B. S., Olmos-Serrano, J. L., Kratovac, S., Nelson, D. L., Corbin, J. G., & Huntsman, M. M. (2013). Homeostatic responses fail to correct defective amygdala inhibitory circuit maturation in fragile X syndrome. *J Neurosci, 33*(17), 7548-7558. doi:10.1523/JNEUROSCI.2764-12.2013

Wahlstrom-Helgren, S., & Klyachko, V. A. (2015). GABAB receptor-mediated feed-forward circuit dysfunction in the mouse model of fragile X syndrome. *J Physiol, 593*(22), 5009-5024. doi:10.1113/JP271190

Wakita, M., Oyama, Y., Takase, Y., & Akaike, N. (2015). Modulation of excitatory synaptic transmission in rat hippocampal CA3 neurons by triphenyltin, an environmental pollutant. *Chemosphere, 120*, 598-607. doi:10.1016/j.chemosphere.2014.09.073

Wang, Q., Gao, E., & Burkhalter, A. (2011). Gateways of ventral and dorsal streams in mouse visual cortex. *J Neurosci, 31*(5), 1905-1918. doi:10.1523/JNEUROSCI.3488-10.2011

Wang, Q., Sporns, O., & Burkhalter, A. (2012). Network analysis of corticocortical connections reveals ventral and dorsal processing streams in mouse visual cortex. *J Neurosci, 32*(13), 4386-4399. doi:10.1523/JNEUROSCI.6063-11.201

Wang, L. W., Berry-Kravis, E., & Hagerman, R. J. (2010). Fragile X: leading the way for targeted treatments in autism. *Neurotherapeutics, 7*(3), 264-274. doi:10.1016/j.nurt.2010.05.005

Weiler, I. J., & Greenough, W. T. (1993). Metabotropic glutamate receptors trigger postsynaptic protein synthesis. *Proc Natl Acad Sci U S A, 90*(15), 7168-7171.

Weiler, I. J., Irwin, S. A., Klintsova, A. Y., Spencer, C. M., Brazelton, A. D., Miyashiro, K., . . . Greenough, W. T. (1997). Fragile X mental retardation protein is translated near synapses in response to neurotransmitter activation. *Proc Natl Acad Sci U S A, 94*(10), 5395-5400.

Wilson, B. M., & Cox, C. L. (2007). Absence of metabotropic glutamate receptor-mediated plasticity in the neocortex of fragile X mice. *Proc Natl Acad Sci U S A, 104*(7), 2454-2459. doi:10.1073/pnas.0610875104

Yan, Q. J., Asafo-Adjei, P. K., Arnold, H. M., Brown, R. E., & Bauchwitz, R. P. (2004). A phenotypic and molecular characterization of the fmr1-tm1Cgr fragile X mouse. *Genes Brain Behav, 3*(6), 337-359. doi:10.1111/j.1601-183X.2004.00087.x

Yan, Q. J., Rammal, M., Tranfaglia, M., & Bauchwitz, R. P. (2005). Suppression of two major Fragile X Syndrome mouse model phenotypes by the mGluR5 antagonist MPEP. *Neuropharmacology, 49*(7), 1053-1066. doi:10.1016/j.neuropharm.2005.06.004

Zhang, Y., Bonnan, A., Bony, G., Ferezou, I., Pietropaolo, S., Ginger, M., . . . Frick, A. (2014). Dendritic channelopathies contribute to neocortical and sensory hyperexcitability in Fmr1(-/y) mice. *Nat Neurosci, 17*(12), 1701-1709. doi:10.1038/nn.3864

Zhao, M. G., Toyoda, H., Ko, S. W., Ding, H. K., Wu, L. J., & Zhuo, M. (2005). Deficits in trace fear memory and long-term potentiation in a mouse model for fragile X syndrome. *J Neurosci, 25*(32), 7385-7392. doi:10.1523/JNEUROSCI.1520-05.2005

Zou, J., Jiang, J. Y., & Yang, J. J. (2017). Molecular Basis for Modulation of Metabotropic Glutamate Receptors and Their Drug Actions by Extracellular Ca2. *Int J Mol Sci, 18*(3). doi:10.3390/ijms18030672

CHAPTER II: MGLUR-MEDIATED MODULATION OF VISUAL NEOCORTICAL PYRAMIDAL CELL EXCITATION IN A FRAGILE X MOUSE

2.1 Introduction

Fragile X syndrome is a heritable disease of intellectual disability, and also the most common genetic cause of autism (Kaufman et al., 2004). It affects 1 in 4000 males and 1 in 8000 females (Hagerman et al., 2008), and causes moderate to severe intellectual impairment in all full mutation carriers. FXS also leads to a variety of neurological and psychiatric clinical manifestations include hypersensitivity to tactile stimuli, anxiety, mood instability, sleep disturbances, seizure disorder, and autistic features (Huber et al., 2002). Development of FXS occurs when the FMR1 gene, located on the X chromosome, is hypermethylated due to replication of CGG repeats (>200) in the 5' untranslated region. Hypermethylation of the gene subsequently leads to little or no production of the gene product FMRP. FMRP is expressed throughout most neurons, and is known to localize abundantly in dendrites, where it serves as a negative regulator of protein translation at the synapse (Antar et al., 2004). It has been shown to affect long term changes in synaptic efficacy, including long term potentiation (LTP) and long term depression (LTD). Exaggerated LTD, mediated by group I metabotropic glutamate receptors (mGluRs), in the *Fmr1* KO hippocampus and cerebellum is one of the hallmark pathophysiological changes observed in the *Fmr1* KO mouse (Huber et al., 2002). These plasticity studies led to the hypothesis that loss of FMRP leads to exaggeration of group I mGluR signaling, and this is the likely mediator of several seemingly different symptoms in FXS. Subsequently, over a decade of studies have shown that reduction of group I mGluR activation, both genetically and pharmacologically, leads to the restoration of hippocampal-mediated learning in mice on a variety of behavioral assessments (Dolen et al., 2007), as well as recovery

of abnormal synaptic morphology in the neocortex. Group I mGluRs have also been associated with epileptogenic activity in the *Fmr1* KO mouse. In mice, loss of FMRP leads to enhanced epileptogenic activity in hippocampal slices, and this activity is mediated by overactive group I mGluRs (Chuang et al., 2005). Taken together, these studies have built strong scientific support in favor of the role of group I mGluRs in the pathogenesis of Fragile X syndrome.

However, the extent to which group I mGluRs, and for that matter other mGluRs, mediate pathological neocortical mechanisms in Fragile X is currently unknown. Although several neocortical studies have demonstrated that loss of FMRP leads to altered synaptic plasticity it does so in a way that differs from that seen in the hippocampus and cerebellum. Thus, it is highly likely that the pathophysiological mechanisms plaguing the hippocampus, do not directly translate to other brain regions.

Understanding that a gap in knowledge exists regarding the role of neocortical mGluRs in the pathophysiology of FXS, I began my investigation of metabotropic receptor modulation in the visual neocortex of *Fmr1* KO mice. Previous studies have shown that the dendritic spine morphology in layer 5/6 visual neocortical neurons of the *Fmr1* KO mouse, mimic the immature spine morphology seen in Golgi-impregnated stains of human visual neocortical spines (Hinton et al., 1991; Irwin, Galvez, & Greenough, 2000; Irwin et al., 2001; Rudelli et al., 1985); this immature spine morphology can be rescued with genetic reduction of group I mGluRs in the *Fmr1* KO mouse (Dolen 2007). Further, published findings from our lab have shown that group I mGluR-mediated synaptic plasticity in layer 5/6 visual neocortical neurons is absent in the *Fmr1* KO mouse (Wilson & Cox, 2007). With this in mind, I hypothesized that group I mGluR-mediated modulation of layer 5/6 neocortical microcircuits are altered in FXS. Additionally, given the ever growing support of FMRP as a regulator of presynaptic mRNA translation (Akins

2009), I also investigated the effects of group II metabotropic glutamate receptors, as they are well-documented to exist abundantly at presynaptic terminals (Anwyl et al., 1999). Here, I show that group I and group II mGluRs modulate the postsynaptic membrane potential of visual neocortical pyramidal neurons, and that both of these glutamate receptors regulate synaptic transmission in the layer 5/6. I then determine that mGluR-mediated modulation of excitatory transmission onto pyramidal neurons is intact in the *Fmr1* KO mouse in both layer 5/6 and 2/3 of the primary visual neocortex.

2.2 Materials and Methods

All experimental procedures were performed in accordance with the National Institutes of Health *Guide for Care and Use if Laboratory Animals* and were approved by the Michigan State University Institutional Animal Care and Use Committee.

Mice on the FVB background (postnatal age 16-21 days) of either sex were anesthetized with isoflurane and perfused with cold, oxygenated (5% CO_2-95% O_2), modified saline prior to decapitation. Brains were removed and transferred to cold (4°C), oxygenated slicing solution containing the following (in mM): 2.5 KCl, 1.25 NaH_2PO_4, 10.0 $MgSO_4$, 0.5 $CaCl_2$, 26.0 $NaHCO_3$, 10.0 glucose, and 234.0 sucrose. Slices (300 μm thickness) were collected in a coronal plane were collected using a Leica vibrating tissue slicer, and then transferred to a holding chamber filled with oxygenated physiological saline containing (in mM): 126.0 NaCl, 2.5 KCl, 1.25 NaH_2PO_4, 2.0 $MgCl_2$, 2.0 $CaCl_2$, 26.0 $NaHCO_3$, and 10.0 glucose. Slices were incubated at 32 ± 1°C for at least 30 minutes, and then left to rest at room temperature for at least 30 minutes prior to recording.

Whole-cell intracellular recordings were obtained using a Zeiss microscope equipped with differential interface contrast optics (Zeiss, Thornwood, NY). Single slices were transferred

to a submersion chamber continuously superfused at 2.5ml/min with oxygenated physiological saline heated to 32◦C. Visual neocortex was identified with a low power (5x) objective and individual pyramidal neurons were identified using a water-immersion objective (63x). Pyramidal neurons were targeted by visual identification of pyramidal-shaped soma with a diameter greater than 20 μm, and confirmed by their characteristic electrophysiological properties as determined using an 800-2000 ms current step injection protocol. The majority of pyramidal neurons (62%) exhibit a regular spiking (RS) slowly adapting firing pattern, with a moderate sized late after-hyperpolarizing potential (AHP) and most often no visible early (AHP) or depolarizing afterpotential (DAP) (Chang and Luebke, 2007; Larkman and Mason; 1990). Another less common (5%), but easily distinguished electrophysiological profile of layer 5/6 pyramids was that of intrinsic bursting firing (IB) of 3-6 bursts of APs (Chang and Luebke, 2007; Larkman and Mason; 1990). For recordings, pipettes made of borosilicate capillary glass were pulled to tip resistances of 4-6MΩ and then filled with intracellular solution containing (in mM): 117.0 K-gluconate, 13.0 KCl, 1.0 MgCl2, 0.07 CaCl2, 0.1 EGTA, 10.0 HEPES, 2.0 Na2-ATP, 0.4 Na-GTP, and 0.2% biocytin. Only cells with a membrane potential ≥ -50 mV and overshooting action potentials were included for analysis. Access resistance was monitored throughout the experiments and recordings were not included if the access resistance increased to >20MΩ.

A. Membrane Potential Drug Application Protocol

For the membrane studies, membrane potential was recorded in current clamp mode. A series of metabotropic glutamate agonists were applied via bolus injection to determine the effects of mGluRs on the postsynaptic cell membrane potential. First, a general mGluR agonist (1S,3R)-1-Aminocyclopentane-1,3-dicarboxylic acid (ACPD) was applied (75 μM, 40 s). Upon

complete washout of the drug, specific mGluR agonists were applied for group I or group II mGluRs. The order of drug application of the specific agonists was varied to prevent convoluted drug effects. (RS)-3,5-dihydroxyphenylglycine (DHPG), a group I mGluR agonist, was applied for 30 seconds at 50 μM and allowed to completely washout before application of group II mGluR agonist, (2R,4R)-4-aminopyrrolidine-2,4-dicarboxylate (APDC, 75μM, 40 s). All recordings were done in the presence of tetrodotoxin (1μM) to isolate the postsynaptic response.

B. Stimulation Protocol

In layer 5/6 neuron recordings, excitatory postsynaptic currents (EPSCs) were evoked by electrical stimulation of afferents in layer 2/3 **(Figure 2.1, left panel)**. For layer 2/3 recordings, a stimulating electrode was placed in layer 4 of the visual neocortex **(Figure 2.1, right panel)**. For EPSC recordings, the chloride channel blocker, 4,4'-dinitrostilbene-2,2'-disulfonic acid (DNDS,1 mM) was included in the recording pipette to block postsynaptic chloride channels. $GABA_A$ receptors are chloride channels, and so DNDS blocks inhibitory postsynaptic currents (IPSCs) generated from these channels. We are thus able to effectively isolate EPSCs in the recorded neurons. Stimuli were delivered at 0.1 Hz, and the peak amplitudes of the evoked EPSC was measured before, during, and after washout of the selective group I and group II mGluR agonists, (RS)-3,5-dihydroxyphenylglycine (DHPG) and (2R,4R)-4-aminopyrrolidine-2,4-dicarboxylate (APDC) respectively.

All compounds used in this study were prepared from stock solutions and diluted to the final concentration with physiological saline prior to administration. All agonists were delivered by bolus injection to the central line of the recording chamber using a syringe pump. Based upon the calculated flow rate of the main line, the delivered drug concentration was estimated to be

one-fourth of the initial drug concentration. DNDS was purchased from Life Technologies, while all other compounds were purchased from Tocris and Sigma-Aldrich.

All recordings were acquired using a Multiclamp 700B amplifier (Molecular Devices). Data was filtered at 2.5 kHz and digitized at 10 kHz using pClamp software. For membrane potential experiments, 12 consecutive sweeps were averaged to determine the membrane potential at baseline and 3 consecutive sweeps were average during the maximal depolarizing or hyperpolarizing drug response. A positive drug response was defined as a change in membrane potential that was greater than 2 standard deviations of the baseline response. For evoked experiments, 12 consecutive sweeps (2 minutes) were averaged to determine the baseline peak amplitude of the synaptic response. The drug effect was determined as the average of 3 consecutive sweeps during the maximal drug response. A positive drug response was defined as a change in amplitude that was greater than 2 standard deviations of the baseline response. All data are reported as the mean ± SEM and analyzed using either paired or independent t-test were applicable. A p-value <0.05 was considered statistically significant.

2.3 Results

A. The intrinsic properties of Fmr1 KO pyramidal neurons are similar to wild type in layer 5/6 of the visual neocortex.

Prior to exploring the synaptic integrity of the visual neocortex in Fragile X Syndrome, we first set out to determine whether any differences in baseline intrinsic properties exist between WT and *Fmr1* KO mice pyramidal neurons. We performed current step protocols in layer 5/6 WT **(Figure 2.2Ai)** and *Fmr1* KO **(Figure 2.2Aii)** pyramidal neurons and looked at the current-voltage relationships to determine the input resistance. We also measured the resting membrane potential prior to current step injections. In control mice, layer 5/6 visual neocortical

pyramidal neurons have an average input resistance of 144.6 ± 10.8 MΩ (n=48; **Figure 2.2B**). *Fmr1* KO animals, showed a small increase in input resistance (175.149 ± 16.4 MΩ, n=47, **Figure 2.2B**), however, this increase was determined not to be significant ($p > 0.05$, t-test, **Figure 2.2B**). Next, we quantified the membrane potential of these neurons. In WT conditions, the average membrane potential at rest was -73.8 ± 0.5 mV (n=48, **Figure 2.2C**). *Fmr1* KO pyramidal neuron input resistance was -74.3 ± 0.7 mV, and this was statistically similar to layer 5/6 WT pyramidal cells ($p> 0.05$, independent t-test, **Figure 2.2C**). These results are summarized in the following table (**Table 2.1**).

Table 2.1. Intrinsic properties of layer 5/6 pyramidal neurons in WT and *Fmr1* KO mice.

	Input Resistance (MΩ)	***Membrane Potential (mV)***
Wild Type	*144.6 ± 10.8 (n=48)*	*-73.8 ± 0.5 (n=48)*
Fmr1 KO	175.1 ± 16.4 (n=47)	-74.3 ± 0.7 (n=47)
p	0.13 t-test	0.58 t-test

B. mGluR-mediated modulation of pyramidal neuron membrane potential is intact in the Fmr1 KO mouse.

We next asked how pharmacological activation of metabotropic glutamate receptors could modulate membrane potential. Specifically, we were interested in quantifying changes in the membrane potential of layer 5/6 pyramidal neurons in response to brief pharmacological activation of both general and specific mGluR agonists. Application of the general agonist, ACPD (75μM, 40s) in the presence of tetrodotoxin (TTX, 1μM) led to either depolarizations or hyperpolarizations in both WT and *Fmr1* KO pyramidal neurons **(Figure 2.3 Ai-ii)**. In WT neurons, 11 of 17 cells depolarized in the presence of ACPD, with the average depolarizing response amplitude measuring 3.3 ± 0.8 mV **(Figure 2.3Ai and 2.3B)**. In *Fmr1* KO mice,

pyramidal neuron depolarizations were of similar amplitude to WT neurons (8 of 20 cells, 3.3 ± 0.5 mV, p >0.05 t-test, **Figure 2.3Aii and 2.3B**). Hyperpolarizations to ACPD in WT neurons were larger in amplitude (6 of 17 cells, 7.1 ± 1.5 mV) on average than WT depolarizations but were seen less often than hyperpolarizations **(Figure 2.3B)**. This is in contrast to *Fmr1* KO neurons, where hyperpolarizations were more likely to be observed (11 of 20 cells). However, the amplitude of these hyperpolarizations (6.6 ± 1.2 mV) was not significantly different than WT cells (p>.05, independent t-test, **(Figure 2.3B**).

Next, to determine the specific metabotropic receptors underlying the variable responses to ACPD, we applied specific agonists of both group I and group II mGluRs **(Figure 2.3Ai-ii)**. Brief application of the specific group I mGluR agonist, (*RS*)-3,5-Dihydroxyphenylglycine (DHPG, 50 μM, 30s) led to depolarizations in both the WT (n=13) and *Fmr1* KO (n=16) pyramidal neurons **(Figure 2.3 Ai-ii)**. Comparison of response amplitudes across the two genotypes led to similar results (WT: 4.8 ± 0.8 mV, *Fmr1* KO: 4.5 ± 0.9 mV, p>.05, independent t-test, **Figure 2.3 B**). Interestingly, in the *Fmr1* KO mouse 5 cells failed to show a response to DHPG although all WT neurons had a significant drug response to DHPG.

Finally, to confirm the metabotropic source of the ACPD-induced membrane hyperpolarizations in these pyramidal neurons, we briefly applied specific group II mGluR agonist, (2*R*,4*R*)-4-Aminopyrrolidine-2,4-dicarboxylate (APDC, 75 μM, 40s). In the WT mouse, neurons hyperpolarized with a response amplitude of 2.4 ± 0.6 mV (n=11, **Figure 2.3 Ai**). The *Fmr1* KO pyramidal cells also hyperpolarized to APDC application, with an average response of 3.4 ± 0.7mV (n=15, **Figure 2.3 Aii**). Similar to our observations with group I agonists, application of APDC to *Fmr1* KO neurons led to a population of cells that failed to respond (n=6). In contrast, all WT cells tested had a significant drug response. These results determined

that group I and group II mGluRs postsynaptically alter the membrane potential of layer 5/6 pyramidal neurons. However, these postsynaptic effects of mGluRs are unaltered in the *Fmr1* KO. A summary of these results is reported in the table below.

Table 2.2. Layer 5/6 pyramidal neuron membrane potential responses to application of general mGluR agonist (ACPD) and specific mGluR I (DHPG) and II (APDC) agonists.

	ACPD		DHPG		APDC	
	WT	**KO**	**WT**	**KO**	**WT**	**KO**
Depolarizations	65% (11/17)	40% (8/20)	100% (13/13)	76% (16/21)	0% (0/11)	0% (0/21)
Hyperpolarizations	35% (6/17)	55% (11/20)	0% (0/13)	0% (0/21)	100% (11/11)	71% (15/21)
No change	0% (0/17)	5% (1/20)	0% (0/13)	24% (5/21)	0% (0/11)	29% (6/21)

C. Group I mGluRs do not modulate excitatory synaptic transmission onto visual neocortical pyramidal neurons in layer 5/6.

After determining whether intrinsic properties are affected in FXS, we next sought to investigate the mGluR-mediated modulation of synaptic transmission in layer 5/6 visual neocortical pyramidal neurons. To that end, we recorded evoked excitatory currents (EPSCs) from pyramidal neurons in both WT **(Figure 2.4 Ai)** and *Fmr1* KO mice **(Figure 2.4 Bi)**. We then quantified peak amplitude in the presence of specific mGluR agonist DHPG (25 μM, 30s). The baseline amplitude of evoked EPSCs in the WT was 181.5 ± 28.2 pA, and application of DHPG did not significantly alter EPSC amplitude (n=24, DHPG: 150.7 ± 21.8 pA, $p>0.05$, paired t-test, **Figure 2.4 Aii-iii**). In *Fmr1* KO neurons, DHPG also failed to alter EPSC amplitude (n=21, Pre: 230.8 ± 26.1 pA, DHPG: 210.4 ± 25.2 pA, $p>0.05$, paired t-test). **Figure 2.4 Bii-iii**). A comparison of the average EPSC amplitude response to DHPG between WT and

Fmr1 KO was not statistically significant. (WT: 86.8 ± 2.9 %, KO: 90.1 ± 3.0 %, p > 0.05, t-test, **Figure 2.4 C**).

D. *Group II mGluR activation leads to suppression of excitatory synaptic transmission onto layer 5/6 visual neocortical pyramidal neurons in the WT and Fmr1 KO mouse.*

The second mGluR agonist we tested, APDC (75μM, 40s), also decreased EPSC amplitude in WT **(Figure 2.5 Ai-iii)** and *Fmr1* KO **(Figure 2.5 Bi-iii)** pyramidal neurons, albeit the reduction was larger in magnitude than the decrease we observed upon activating group I mGluRs. In WT mice, the average baseline amplitude of the EPSC was 248.7 ± 28.7 pA (n=16, **Figure 2.5 C**), and APDC decreased this peak amplitude to 80.1 ± 9.8 pA. *Fmr1* KO neurons exhibited a similar decrease in EPSC amplitude that was not statistically different from control neurons (Pre: 221.4 ± 31.2 pA, APDC: 77.1 ± 13.3 pA, p>0.05, t-test, **Figure 2.5 C**).

E. The intrinsic properties of Fmr1 KO pyramidal neurons are similar to wild type in layer 2/3 of the visual neocortex.

We next recorded from layer 2/3 WT **(Figure 2.6 Ai)** and *Fmr1* KO **(Figure 2.6 Aii)** pyramidal neurons and quantified their input resistance and membrane potential from a current-step protocol. In the layer 2/3 of the visual neocortex, wild type pyramidal neurons had an increased input resistance relative to layer 5/6 WT pyramidal neurons (279.0 ± 32.2 MΩ, n=9, **Figure 2.6B**). A similar trend was observed in layer 2/3 *Fmr1* KO pyramidal neurons when compared to *Fmr1* KO layer 5/6 neurons (209.1 ± 30.2 MΩ, n=10, **Figure 2.6 B**). No notable differences were observed between WT and *Fmr1* KO layer 2/3 pyramidal neurons (p>0.05, t-test, **Figure 2.6 B**). The membrane potential of the superficial pyramidal neurons was more hyperpolarized relative to the layer 5/6 pyramidal neurons in both WT (n=9) and *Fmr1* KO (n=10) animals (WT: -83.5 ± 1.3 mV, *Fmr1* KO: -87.1 ± 1.4 mV, **Figure 2.6C**). Compared to

WT cells, the membrane potential observed in the *Fmr1* KO neurons was more hyperpolarized, and this was just outside of significance (p=0.07, t-test, **Figure 2.6 C**). For a summary of these results, see **Table 2.3**.

Table 2.3. Intrinsic properties of layer 2/3 pyramidal neurons in WT and *Fmr1* KO mice.

	Input Resistance (MΩ)	***Membrane Potential mV***
Wild Type	*279.7 ± 32.2 (n=9)*	*-83.5 ± 1.3 (n=9)*
Fmr1 KO	209.1 ± 30.2 (n=10)	-87.1 ± 1.4 (n=10)
p	0.13 t-test	0.07 t-test

F. Group I mGluRs do not modulate excitatory synaptic transmission onto visual neocortical pyramidal neurons in layer 2/3.

To determine whether the mGluR-mediated modulation of synaptic transmission we observed was unique to layer 5/6 pyramidal neurons, we next tested whether group I mGluRs modulate glutamatergic synaptic transmission in layer2/3 pyramidal neurons of WT and *Fmr1* KO mice (**Figure 2.7 Ai and Bi**). We recorded electrically evoked EPSCs in layer 2/3 of the visual neocortex with an electrode placed in layer 4 **(Figure 2.1)**. The average amplitude of the evoked response in wild type animals was 159.0 ± 17.7 pA (n=5), and brief application of specific mGluR I agonist DHPG (25 μM, 30s) reduced the peak amplitude of the response to 147.0 ± 17.9 pA (n=7, **Figure 2.7Aii-iii**). However, this decrease was not statistically significant (p>0.05, paired t-test). A similar trend was observed in the *Fmr1* KO mouse. The average pre-drug amplitude in the *Fmr1* KO was 333.0 ± 148.5 pA **(n=8, Figure 2.7Bii-iii)** and DHPG significantly reduced the EPSC amplitude (311.7 ± 138.8 pA, n=8, $p < 0.05$, paired t-test). We conclude that group I mGluRs do not modulate synaptic transmission in the layer 2/3.

G. Group II mGluR activation leads to suppression of excitatory synaptic transmission onto layer 2/3 visual neocortical pyramidal neurons in the WT and Fmr1 KO mouse.

In the case of specific group II mGluR agonist APDC, both WT and *Fmr1* KO pyramidal neurons EPSC were responsive (**2.8 Ai and Bi**). In WT neurons, pre-drug EPSC amplitude was 160.8 ± 35.4 pA (n=8) and application of APDC (75μM, 40s) produced a significant decrease in the response (41.3 ± 8.5 pA, n=8, $p < 0.05$, paired t-test, **Figure 2.8ii-iii**). For the *Fmr1* KO, average pre-drug amplitude of the EPSC was 350.8 ± 65.2 pA (n=7) and the post-drug response was significantly reduced (109.5 ± 30.3 pA, n=7, $p < 0.05$, paired t-test, **Figure 2.8 Bii-iii**). Statistical analysis determined that there were no significant differences in WT vs *Fmr1* KO drug response ($p > 0.05$, t-test, **Figure 2.8 C**).

2.4 Discussion

In our studies, we show that membrane potential and input resistance are similar in WT and *Fmr1* KO pyramidal neurons of the visual neocortex. A few studies have shown that juvenile layer 4 regular-spiking pyramidal neurons of the somatosensory cortex exhibit increased input resistance relative to wild type controls, with no difference in membrane potential (Zhang et al., 2016; Gibson et al., 2008). However, another study done in layer 2/3 determined that there were no changes in input resistance or membrane potential in pyramidal cells of the medial pre-frontal cortex (Meredith et al., 2007). We also report that neither the membrane potential or input resistance of pyramidal neurons in layer 5/6 or 2/3 are altered in the neocortex of the *Fmr1* KO mouse. While it may still be possible that pyramidal neuron intrinsic excitability is a contributing factor leading to visual neocortical hyperexcitability in FXS, we indicate that input resistance and membrane potential are intrinsic properties of these excitatory neurons that do not contribute to visual neocortical microcircuit alterations in the *Fmr1* KO.

We go on to demonstrate that activation of group I mGluRs lead to depolarizations of layer 5/6 pyramidal neuron postsynaptic membrane potentials. The magnitude of these depolarizations is normal in the *Fmr1* KO mouse. Although, previous literature suggests that group I mGluR-mediated postsynaptic LTD is exaggerated in the *Fmr1* KO mouse hippocampus (Huber et al., 2002), our data show that not all mGluR-mediated postsynaptic mechanisms are altered in the *Fmr1* KO. Thus we provide evidence of regional specificity of group I mGluRs in mediating dysfunction in the absence of FMRP. We also showed that group II mGluRs hyperpolarize the postsynaptic pyramidal cell membrane, and that this function is intact in the *Fmr1* KO mouse. Interestingly, in our membrane studies we found that a population of layer 5/6 pyramidal neurons in the *Fmr1* KO mouse were not responsive to the pharmacological glutamate receptor agonists that we used, even though all the WT cells we tested responded to the pharmacological agents. Any number of reasons could be proposed to explain these results, including impaired binding at mGluRs, preferential binding of the agonist to other neuron subtypes, or better clearing of mGluR agonist at the synapse in *Fmr1* KO animals.

We also show that group I mGluR agonist DHPG does not modulate fast excitatory transmission onto layer 5/6 pyramidal neurons in either wild type or *Fmr1* KO mice. In a minority of cells tested, DHPG was seen to reduce excitatory transmission by less than 25%, however the majority of cells tested showed no change. This is interesting given that DHPG yields long term depression in several brain regions, including the visual neocortex (Kirkwood 2005). We speculate that brief application of DHPG does not affect the dynamics of the excitatory response, but that it is the prolonged activation of group I mGluRs that leads to long-lasting alterations in fast excitatory transmission. We also tested the effects of group II mGluRs on the excitatory response, and activation of these receptors led to a strong suppression of

excitation onto pyramidal neurons. Group II mGluRs modulate fast excitatory transmission in several brain regions (Anwyl et al., 1999), and this mechanism is one means by which hyperexcitability can be prevented (Hovelso et al., 2012). Thus, we were interested in whether this mechanism is intact in the *Fmr1* KO mouse, and we determined that group II mGluR-mediated suppression of excitatory currents onto pyramidal neurons is comparable to that observed in the WT.

Although none of the parameters we tested in layer 5/6 pyramidal neurons were significantly altered in *Fmr1* KO mice, we set out to determine whether this was the case in layer 2/3. Indeed, it has been shown that *Fmr1* KO mice pyramidal neurons show greater spine densities in layer 2/3 in addition to layer 5/6 (Dolen et al., 2007, Irwin et al., 2000), and deficits in group I mGluR-mediated modulation of synaptic transmission onto neurons in layer 2/3 have been reported in the *Fmr1* KO (Paluskiewicz et al., 2011). With this information we set out to determine whether mGluR-mediated modulation of layer 2/3 pyramidal neurons is intact in the *Fmr1* KO, and we report that none of the parameters we tested were observably altered.

These experiments have shown the extent to which activation of group I and group II mGluRs alter the membrane potential of pyramidal neurons and the extent to which they modulate excitatory transmission onto these cells. We further demonstrated that the effects of both group I and group II mGluRs are intact in the *Fmr1* KO mouse. We add to the body of literature on the effects of group I mGluRs in the neocortex, while simultaneously investigating group II mGluR modulation in the neocortex in Fragile X. This investigation has not been done previously, despite evidence suggesting that group II mGluR pharmacology can restore exaggerated LTD in the hippocampus (Choi et al., 2007). The observation that these experiments yield no change between WT and *Fmr1* KO pyramidal neurons, does not exclude the possibility

that alterations of group I and group II mGluR signaling may still be contributing to hyperexcitability of V1 neuronal circuits. Inhibition is equally important in maintaining the excitatory/inhibitory balance of neocortical circuitry, and there are multiple different interneuron subtypes in the visual neocortex that accomplish this task. Thus, further studies must be done to investigate the role of mGluRs in modulating GABAergic cells in the visual neocortex (Chapter 3).

APPENDIX

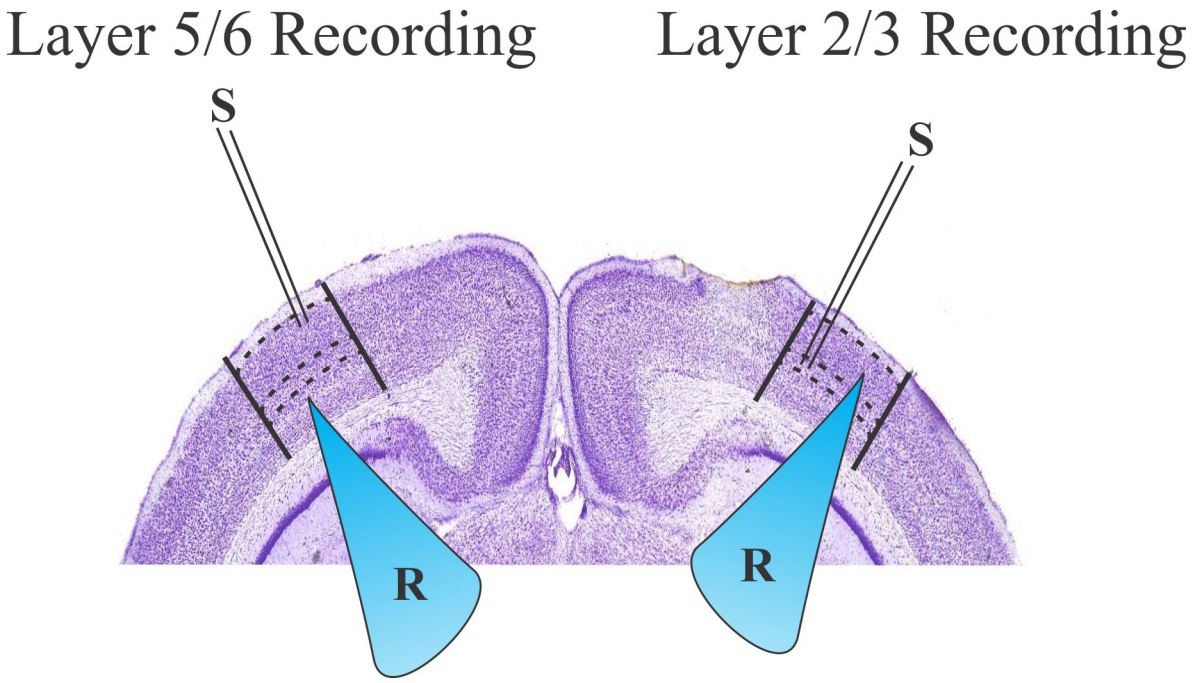

Figure 2.1. Schematic diagram of stimulation protocol.
For layer 5/6 recordings, a stimulating electrode was placed into layer 2/3 off-column, and neurons in layer 5/6 were recorded from in whole-cell patch clamp configuration. For layer 2/3 recordings, a stimulating electrode was placed into layer 4 off-column, and neurons in layer 2/3 were recorded from also in whole-cell patch clamp configuration.

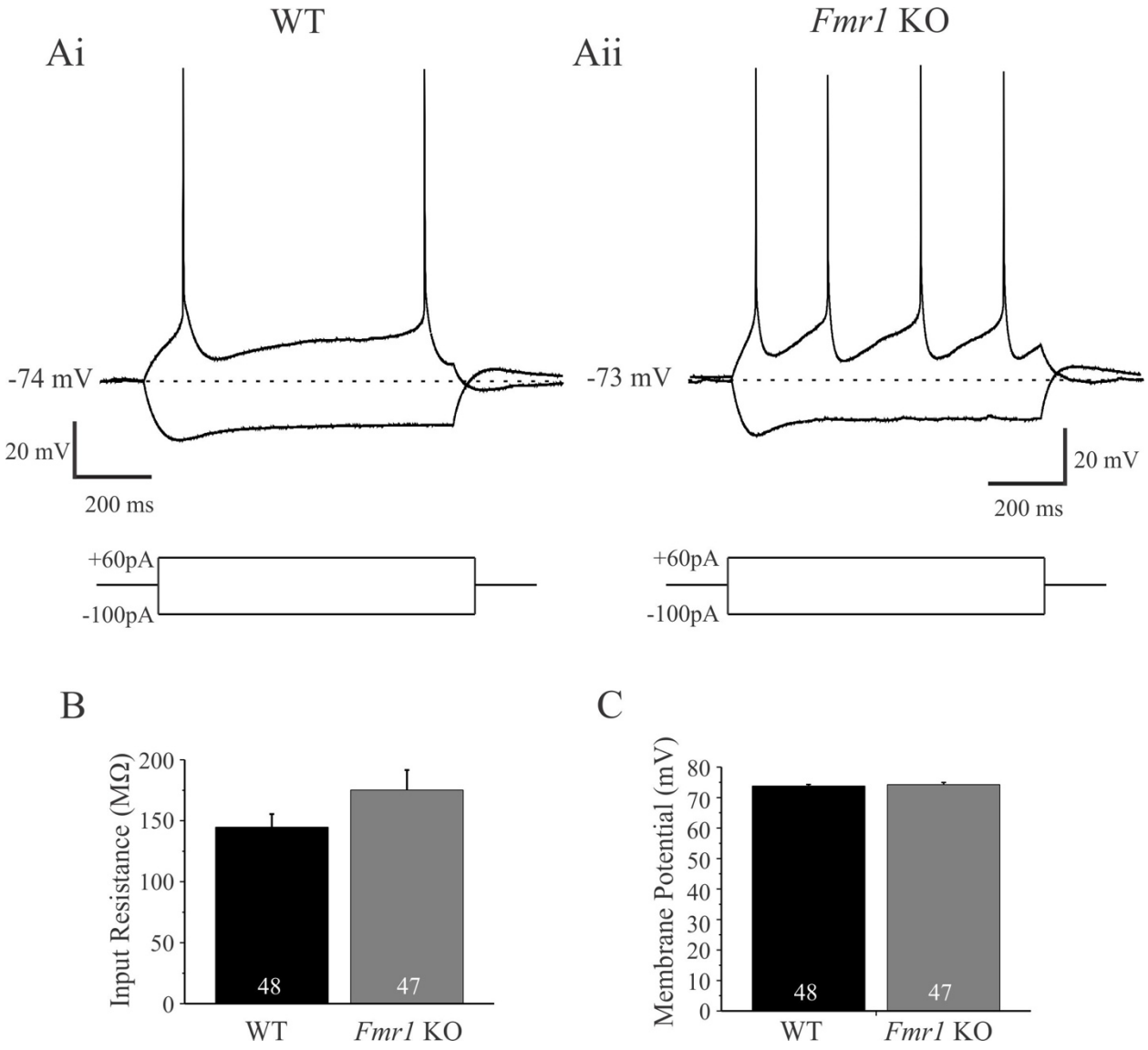

Figure 2.2. The intrinsic excitability of *Fmr1* KO pyramidal neurons is unaltered in layer 5/6 visual neocortex.

Figure Ai. Representative tracing of a wild type pyramidal cell during a current-step injection protocol. Aii. Similar to figure Ai but recorded in pyramidal neurons from the *Fmr1* KO mouse. B. Population data showing the average input resistance in wild type and *Fmr1* KO cells (WT=48, KO=47 $p > 0.05$, t-test). C. Population data showing the average membrane potential of wild type and *Fmr1* KO cells (WT=48, KO=47, $p > 0.05$, t-test)

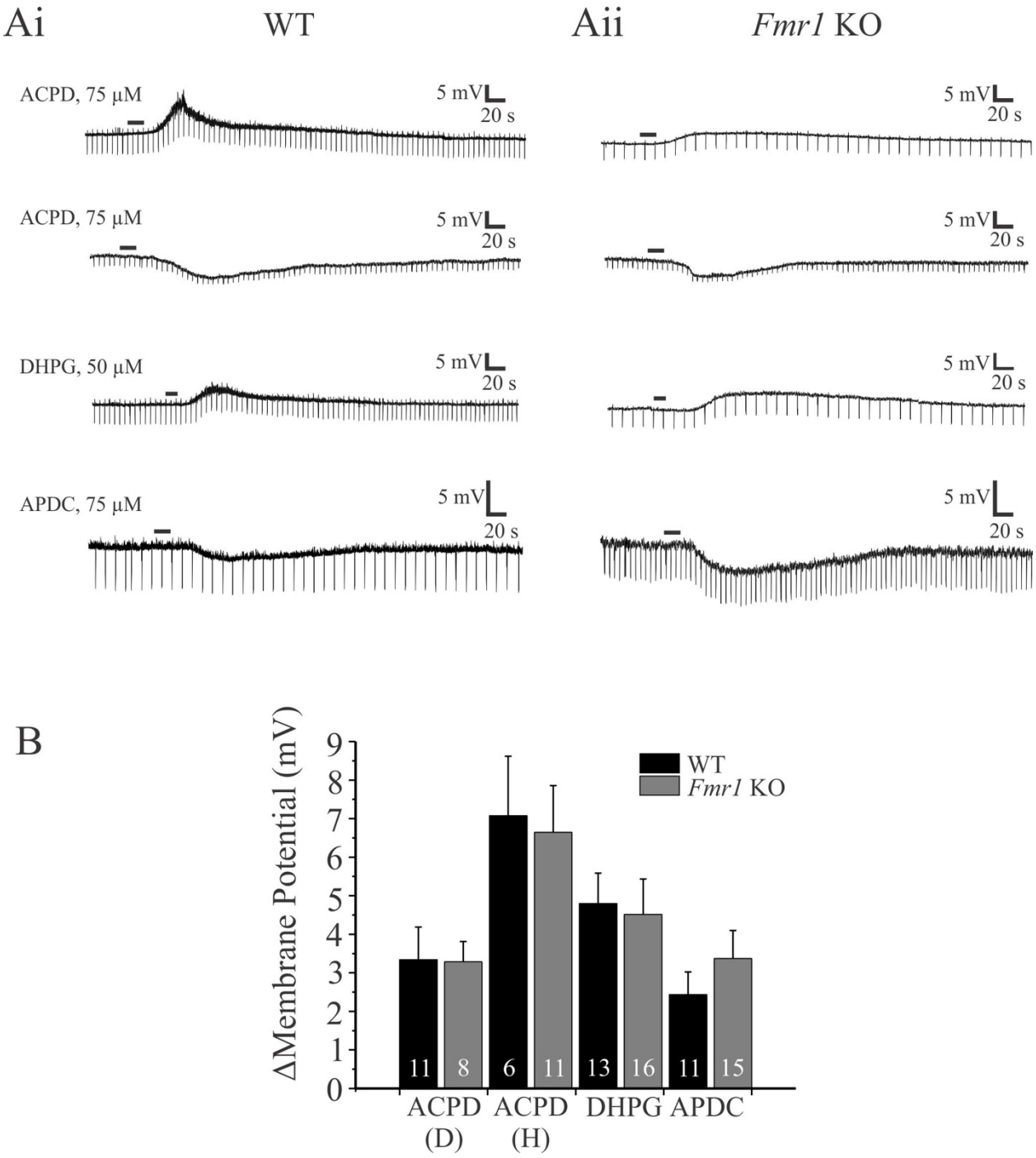

Figure 2.3. mGluR-mediated modulation of pyramidal neuron membrane potential is intact in layer 5/6 of the *Fmr1* KO mouse.

Ai. Wild type layer 5/6 pyramidal neuron membrane potential response to application of a general group I/II mGluR agonist (APDC) and specific agonists for either group I mGluRs (DHPG) or group II mGluRs (APDC). All experiments were done in the presence of TTX (1µM) to isolate the postsynaptic response. Aii. Same as Ai, but for layer 5/6 *Fmr1* KO pyramidal neurons. B. Graph showing population data for the change in membrane potential to various mGluR agonists in both WT an *Fmr1* KO mouse. Numbers are reported as absolute

Figure 2.3. (cont'd)

values. ACPD produced both depolarizations and hyperpolarizations in the WT and *Fmr1* KO. Group I mGluR agonist DHPG produced depolarizations, and group II mGluR agonist APDC produced hyperpolarizations. No statistically significant differences were observed between genotypes for any of the drug applications. ($p > 0.05$, t-test).

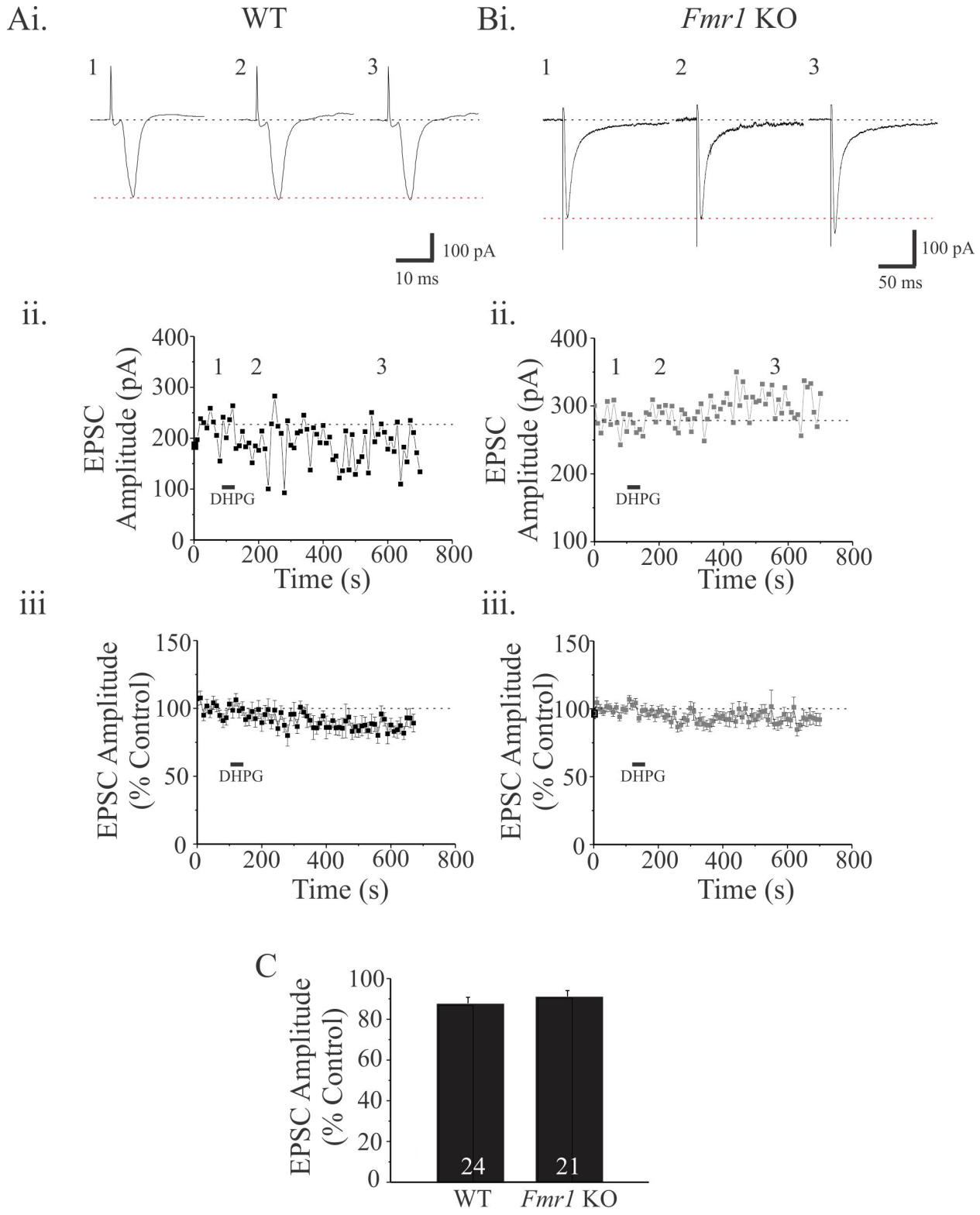

Figure 2.4. Group I mGluRs do not suppress excitatory synaptic transmission of layer 5/6 pyramidal neurons.

Figure 2.4. (cont'd)

Ai. Representative trace showing the response of a layer 5/6 wild type pyramidal neuron EPSC to brief application of group I mGluR agonist DHPG (25μM). Aii. Raw time course of the changes in peak amplitude in a single wild type pyramidal cell. Aiii. Wild type normalized time course of the population peak amplitude change (n=24). Bi-iii. Same as Ai-iii, but for *Fmr1* KO pyramidal neurons. C. Average EPSC amplitude expressed as % of control for all cells tested in both WT and *Fmr1* KO (WT=24, KO=21). A comparison of the EPSC amplitude of WT and *Fmr1* KO pyramidal neurons in the presence of DHPG found no significant differences ($P > 0.05$, t-test).

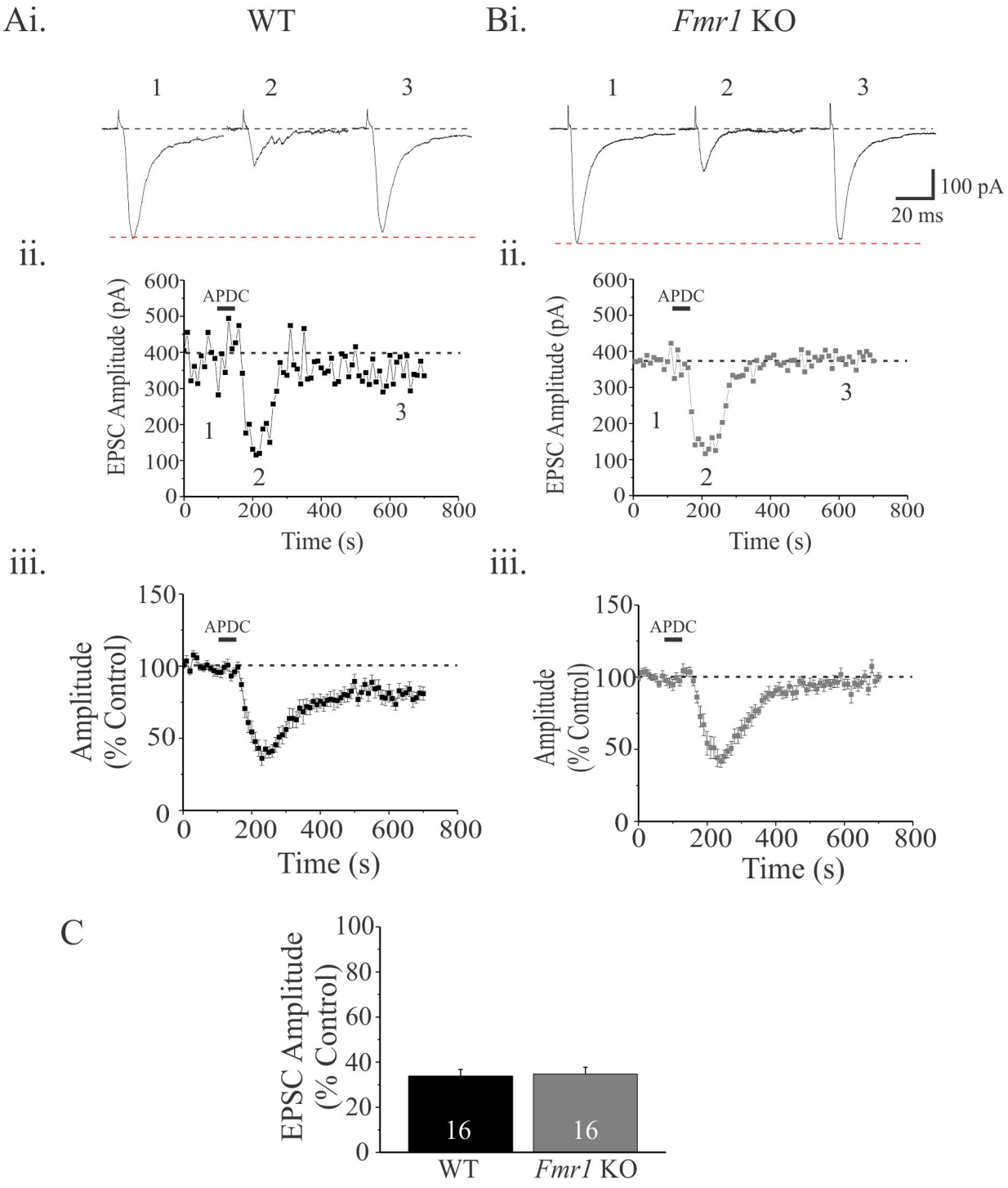

Figure 2.5. Group II mGluR activation leads to suppression of excitatory synaptic transmission onto layer 5/6 visual neocortical pyramidal neurons in the WT and *Fmr1* KO mouse.

Ai. Representative trace showing a wild type EPSC evoked by electrical stimulation of layer 2/3. Traces show wild type EPSC response before, during, and after brief application of APDC (75μM). Aii. Raw time course of the change in wild type EPSC amplitude before, during, and

Figure 2.5. (cont'd)

after APDC application. Aiii. WT population data showing the normalized time course of the change in peak amplitude in response to APDC (n=16). Bi-iii. Same as Ai-iii but for *Fmr1* KO. C. Average population EPSC amplitude in the presence of APDC expressed as percent of control for both wild type and *Fmr1* KO (WT=16, KO=16). No statistical differences were found between peak amplitude of WT and *Fmr1* KO in the presence of APDC ($p > 0.05$, t-test).

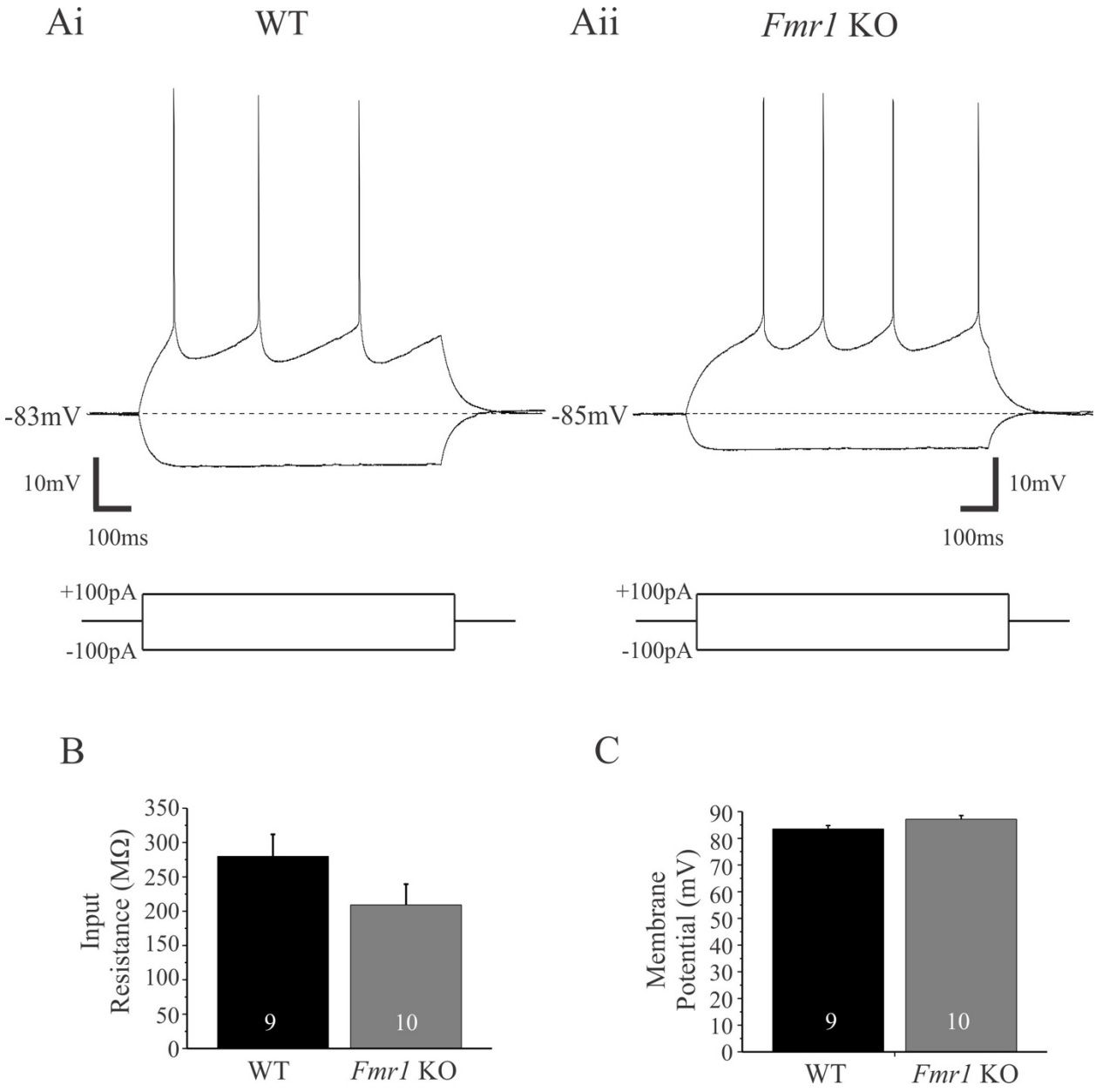

Figure 2.6. The intrinsic properties of *Fmr1* KO layer 2/3 pyramidal neurons are similar to wild type.

Ai. Representative tracing of a layer 2/3 wild type pyramidal cell during a current-step injection protocol. Aii. Similar to figure Ai but recorded in layer 2/3 pyramidal neurons from the *Fmr1* KO mouse. B. Population data showing the average input resistance in wild type and *Fmr1* KO cells (WT=9, KO=10, $p > 0.05$, t-test). C. Population data showing the average membrane potential of wild type and *Fmr1* KO cells (WT=9, KO=10 $p > 0.05$, t-test). No statistical differences between genotypes were observed for either input resistance or membrane potential ($p>0.05$, t-test).

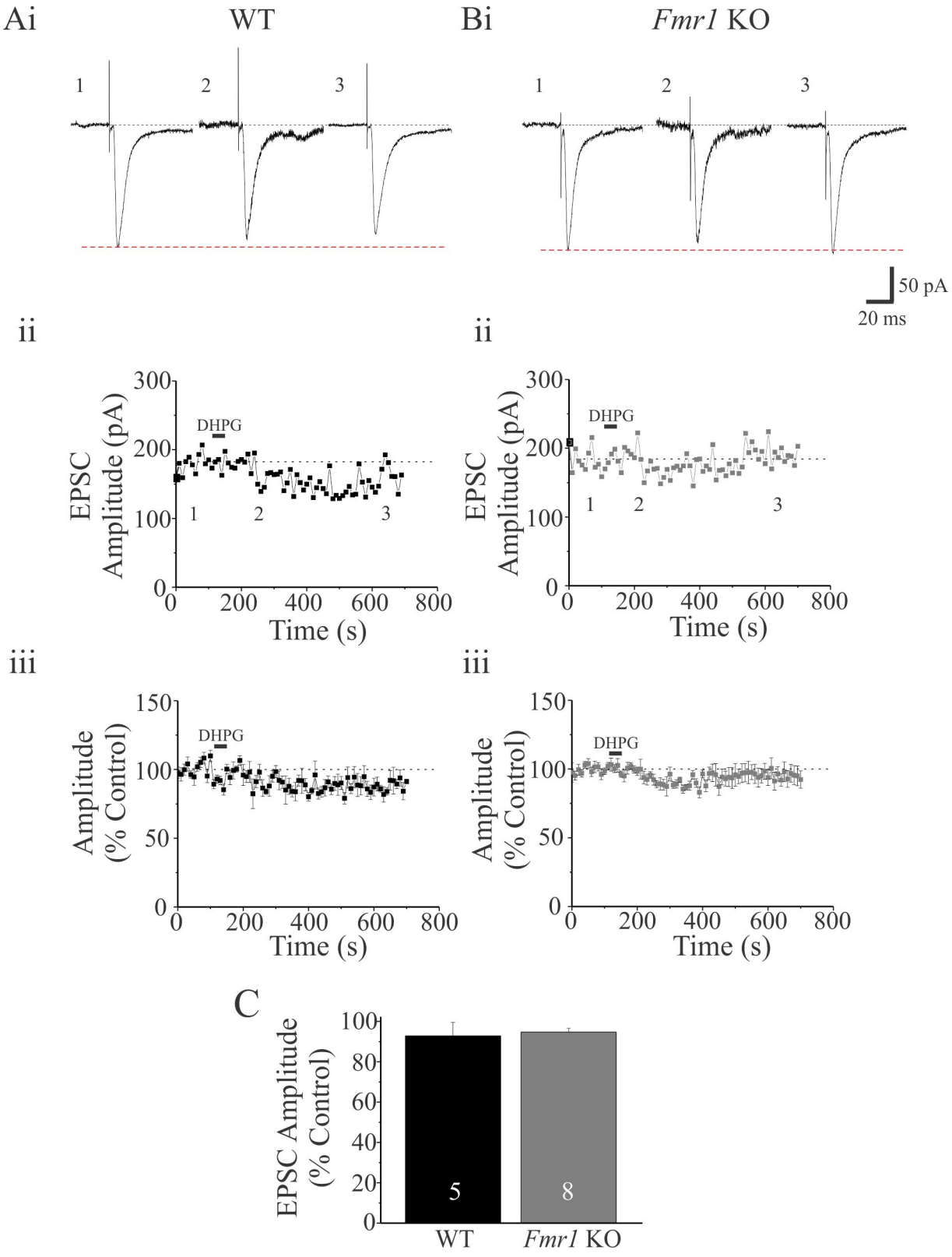

Figure 2.7. DHPG does not alter EPSCs in layer 2/3 pyramidal neurons from WT and *Fmr1* KO mice.

Figure 2.7. (cont'd)

Ai. Representative trace showing the response of a layer 2/3 wild type pyramidal neuron EPSC to brief application of group I mGluR agonist DHPG (25μM). Aii. Raw time course of the changes in peak amplitude in a single wild type pyramidal cell. Aiii. Wild type normalized time course of the population peak amplitude change (n=5). Bi-iii. Same as Ai-iii, but for *Fmr1* KO. C. Average EPSC amplitude expressed as % of control for all cells tested in both WT and *Fmr1* KO (WT=5, KO=8). Statistical comparison of peak amplitude change in response to DHPG shows no difference between wild type and *Fmr1* KO pyramidal neurons ($P > 0.05$, t-test).

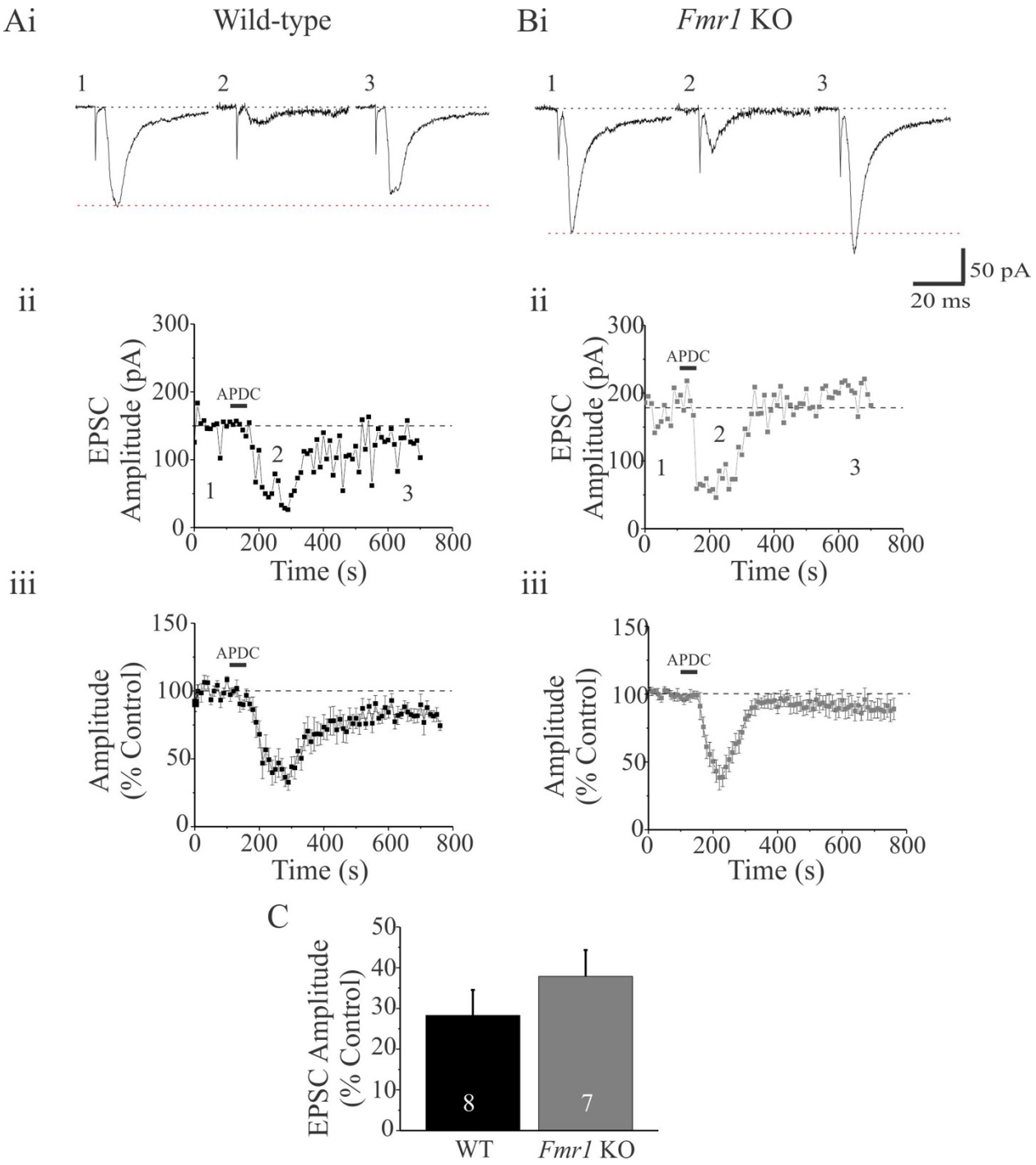

Figure 2.8. Group II mGluR activation leads to suppression of excitatory synaptic transmission onto layer 2/3 visual neocortical pyramidal neurons in the WT and *Fmr1* KO mouse.

Ai. Representative trace showing a layer 2/3 wild type pyramidal EPSC evoked by electrical stimulation of layer 2/3. Traces show wild type EPSC response before, during, and after brief application of APDC (75μM). Aii. Raw time course of the change in wild type EPSC amplitude before, during, and after APDC application. Aiii. WT population data showing the normalized

Figure 2.8. (cont'd)

time course of the change in peak amplitude in response to APDC (n=8). Bi-iii. Same as Ai-iii but for *Fmr1* KO (n=7). C. Average population EPSC amplitude in the presence of APDC expressed as % of control for both wild type and *Fmr1* KO (WT=8, KO=7). No statistical differences were found between peak amplitude of WT and *Fmr1* KO in the presence of APDC ($p > 0.05$, t-test).

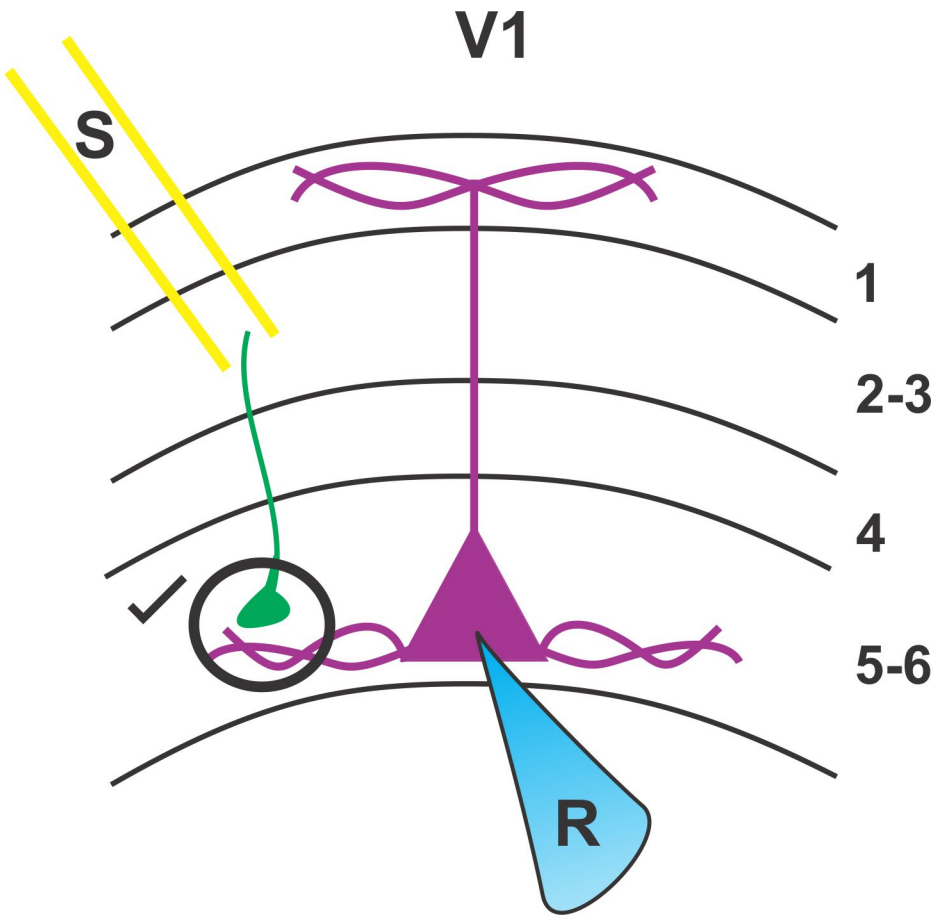

Figure 2.9. Group II mGluR-mediated suppression of EPSCs on pyramidal neurons is normal in the *Fmr1* KO mouse.
In chapter 2, excitatory postsynaptic currents (EPSCs) were evoked using a stimulating electrode placed in layer 2/3 (S). We show that activation of group II mGluRs leads to suppression of EPSCs at glutamatergic synapses onto layer 5/6 pyramidal neurons in both the WT and *Fmr1* KO (black circle). The magnitude of this suppression is similar between WT and *Fmr1* KO mouse (black checkmark).

REFERENCES

REFERENCES

Akins, M. R., Berk-Rauch, H. E., & Fallon, J. R. (2009). Presynaptic translation: stepping out of the postsynaptic shadow. *Front Neural Circuits, 3*, 17. doi:10.3389/neuro.04.017.2009

Antar, L. N., Afroz, R., Dictenberg, J. B., Carroll, R. C., & Bassell, G. J. (2004). Metabotropic glutamate receptor activation regulates fragile x mental retardation protein and FMR1 mRNA localization differentially in dendrites and at synapses. *J Neurosci, 24*(11), 2648-2655. doi:10.1523/JNEUROSCI.0099-04.2004

Anwyl, R. (1999). Metabotropic glutamate receptors: electrophysiological properties and role in plasticity. *Brain Res Brain Res Rev, 29*(1), 83-120.

Chang, Y. M., & Luebke, J. I. (2007). Electrophysiological diversity of layer 5 pyramidal cells in the prefrontal cortex of the rhesus monkey: in vitro slice studies. *J Neurophysiol, 98*(5), 2622-2632. doi:10.1152/jn.00585.2007

Choi, C. H., Schoenfeld, B. P., Bell, A. J., Hinchey, P., Kollaros, M., Gertner, M. J., . . . McBride, S. M. (2011). Pharmacological reversal of synaptic plasticity deficits in the mouse model of fragile X syndrome by group II mGluR antagonist or lithium treatment. *Brain Res, 1380*, 106-119. doi:10.1016/j.brainres.2010.11.032

Chuang, S. C., Zhao, W., Bauchwitz, R., Yan, Q., Bianchi, R., & Wong, R. K. (2005). Prolonged epileptiform discharges induced by altered group I metabotropic glutamate receptor-mediated synaptic responses in hippocampal slices of a fragile X mouse model. *J Neurosci, 25*(35), 8048-8055. doi:10.1523/JNEUROSCI.1777-05.2005

Dolen, G., Osterweil, E., Rao, B. S., Smith, G. B., Auerbach, B. D., Chattarji, S., & Bear, M. F. (2007). Correction of fragile X syndrome in mice. *Neuron, 56*(6), 955-962. doi:10.1016/j.neuron.2007.12.001

Gibson, J. R., Bartley, A. F., Hays, S. A., & Huber, K. M. (2008). Imbalance of neocortical excitation and inhibition and altered UP states reflect network hyperexcitability in the mouse model of fragile X syndrome. *J Neurophysiol, 100*(5), 2615-2626. doi:10.1152/jn.90752.2008

Hagerman, P. J. (2008). The fragile X prevalence paradox. *J Med Genet, 45*(8), 498-499. doi:10.1136/jmg.2008.059055

Hagerman, P. J., & Stafstrom, C. E. (2009). Origins of epilepsy in fragile X syndrome. *Epilepsy Curr, 9*(4), 108-112. doi:10.1111/j.1535-7511.2009.01309.x

Hinton, V. J., Brown, W. T., Wisniewski, K., & Rudelli, R. D. (1991). Analysis of neocortex in three males with the fragile X syndrome. *Am J Med Genet, 41*(3), 289-294. doi:10.1002/ajmg.1320410306

Hovelso, N., Sotty, F., Montezinho, L. P., Pinheiro, P. S., Herrik, K. F., & Mork, A. (2012). Therapeutic potential of metabotropic glutamate receptor modulators. *Curr Neuropharmacol, 10*(1), 12-48. doi:10.2174/157015912799362805

Huber, K. M., Gallagher, S. M., Warren, S. T., & Bear, M. F. (2002). Altered synaptic plasticity in a mouse model of fragile X mental retardation. *Proc Natl Acad Sci U S A, 99*(11), 7746-7750. doi:10.1073/pnas.122205699

Irwin, S. A., Idupulapati, M., Gilbert, M. E., Harris, J. B., Chakravarti, A. B., Rogers, E. J., . . . Greenough, W. T. (2002). Dendritic spine and dendritic field characteristics of layer V pyramidal neurons in the visual cortex of fragile-X knockout mice. *Am J Med Genet, 111*(2), 140-146. doi:10.1002/ajmg.10500

Irwin, S. A., Galvez, R., & Greenough, W. T. (2000). Dendritic spine structural anomalies in fragile-X mental retardation syndrome. *Cereb Cortex, 10*(10), 1038-1044.

Irwin, S. A., Patel, B., Idupulapati, M., Harris, J. B., Crisostomo, R. A., Larsen, B. P., . . . Greenough, W. T. (2001). Abnormal dendritic spine characteristics in the temporal and visual cortices of patients with fragile-X syndrome: a quantitative examination. *Am J Med Genet, 98*(2), 161-167.

Kaufmann, W. E., Cortell, R., Kau, A. S., Bukelis, I., Tierney, E., Gray, R. M., . . . Stanard, P. (2004). Autism spectrum disorder in fragile X syndrome: communication, social interaction, and specific behaviors. *Am J Med Genet A, 129A*(3), 225-234. doi:10.1002/ajmg.a.30229

Kirkwood, A., Rozas, C., Kirkwood, J., Perez, F., & Bear, M. F. (1999). Modulation of long-term synaptic depression in visual cortex by acetylcholine and norepinephrine. *J Neurosci, 19*(5), 1599-1609.

Larkman, A., & Mason, A. (1990). Correlations between morphology and electrophysiology of pyramidal neurons in slices of rat visual cortex. I. Establishment of cell classes. *J Neurosci, 10*(5), 1407-1414.

Meredith, R. M., Holmgren, C. D., Weidum, M., Burnashev, N., & Mansvelder, H. D. (2007). Increased threshold for spike-timing-dependent plasticity is caused by unreliable calcium signaling in mice lacking fragile X gene FMR1. *Neuron, 54*(4), 627-638. doi:10.1016/j.neuron.2007.04.028

Paluszkiewicz, S. M., Olmos-Serrano, J. L., Corbin, J. G., & Huntsman, M. M. (2011). Impaired inhibitory control of cortical synchronization in fragile X syndrome. *J Neurophysiol, 106*(5), 2264-2272. doi:10.1152/jn.00421.2011

Rudelli, R. D., Brown, W. T., Wisniewski, K., Jenkins, E. C., Laure-Kamionowska, M., Connell, F., & Wisniewski, H. M. (1985). Adult fragile X syndrome. Clinico-neuropathologic findings. *Acta Neuropathol, 67*(3-4), 289-295.

Zhang, Y., Bonnan, A., Bony, G., Ferezou, I., Pietropaolo, S., Ginger, M., . . . Frick, A. (2014). Dendritic channelopathies contribute to neocortical and sensory hyperexcitability in Fmr1(-/y) mice. *Nat Neurosci, 17*(12), 1701-1709. doi:10.1038/nn.3864

CHAPTER III: MGLUR-MEDIATED MODULATION OF VISUAL NEOCORTICAL PYRAMIDAL CELL INHIBITION IN A FRAGILE X MOUSE

3.1 Introduction

Fragile X Syndrome is a genetic form of intellectual disability (Hagerman et al., 2009). Studies using an *Fmr1* KO mouse, have uncovered a wide array of defects with glutamatergic transmission. However, less is known about the effects of loss of FMRP on GABAergic transmission, particularly as it pertains to neocortex, where interneurons comprise 20% of all cells (Rudy et al., 2011). Most neocortical studies on GABA dysfunction have looked at mRNA expression of $GABA_A$ subunits. $GABA_A$ receptors mediate fast ionotropic inhibitory transmission, and any changes in the expression level of $GABA_A$ subunits would be hypothesized to affect inhibitory function at the synapse. Several studies in the *Fmr1* KO show decreased mRNA levels of $GABA_A$ subunits in the hippocampus and neocortex of Fragile X mice (Gantois, I. et al, 2006; Hong, et al 2012). This underexpression includes the subunits α1, β2, and γ2, which together comprise the most abundant $GABA_A$ receptor in the CNS. Protein expression of $GABA_A$ subunits has also been shown to be reduced in the neocortex, hippocampus, diencephalon, and brainstem of *Fmr1* KO mice (El Idrissi et al., 2005, Adusei et al., 2010). Additionally, mRNA expression of proteins important for GABA synthesis, transport, and degradation, have been shown to be decreased in both the neocortex and cerebellum (D'Hulst et al. 2008). Despite these results, we still have no idea what the functional consequences are of underexpression of neocortical GABAergic compounds in the *Fmr1* KO. The electrophysiological studies investigating functional changes in GABAergic signaling to-date have documented both increases and decrease in tonic inhibition that appear to be dependent on the brain region under examination. Increases in the frequency of spontaneous and miniature

inhibitory currents have been reported in the subiculum (Centonze et al., 2008), indicating an increase in tonic inhibition. However, decreased tonic inhibition has also been reported in the subiculum (Curia et al., 2009), amygdala (Olmos-Serrano, et al., 2010; Martin et al., 2014), and hippocampus (Sabonov et al., 2017). Phasic inhibition has also been shown to be decreased in the amygdala (Olmos-Serrano et al., 2010). Although we would expect that the decreased expression of $GABA_A$ subunits in the neocortex might lead to decreased inhibition in the neocortex, that question remains unanswered due to the lack of electrophysiological studies on GABAergic transmission in neocortex. While deficits in excitatory drive onto interneurons in the somatosensory neocortex have been reported (Gibson et al., 2008; Paluszkiewicz et al., 2011), no changes in neocortical GABAergic transmission have been reported (Gibson et al., 2008). This is interesting considering another study showed a significant decrease in the density of FS interneurons in the somatosensory cortex, as well as altered laminar distributions of these neurons (Selby, Zhang & Sun, 2006). Clearly, more electrophysiological studies need to be done before we understand what is happening to GABAergic transmission in the neocortex.

In Chapter 2, I previously determined that mGluR-mediated modulation of glutamatergic transmission onto pyramidal neurons is unaltered in the layer 5/6 visual neocortex of the *Fmr1* KO mouse. Given that several human studies suggest that the neocortex is hyperexcitable in FXS, it is possible that hyperexcitable neocortical circuitry occurs due to defective inhibition rather than enhanced excitation. In the neocortex, mGluRs have been shown to modulate GABAergic transmission (Sladeczek et al., 2016; Liu, Petrof & Sherman, 2014). Since mGluRs are heavily implicated in the pathogenesis of the Fragile X mouse model, I hypothesize that mGluR-mediated modulation of GABAergic neurotransmission in the layer 5/6 neocortex is altered in the *Fmr1* KO mouse. Group II mGluRs, in particular seem to be extremely effective at

suppressing neurotransmission at both glutamatergic and GABAergic synapses (Liu, Petrof, & Sherman, 2014; Flavin, Jin & Daw., 2000). Consequently, in this chapter I focused on the effects of group II mGluRs in modulating GABAergic transmission. I recorded inhibitory currents from pyramidal neurons before, during, and after application of a group II mGluR agonist in an attempt to observe and quantify changes in the amplitude of this response in the *Fmr1* KO. I also determined the location of group II mGluRs at GABAergic interneuron synapses onto pyramidal cells.

3.2 Materials and Methods

All experimental procedures were performed in accordance with the National Institutes of Health *Guide for Care and Use if Laboratory Animals* and were approved by the Michigan State University Institutional Animal Care and Use Committee.

Mice on the FVB background (postnatal age 16-21 days) of either sex were anesthetized with isofluorane and perfused with cold, oxygenated (5% CO_2-95% O_2), modified saline prior to decapitation. Brains were removed and transferred to cold (4°C), oxygenated slicing solution containing the following (in mM): 2.5 KCl, 1.25 NaH_2PO_4, 10.0 $MgSO_4$, 0.5 $CaCl_2$, 26.0 $NaHCO_3$, 10.0 glucose, and 234.0 sucrose. Slices (300 μm thickness) were collected in a coronal plane were collected using a Leica vibrating tissue slicer, and then transferred to a holding chamber filled with oxygenated physiological saline containing (in mM): 126.0 NaCl, 2.5 KCl, 1.25 NaH_2PO_4, 2.0 $MgCl_2$, 2.0 $CaCl_2$, 26.0 $NaHCO_3$, and 10.0 glucose. Slices were incubated at 32 ± 1°C for at least 30 minutes, and then left to rest at room temperature for at least 30 minutes prior to recording.

Whole-cell recordings were obtained using a microscope equipped with differential interface contrast optics (Zeiss, Thornwood, NY). Single slices were transferred to a submersion

chamber continuously superfused at 2.5ml/min with oxygenated physiological saline heated to 32˚C. Visual neocortex was identified with a low power (5x) objective and individual neurons were identified using a water-immersion objective (63x). Pyramidal neurons were identified through preferential targeting of pyramidal-shaped soma with a diameter greater than 20 μm. The majority of pyramidal neurons (62%) exhibit a regular spiking (RS) slowly adapting firing pattern, with a moderate sized late after-hyperpolarizing potential (AHP) and most often no visible early (AHP) or depolarizing afterpotential (DAP) (Chang and Luebke, 2007; Larkman and Mason; 1990). Another less common (5%), but easily distinguished electrophysiological profile of layer 5/6 pyramids was that of intrinsic bursting firing (IB) of 3-6 bursts of APs (Chang and Luebke, 2007; Larkman and Mason; 1990). For recordings, pipettes made of borosilicate capillary glass were pulled to tip resistances of 4-6MΩ and then filled with a cesium-based intracellular solution containing (in mM): 117.0 Cs-gluconate, 13.0 CsCl, 1.0 $MgCl_2$, 0.07 $CaCl_2$, 0.1 EGTA, 10.0 HEPES, 2.0 Na_2-ATP, and 0.4 Na-GTP. Only cells with a membrane potential ≥ -50 mV and overshooting action potentials were included for analysis. Access resistance was monitored throughout the experiments and recordings were not included if the access resistance increased to >20MΩ.

In recordings from layer 5/6 pyramidal neurons, inhibitory postsynaptic currents (IPSCs) were evoked by electrical stimulation of afferents in layer 2/3 (**Figure 2.1, left panel**). Stimuli were delivered at 0.1 Hz, and the peak amplitude of the evoked IPSC was measured before, during, and after washout of the selective group II mGluR agonist, (2R,4R)-4-aminopyrrolidine-2,4-dicarboxylate (APDC). Spontaneous IPSCs (sIPSCs) and miniature IPSCs (mIPSCs) were recorded in the absence of electrical stimulation while the cell was held at 0 mV. mIPSCs were recorded in the presence of tetrodotoxin (1μM).

All compounds used in this study were prepared from stock solutions stored at the appropriate temperature and diluted to the correct concentration with physiological saline prior to administration. APDC was delivered by bolus injection to the central line of the recording chamber using a syringe pump. Antagonist application was applied in the bath physiological saline. Based upon the calculated flow rate of the main line, the delivered drug concentration was estimated to be one-fourth of the initial drug concentration. All compounds were purchased from Tocris and Sigma-Aldrich.

All recordings were acquired using a Multiclamp 700B amplifier (Molecular Devices). Data was filtered at 2.5 kHz and digitized at 10 kHz using pClamp software. For evoked experiments, 12 consecutive sweeps (2 minutes) were averaged to determine the IPSC baseline peak amplitude of the synaptic response. The drug effect was determined as the average of 3 consecutive sweeps during the maximal drug response. A positive drug response was defined as a change in amplitude that was greater than 2 standard deviations of the baseline response. The frequency and amplitude of spontaneous and miniature IPSCS were analyzed using MiniAnalysis software (Synaptosoft). Kolmogorov-Smirnoff tests were used within cells to determine if sIPSC and mIPSC frequency and/or amplitude were altered by drug application. All data are reported as the mean ± SEM and analyzed using either paired or independent t-test were applicable. A p-value <0.05 was considered statistically significant.

3.3 Results

A. Group II mGluR-mediated suppression of IPSCs on layer 5/6 pyramidal neurons is exaggerated in the Fmr1 KO mouse.

To determine whether activation of group II mGluRs leads to altered GABAergic inhibition onto pyramidal neurons in the *Fmr1* KO, whole cell patch clamp recordings were

obtained from layer 5/6 pyramidal neurons in the visual neocortex of WT (**Figure 3.1 Ai**) and *Fmr1* KO animals (**Figure 3.1 Bi**). A cesium based internal solution and a holding potential of 0 mV were used to optimize recordings of inhibitory postsynaptic currents (IPSCs). Synaptic responses were evoked using a bipolar stimulating electrode inserted into layer 2/3. In WT animals (n=16), the baseline ISPC averaged 1333.2 ± 143.9 pA. Following application of APDC (75 μM, 40 s), the IPSC was reduced to 685.4 ± 117.1 pA, and this decrease was statistically significant ($p<0.001$, paired t-test, **Figure 3.1 Aii-iii**). In neurons from *Fmr1* KO animals, APDC also significantly suppressed the IPSC (Pre-drug: 959.7 ± 121.3 pA; APDC: 272.5 ± 65.6 pA, n=8, $p<0.001$, paired t-test, **Figure 3.1 Bii-iii**). The average amplitude of the WT IPSC upon application of APDC was 45.3 ± 5.5 % of the control IPSC amplitude, while the *Fmr1* KO was 26.4 ± 5.3 % of the control response, indicating a suppression of the IPSC in the *Fmr1* KO that was nearly 20% larger than the WT. This difference was determined to be statistically significant ($p=0.023$, t-test, **Figure 3.1C**). Thus, we show that activation of group II mGluRs leads to increased suppression of inhibition onto pyramidal neurons in the *Fmr1* KO.

B. In the absence of excitatory drive onto interneurons, group II mGluR-mediated suppression of IPSCs is normal in the Fmr1 KO mouse.

Is the increased suppression of inhibitory currents we observe in *Fmr1* KO pyramidal neurons due to the presence of group II mGluRs at GABA synapses? To answer this question, we next sought to record evoked inhibitory currents in the presence of 3-(2- carboxypiperazin-4-yl)-propyl-1-phosphonic acid (CPP, 20 μM) and 6,7-dinitroquinoxaline-2,3-dione (DNQX, 40 μM) to isolate interneuron synapses onto pyramidal neurons. In the presence of CPP and DNQX, APDC significantly reduced the amplitude of the IPSCs in WT cells (**Figure 3.2 Ai**). The average baseline response of the IPSC was 439.3 ± 104.4 pA. Following application of

APDC, this response decreased to 314.1 ± 83.8 pA (n=9, p<0.05, paired t-test, **Figure 3.2 Aii-iii**). In *Fmr1* KO pyramidal neurons, the average baseline response in the presence of CPP and DNQX was 122.2 ± 27.7 pA, and APDC decreased this amplitude to 60.7 ± 9.3 pA (n=4, p<0.05, paired t-test, **Figure 3.2 Bii-iii**). A comparison of the IPSC amplitude in response to APDC expressed as a % of the control response, was made between WT and *Fmr1* KO. No statistical differences were observed between genotypes (WT: 69.5 ± 5.9 %; *Fmr1* KO: 52.9 ± 6.0%, p>0.05, t-test, **Figure 3.2 C)**. These data indicate that group II mGluRs directly modulate GABAergic transmission in layer 5/6 of the visual neocortex. Furthermore, the exaggerated inhibition of pyramidal neurons by group II mGluRs is not caused by direct changes in GABAergic transmission onto pyramidal neurons.

C. Suppression of IPSCs onto pyramidal neurons is due to either pre- or post- synaptic group II mGluRs.

We show group II mGluRs directly modulate GABAergic transmission in layer 5/6 of the visual neocortex. However, we do not know where these mGluRs are located at GABAergic synapses. To locate the group II mGluRs we first recorded spontaneous IPSCs in layer 5/6 pyramidal neurons (**Figure 3.3 Ai and Bi**). In the WT mouse, 3 of 5 cells showed a statistically significant change in sIPSC amplitude in response to brief application of APDC (K.S. test, $p < 0.05$, **Figure 3.3 Aii**). The average baseline amplitude of sIPSCs was 27.5 ± 2.1 pA, and application of APDC reduced the average amplitude to 26.5 ± 2.6 pA (n=5). This results in a response amplitude that is 96.1 ± 2.7 % of the control amplitude (**Figure 3.3 C**). In the *Fmr1* KO, a similar observation was made. In 6 of 10 cells, APDC significantly decreased the amplitude of the sIPSC, from an average baseline of 29.5 ± 2.0 pA, to a post-drug average of 27.2 ± 1.7 pA (K.S. test, $p < 0.05$, **Figure 3.3 Bii**). This led to a response amplitude that was, on

average, 92.7 ± 2.0 % of the control response (**Figure 3.3C**). A comparison of WT and *Fmr1* KO sIPSCs determined that there was no significant difference in the amplitude between genotypes (WT: 96.1 ± 2.7 %, *Fmr1* KO: 92.7 ± 2.0 %, $p > 0.05$, t-test, **Figure 3.3 C**). The average frequency of WT sIPSCs was also significantly decreased by APDC application (4 of 5 cells, $p < 0.05$, K.S. test, **Figure 3.3 Aiii**). APDC reduced sIPSC frequency from 17.6 ± 5.5 Hz to 14.4 ± 4.9 Hz (n=5). In the *Fmr1* KO, APDC reduced the average sIPSC frequency from 17.0 ± 4.7 Hz to 14.4 ± 4.1 Hz (n=10, $p < 0.05$, K.S. test, **Figure 3.3 Biii**). Comparison of the average event frequency expressed as % of control for both WT and *Fmr1* KO determined that there were no significant differences between genotypes (WT: 77.1 ± 6.6 %, *Fmr1* KO: 84.4 ± 2.0 %, $p > 0.05$, t-test, **Figure 3.3 D**). From these data, we cannot conclude where the suppression of sIPSCs is occurring at the GABA synapse upon activation of group II mGluRs.

To better assess the location of the group II mGluR effect at GABA synapses, we next recorded miniature IPSCs in the presence of TTX to isolate AP-independent release from the terminals of interneuron inputs onto pyramidal neurons of WT and *Fmr1* KO mice. In the presence of TTX, APDC significantly decreased mIPSC amplitude in 3 of 8 wild type cells (K.S. test, $p<0.05$, **Figure 3.4Ai**). Pooled data show that the average mIPSC amplitude of all wild type cells was 31.1 ± 3.6 pA, and after APDC this amplitude was not significantly different (n=8, APDC: 31.4 ± 4.7 pA, $p>0.05$, paired t-test, **Figure 3.4 Aii**). In the presence of APDC, all 8 WT cells tested showed a significant decrease in the frequency of the response ($p<0.05$, K.S. test). A pooled average from all WT pyramidal neurons, showed that mIPSC frequency decreased in response to group II mGluR activation (Pre-drug: 9.9 ± 1.7 Hz, APDC: 7.8 ± 1.6 Hz, $p<0.05$, paired t-test, **Figure 3.4 Aiii**). In *Fmr1* KO pyramidal neurons, mIPSC amplitude also decreased in the presence of APDC (**Figure 3.4 Bi**). Specifically, 5 of 12 *Fmr1* KO cells show a

statistically significant decrease in mIPSC amplitude ($p<0.05$, K.S. test). The pooled amplitude of all mIPSCs for the *Fmr1* KO was 27.7 ± 2.2 pA, and APDC did not change the amplitude of this response (n=12, APDC: 26.8 ± 2.1 pA, $p>0.05$, paired t-test, **Figure 3.4Bii**). However, presence of APDC decreased the frequency of *Fmr1* KO mIPSCs in 9 of 12 cells ($p<0.05$, K.S. test). Pooled data showed a statistically significant decrease in the frequency of *Fmr1* KO pyramidal mIPSCs in response to APDC application (n=12, Pre-drug: 16.1 ± 3.9 Hz, APDC: 14.1 ± 3.4 Hz, $p<0.05$, paired t-test, **Figure 3.4Biii**). From the above data, we conclude that group II mGluRs are predominantly acting at presynaptic interneuron terminals to decrease GABAergic transmission. We also observe that this GABAergic modulation is intact in the *Fmr1* KO mouse, indicating that exaggerated suppression of inhibition onto pyramidal neurons in the *Fmr1* KO is due to changes in group II mGluR processes upstream of the GABA synapse.

3.4 Discussion

In this chapter, we determine if activation of group II mGluRs could differentially modulate GABAergic inhibition in layer 5/6 pyramidal neurons in WT and *Fmr1* KO animals. In addition to modulating glutamatergic transmission across all layers of the visual neocortex (Flavin, Jin & Daw, 2000), group II mGluRs have been shown to mediate inhibition of GABAergic currents in hippocampus (Jouvenceau et al. 1995), thalamus (Salt and Eaton, 1995; Salt and Turner, 1998), olfactory bulb (Hayashi et al., 1993), striatum (Hanania and Johnson, 1999), tectum (Neale and Salt, 2006), and certain regions of the brainstem (Chen and Bonham, 2005; Liu, Petrof & Sherman, 2014). Upon activation, these group II mGluRs have also been shown to decrease GABAergic transmission onto both layer 2/3 and layer 4 excitatory pyramidal neurons in the auditory and visual cortices (Liu, Petrof & Sherman). In this chapter, we report that group II mGluRs also inhibit GABAergic transmission onto layer 5/6 pyramidal neurons, as

measured by a decrease in evoked IPSC amplitude is response to pharmacological activation of group II mGluRs. We further demonstrate that this effect is exaggerated by 20% in the *Fmr1* KO mouse, leading to a decrease in inhibition onto layer 5/6 pyramidal neurons. This is the first electrophysiological study to show a functional defect in group II mGluR signaling in FXS. Additionally, we show that group II mGluRs are present at both GABAergic terminals and at postsynaptic pyramidal neurons. Interestingly, neither of these group II mGluR populations are responsible for mediating the exaggerated suppression of inhibition that we see in the *Fmr1* KO. Blocking glutamatergic excitation of interneurons led to a suppression of the evoked IPSC by group II mGluRs that was similar between WT and *Fmr1* KO. We also recorded both sIPSC and mIPSC recordings and confirmed that group II mGluR-mediated suppression of IPSC frequency and amplitude is similar in WT and *Fmr1* KO mice, further supporting the idea that there is normal group II mGluR-mediated modulation of GABAergic transmission onto pyramidal neurons in the layer 5/6. Together these results suggest that the changes we observe are due to group II mGluRs residing upstream of the GABAergic terminals. We hypothesize that the group II mGluR-mediated suppression of inhibition in *Fmr1* KO pyramidal neurons is actually disinhibition caused by exaggerated suppression of excitation onto layer 5/6 interneurons upon activation of group II mGluRs. We also add to the literature by showing that group II mGluR-mediated modulation of GABA synapses are intact in the *Fmr1* KO. Interestingly, the only functional studies that have shown impairments in inhibition of the neocortex, both find that excitatory drive onto interneurons and/or modulation of excitatory drive is deficient (Gibson et al., 2008; Paluszkiewicz et al., 2011). This is also what our data suggest. While defective GABAergic transmission appears to be a major defect in other brain regions such as the amygdala (Olmos-Serrano et al., 2010; Vislay et al., 2013; Martin et al., 2014), it may turn out

that selective loss of excitatory drive onto and/or modulation of interneurons is the major circuit defect in neocortical brain regions. Unfortunately experiments such as these will need to be completed in other neocortical brain regions and layers, before we can be certain. In the following chapter, I will test the hypothesis that activation of group II mGluRs leads to exaggerated suppression of excitatory glutamatergic transmission onto layer 5/6 interneurons (Chapter 4).

APPENDIX

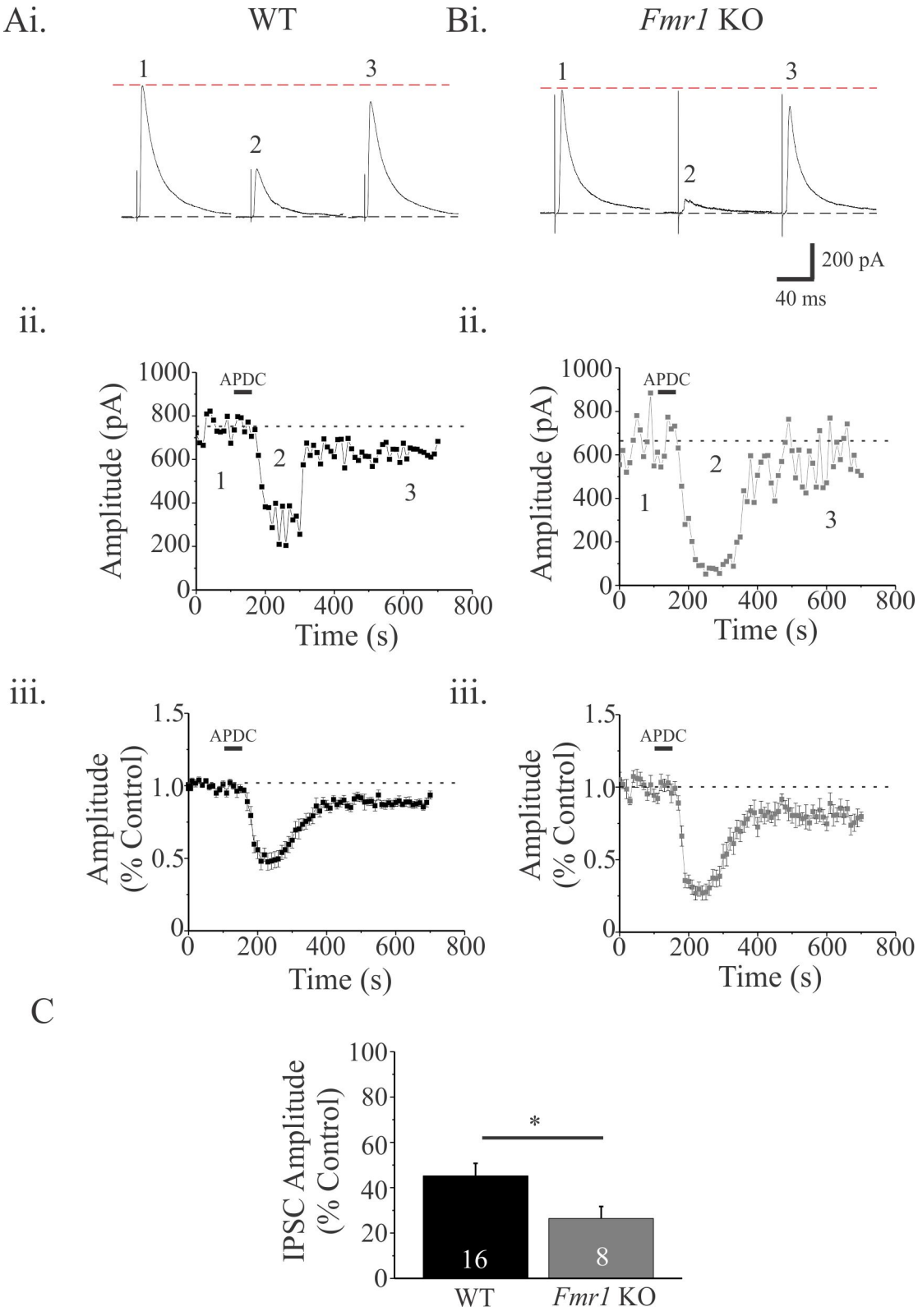

Figure 3.1. Group II mGluR-mediated modulation of IPSCs in layer 5/6 pyramidal neurons is exaggerated in the *Fmr1* KO mouse.

Figure 3.1. (cont'd)

Ai. Representative trace showing the response of a layer 5/6 wild type pyramidal neuron IPSC to brief application of group II mGluR agonist, APDC (75 μM). ii. Raw time course of the change in peak amplitude in a single wild type pyramidal cell. iii. Wild type normalized time course of the population peak amplitude change (n=16). Bi-iii. Same as Ai-iii, but for the *Fmr1* KO (n=8). C. Average IPSC amplitude immediately following APDC application, expressed as % of control for all cells tested in both WT and *Fmr1* KO. Comparison of peak amplitude following APDC application determined that the *Fmr1* KO IPSC suppression mediated by group II mGluR activation is exaggerated relative to wild type pyramidal neuron IPSCs (WT=16, KO=8, p=0.023, t-test).

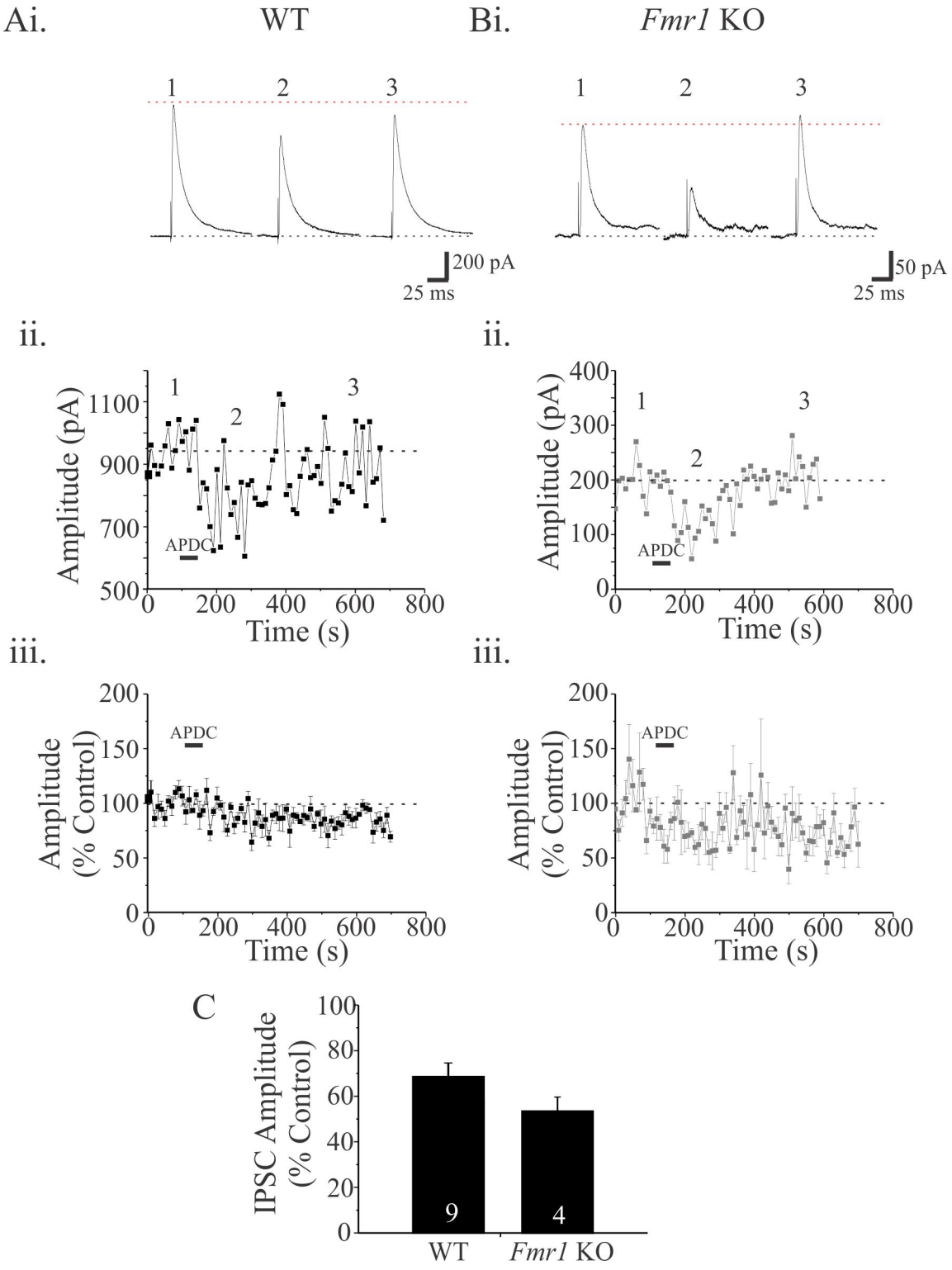

Figure 3.2. Group II mGluRs suppress fast inhibitory transmission onto WT and *Fmr1* KO pyramidal neurons in the absence of excitatory drive onto neocortical interneurons.

Figure 3.2. (cont'd)

Ai. Representative trace showing the presence of a layer 5/6 wild type pyramidal neuron IPSC to brief application of group II mGluR agonist APDC (75 μM), in the presence of bath applied NMDA and AMPA receptor antagonists, CPP (20 μM) and DNQX (40 μM). Aii. Raw time course of the changes in peak amplitude in a single wild type pyramidal cell. Aiii. Wild type normalized time course of the population peak amplitude change (n=9). Bi-iii. Same as Ai-iii, but for *Fmr1* KO. C. Average IPSC amplitude immediately following APDC application, expressed as % of control for all cells tested in both WT and *Fmr1* KO (WT=9, KO=4). A comparison of the population peak amplitude determined that there were no significant differences between WT and *Fmr*1 KO (WT=9, KO=4, $p > 0.05$, t-test).

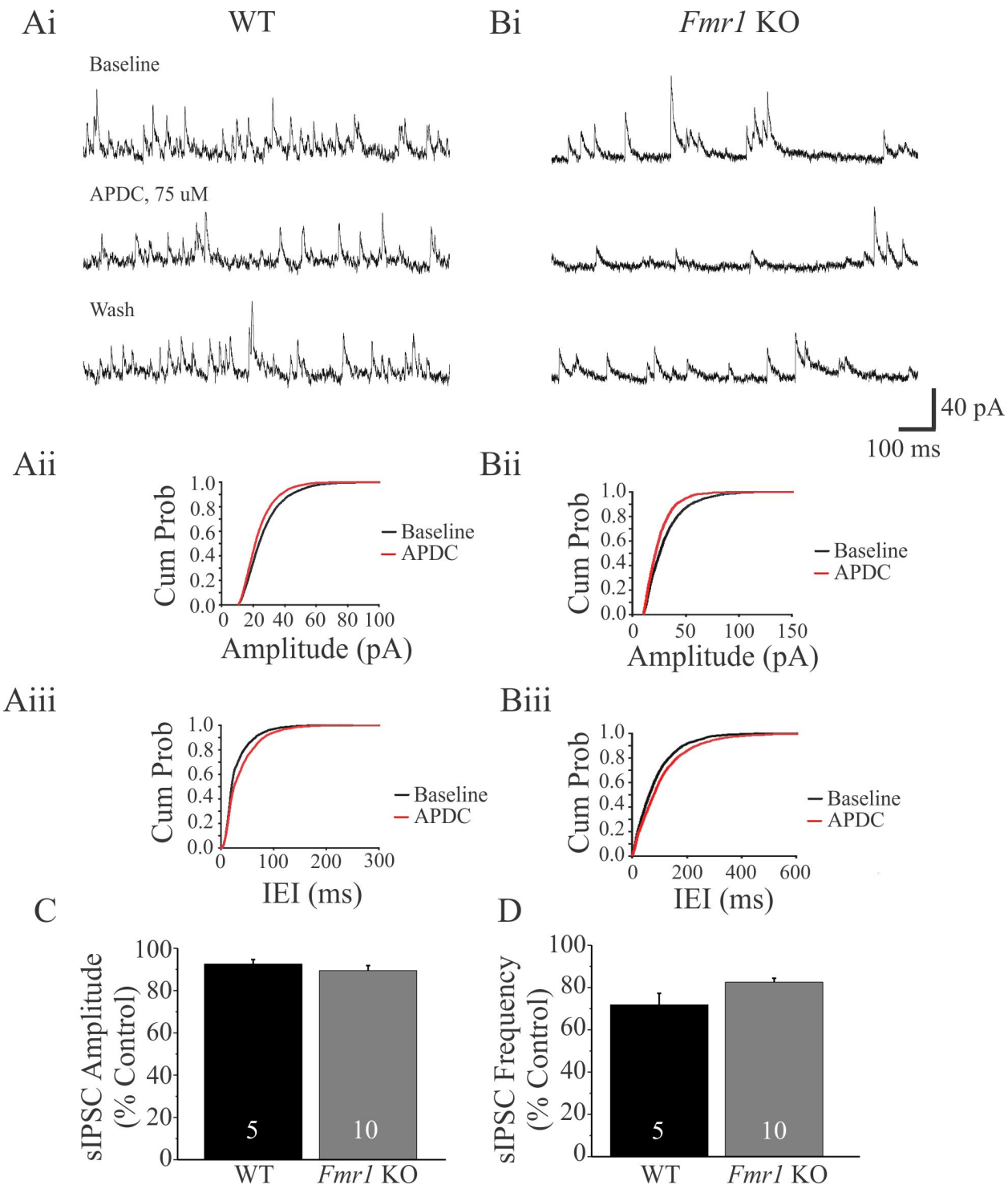

Figure 3.3. Group II mGluRs modulate sIPSC amplitude and frequency similarly between WT and *Fmr1* KO layer 5/6 pyramidal neurons.
Ai. Raw data showing spontaneous IPSCs recorded from WT pyramidal neurons before, during and after application of group II mGluR agonist APDC (75 µM). Aii. Representative cumulative distribution showing a significant decrease in WT amplitude in response to APDC (n=1, $p < 0.05$,

Figure 3.3. (cont'd)

K.S. test). Aiii. Representative cumulative distribution showing a decrease in frequency upon APDC application (n= 1, $p < 0.05$, K.S. test). Bi-iii. Same as Ai-iii, but for *Fmr1* KO. *Fmr1* KO pyramidal neurons also show a shift in the cumulative distribution for amplitude and frequency in response to APDC ($p < 0.05$, K.S. test). C. Comparison of the average population sIPSC response amplitude between WT and *Fmr1* KO was not significant (WT=5, KO=10, $p > 0.05$, t-test). D. Population data for sIPSC frequency was also not statistically different between genotypes (WT=5, KO=10, $p > 0.05$, t-test).

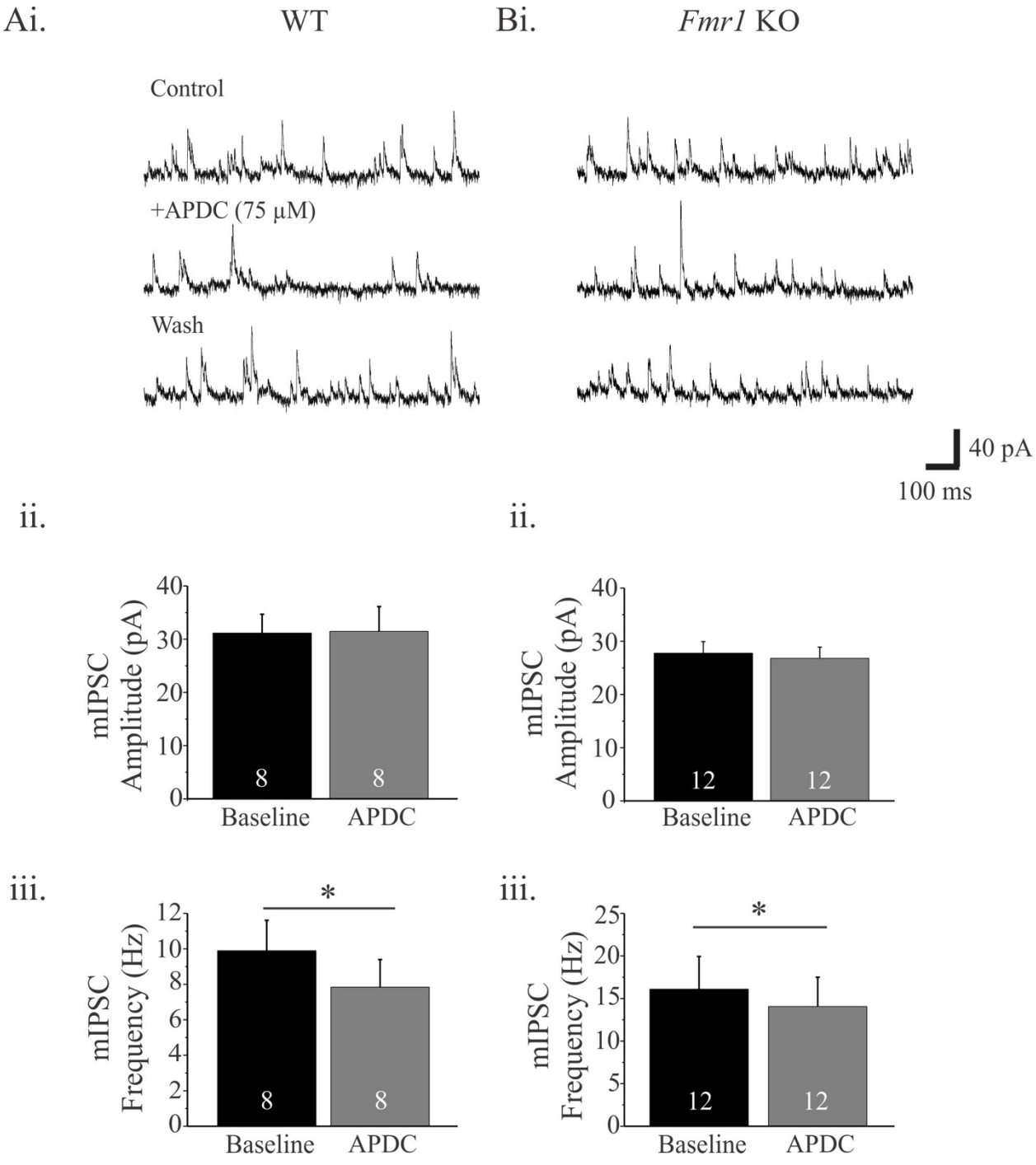

Figure 3.4. Presynaptic mGluRs at the interneuron terminals modulate inhibition similarly between WT and *Fmr1* KO layer 5/6 pyramidal neurons.
Ai. Raw data showing miniature IPSCs recorded from WT pyramidal neurons before, during and after application of group II mGluR agonist APDC (75 μM). Aii. Average wild type population change in mIPSC peak amplitude in response to APDC application (n=8). Aiii. Average wild type population change in mIPSC frequency in response to APDC application (n=8). Bi-iii. Same as Ai-iii, but for the *Fmr1* KO. APDC did not change the amplitude of mIPSCs for either WT or *Fmr1* KO ($p > 0.05$, t-test). Frequency of mIPSCs was statistically decreased in the

Figure 3.4. (cont'd)

presence of APDC for both WT and *Fmr1* KO pyramidal neurons, indicating that group II mGluRs are located presynaptically at GABAergic terminals. No differences were seen between WT and *Fmr1* KO ($p > 0.05$, t-test).

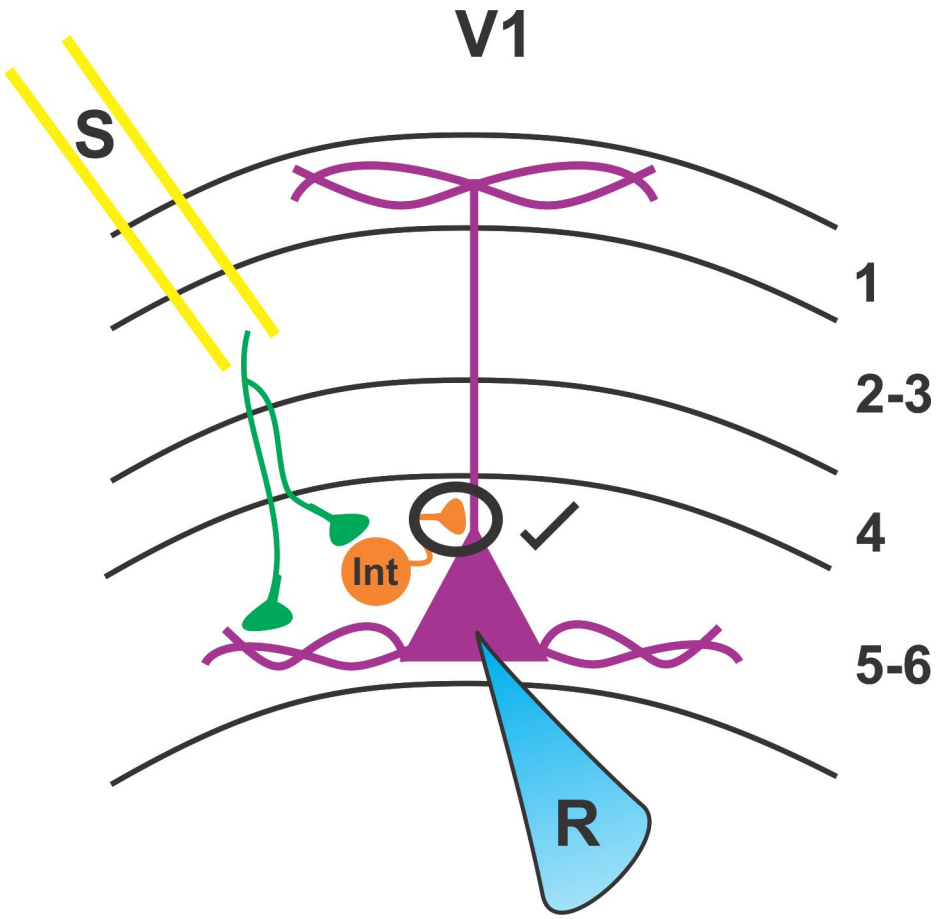

Figure 3.5. Group II mGluR-mediated suppression of IPSCs on pyramidal neurons is normal in the *Fmr1* KO mouse.
In chapter 3, inhibitory postsynaptic currents (IPSCs) were evoked using a stimulating electrode placed in layer 2/3 (S). We show that activation of group II mGluRs leads to suppression of IPSCs at glutamatergic synapses onto layer 5/6 pyramidal neurons in both the WT and *Fmr1* KO (black circle). The magnitude of this suppression is similar between WT and *Fmr1* KO mouse (black checkmark).

REFERENCES

REFERENCES

Adusei, D. C., Pacey, L. K., Chen, D., & Hampson, D. R. (2010). Early developmental alterations in GABAergic protein expression in fragile X knockout mice. *Neuropharmacology, 59*(3), 167-171. doi:10.1016/j.neuropharm.2010.05.002

Centonze, D., Rossi, S., Mercaldo, V., Napoli, I., Ciotti, M. T., De Chiara, V., . . . Bagni, C. (2008). Abnormal striatal GABA transmission in the mouse model for the fragile X syndrome. *Biol Psychiatry, 63*(10), 963-973. doi:10.1016/j.biopsych.2007.09.008

Chang, Y. M., & Luebke, J. I. (2007). Electrophysiological diversity of layer 5 pyramidal cells in the prefrontal cortex of the rhesus monkey: in vitro slice studies. *J Neurophysiol, 98*(5), 2622-2632. doi:10.1152/jn.00585.2007

Chen, C. Y., & Bonham, A. C. (2005). Glutamate suppresses GABA release via presynaptic metabotropic glutamate receptors at baroreceptor neurones in rats. *J Physiol, 562*(Pt 2), 535-551. doi:10.1113/jphysiol.2004.076885

D'Hulst, C., Heulens, I., Brouwer, J. R., Willemsen, R., De Geest, N., Reeve, S. P., . . . Kooy, R. F. (2009). Expression of the GABAergic system in animal models for fragile X syndrome and fragile X associated tremor/ataxia syndrome (FXTAS). *Brain Res, 1253*, 176-183. doi:10.1016/j.brainres.2008.11.075

El Idrissi, A., Ding, X. H., Scalia, J., Trenkner, E., Brown, W. T., & Dobkin, C. (2005). Decreased GABA(A) receptor expression in the seizure-prone fragile X mouse. *Neurosci Lett, 377*(3), 141-146. doi:10.1016/j.neulet.2004.11.087

Flavin, H. J., Jin, X. T., & Daw, N. W. (2000). 2R,4R-4-Aminopyrrolidine-2,4-dicarboxylate (APDC) attenuates cortical EPSPs. *Brain Res, 873*(2), 212-217.

Gantois, I., Vandesompele, J., Speleman, F., Reyniers, E., D'Hooge, R., Severijnen, L. A., . . . Kooy, R. F. (2006). Expression profiling suggests underexpression of the GABA(A) receptor subunit delta in the fragile X knockout mouse model. *Neurobiol Dis, 21*(2), 346-357. doi:10.1016/j.nbd.2005.07.017

Gibson, J. R., Bartley, A. F., Hays, S. A., & Huber, K. M. (2008). Imbalance of neocortical excitation and inhibition and altered UP states reflect network hyperexcitability in the mouse model of fragile X syndrome. *J Neurophysiol, 100*(5), 2615-2626. doi:10.1152/jn.90752.2008

Hagerman, P. J., & Stafstrom, C. E. (2009). Origins of epilepsy in fragile X syndrome. *Epilepsy Curr, 9*(4), 108-112. doi:10.1111/j.1535-7511.2009.01309.x

Hanania, T., & Johnson, K. M. (1999). Regulation of NMDA-stimulated [14C]GABA and [3H]acetylcholine release by striatal glutamate and dopamine receptors. *Brain Res, 844*(1-2), 106-117.

Hayashi, Y., Momiyama, A., Takahashi, T., Ohishi, H., Ogawa-Meguro, R., Shigemoto, R., . . . Nakanishi, S. (1993). Role of a metabotropic glutamate receptor in synaptic modulation in the accessory olfactory bulb. *Nature, 366*(6456), 687-690. doi:10.1038/366687a0

Hong, A., Zhang, A., Ke, Y., El Idrissi, A., & Shen, C. H. (2012). Downregulation of GABA(A) beta subunits is transcriptionally controlled by Fmr1p. *J Mol Neurosci, 46*(2), 272-275. doi:10.1007/s12031-011-9531-5

Larkman, A., & Mason, A. (1990). Correlations between morphology and electrophysiology of pyramidal neurons in slices of rat visual cortex. I. Establishment of cell classes. *J Neurosci, 10*(5), 1407-1414.

Liu, T., Petrof, I., & Sherman, S. M. (2014). Modulatory effects of activation of metabotropic glutamate receptors on GABAergic circuits in the mouse cortex. *J Neurophysiol, 111*(11), 2287-2297. doi:10.1152/jn.00730.2013

Martin, B. S., Corbin, J. G., & Huntsman, M. M. (2014). Deficient tonic GABAergic conductance and synaptic balance in the fragile X syndrome amygdala. *J Neurophysiol, 112*(4), 890-902. doi:10.1152/jn.00597.2013

Neale, S. A., & Salt, T. E. (2006). Modulation of GABAergic inhibition in the rat superior colliculus by a presynaptic group II metabotropic glutamate receptor. *J Physiol, 577*(Pt 2), 659-669. doi:10.1113/jphysiol.2006.119073

Olmos-Serrano, J. L., Paluszkiewicz, S. M., Martin, B. S., Kaufmann, W. E., Corbin, J. G., & Huntsman, M. M. (2010). Defective GABAergic neurotransmission and pharmacological rescue of neuronal hyperexcitability in the amygdala in a mouse model of fragile X syndrome. *J Neurosci, 30*(29), 9929-9938. doi:10.1523/JNEUROSCI.1714-10.2010

Paluszkiewicz, S. M., Olmos-Serrano, J. L., Corbin, J. G., & Huntsman, M. M. (2011). Impaired inhibitory control of cortical synchronization in fragile X syndrome. *J Neurophysiol, 106*(5), 2264-2272. doi:10.1152/jn.00421.2011

Salt, T. E., & Eaton, S. A. (1995). Distinct presynaptic metabotropic receptors for L-AP4 and CCG1 on GABAergic terminals: pharmacological evidence using novel alpha-methyl derivative mGluR antagonists, MAP4 and MCCG, in the rat thalamus in vivo. *Neuroscience, 65*(1), 5-13.

Selby, L., Zhang, C., & Sun, Q. Q. (2007). Major defects in neocortical GABAergic inhibitory circuits in mice lacking the fragile X mental retardation protein. *Neurosci Lett, 412*(3), 227-232. doi:10.1016/j.neulet.2006.11.062

Sladeczek, F., Momiyama, A., & Takahashi, T. (1993). Presynaptic inhibitory action of a metabotropic glutamate receptor agonist on excitatory transmission in visual cortical neurons. *Proc Biol Sci, 253*(1338), 297-303. doi:10.1098/rspb.1993.0117

Vislay, R. L., Martin, B. S., Olmos-Serrano, J. L., Kratovac, S., Nelson, D. L., Corbin, J. G., & Huntsman, M. M. (2013). Homeostatic responses fail to correct defective amygdala inhibitory circuit maturation in fragile X syndrome. *J Neurosci, 33*(17), 7548-7558. doi:10.1523/JNEUROSCI.2764-12.2013

CHAPTER IV: FMR1 KO NON FAST-SPIKING INTERNEURONS EXHIBIT EXAGGERATED RESPONSE TO GROUP II MGLUR MEDIATED SUPPRESSION OF EXCITATORY TRANSMISSION

4.1 Introduction

Fragile X Syndrome (FXS) is the most common inherited form of autism. It is primarily a disorder of intellectual impairment, with approximately 85% of males and 25% of females experiencing severe intellectual difficulties (<70 IQ). However, the syndrome also features a wide array of physical and neuropsychiatric symptoms. Neurological features include hypersensitivity to sensory stimuli across all modalities, autistic features, and seizure disorder (Hagerman, 2008). All of these phenotypes have been speculated to result from hyperexcitable neocortical circuitry. In support of this, functional neocortical studies suggest that neocortical interneurons are dysfunctionally regulated in the neocortex of *Fmr1* KO mice. There are three major interneuron subtypes in the neocortex (Markram, 2004). Of these subtypes, the two largest are the parvalbumin-(PV+) and somatostatin-(SST+) expressing interneurons, together comprising 70% of all neocortical interneurons (Rudy et al., 2001). These interneuron subtypes differ in their morphology, laminar expression, and in the role they play in modulating excitation of the neocortical circuitry. PV+ interneurons exhibit a fast-spiking profile (FS) and synapse onto the soma and proximal dendrites of their target neurons, while SST+ interneurons exhibit non fast-spiking properties (NFS) with low threshold spikes (LTS) and are dendritic targeting (Kawaguchi and Kubota, 1997; Beierlein and Connors, 2000). FS interneurons are particularly well suited for rapid inhibition of their target cell output, whereas NFS interneurons receive highly facilitating excitatory inputs and are speculated to play a more important role during elevated levels of network activity, where they can act to synchronize inhibition (Paluskiewicz et al., 2011; Beierlein and Connors, 2003). Both FS and NFS interneurons are dysfunctionally

regulated in the neocortex of the *Fmr1* KO mouse. In layer 4 of the somatosensory cortex, excitatory drive onto FS interneurons is decreased by 51%, and this contributes to a prolonged duration of upstates observed in the *Fmr1* KO somatosensory cortex (Gibson et al., 2008). Additionally, group I mGluR-mediated modulation of NFS interneurons in layer 2/3 of the somatosensory cortex is decreased, leading to reduced synchronization of inhibition (Paluszkiewicz et al., 2011). These studies provide compelling evidence in favor of decreased excitatory drive of inhibition as a major culprit of neocortical pathogenesis in FXS, albeit it appears that the extent to which different interneuron subtypes are affected may be laminar specific. Further, they specifically implicate aberrant mGluR signaling in the function of these interneurons in FXS. In support of this, we have previously shown an inhibitory defect of layer 5/6 excitatory pyramidal neurons in the visual neocortex of the *Fmr1* KO mouse triggered by pharmacological activation of group II mGluRs. Specifically, activation of these mGluRs leads to enhanced suppression of GABAergic neurotransmission onto pyramidal neurons in the *Fmr1* KO mouse. This would be expected to cause hyperexcitability of visual neocortical circuitry. Interestingly, we also discovered that group II mGluR-mediated modulation of GABA synapses onto excitatory cells is normal in the *Fmr1* KO mouse, suggesting that the alterations we observed in group II mGluR-mediated modulation of inhibition is occurring upstream from the GABA synapse. We hypothesize that group II mGluRs are modulating excitatory transmission onto inhibitory neurons, and that this is the likely location of dysfunction in the *Fmr1* KO mouse. Given that both FS and NFS interneurons have previously been implicated in FXS neocortical pathogenesis, it is possible that one or both of these interneurons are involved in the exaggerated suppression of inhibition that we observe onto layer 5/6 pyramidal neurons. To that end, we performed whole-cell recordings from both FS and NFS interneurons in the layer 5/6, and

quantified the changes we observed in group II mGluR-mediated modulation of excitation onto these neurons. We demonstrate that group II mGluR-mediated suppression of glutamatergic transmission onto FS interneurons remains unaltered in the *Fmr1* KO. In contrast, group II mGluR-mediated modulation of glutamatergic transmission onto NFS interneurons is exaggerated in the *Fmr1* KO mouse, leading to decreased excitation of these interneurons relative to WT NFS cells. We further show that group II mGluRs are mediating this effect presynaptically, presenting new evidence in support of a presynaptic role for FMRP. Finally, we show that this alteration in the *Fmr1* KO mouse is layer specific, as excitatory synapses onto NFS interneurons in the layer 2/3 do not show the same alterations that we observe in the layer 5/6.

4.2 Materials and Methods

All experimental procedures were performed in accordance with the National Institutes of Health *Guide for Care and Use if Laboratory Animals* and were approved by the Michigan State University Institutional Animal Care and Use Committee.

Mice on the FVB background (postnatal age 16-21 days) of either sex were anesthetized with isoflurane and perfused with cold, oxygenated (5% CO_2-95% O_2), modified saline prior to decapitation. Brains were removed and transferred to cold (4°C), oxygenated slicing solution containing the following (in mM): 2.5 KCl, 1.25 NaH_2PO_4, 10.0 $MgSO_4$, 0.5 $CaCl_2$, 26.0 $NaHCO_3$, 10.0 glucose, and 234.0 sucrose. Slices (300 μm thickness) were collected in a coronal plane were collected using a Leica vibrating tissue slicer, and then transferred to a holding chamber filled with oxygenated physiological saline containing (in mM): 126.0 NaCl, 2.5 KCl, 1.25 NaH_2PO_4, 2.0 $MgCl_2$, 2.0 $CaCl_2$, 26.0 $NaHCO_3$, and 10.0 glucose. Slices were

incubated at 32 ± 1°C for at least 30 minutes, and then left to rest at room temperature for at least 30 minutes prior to recording.

Whole-cell recordings were obtained using a microscope equipped with differential interface contrast optics (Zeiss, Thornwood, NY). Single slices were transferred to a submersion chamber continuously superfused at 2.5ml/min with oxygenated physiological saline heated to 32°C. Visual neocortex was identified with a low power (5x) objective and individual neurons were identified using a water-immersion objective (63x). For a subset of experiments, fluorescent microscopy was used to visualize GFP-expressing neurons in two different transgenic mouse lines. These transgenic lines have been shown to express green fluorescent protein (GFP) in a subset of either parvalbumin positive (CB6-Tg(Gad1-EGFP)G42Zjh/J/Jax labs) or somatostatin positive interneurons (FVBTg(GadGFP)45704Swn/Jax labs) under the control of the mouse *Gad1* gene. Neuron subtypes were further distinguished by their characteristic electrophysiological properties as determined using an 800-2000 ms current step injection protocol. PV+ interneurons exhibit the following intrinsic properties: more hyperpolarized membrane potentials, higher threshold to fire action potentials, non-accommodating spike firing, and abrupt episodes of nonadapting repetitive discharges (Kawaguchi and Kubota, 1997). Relative to parvalbumin interneurons, somatostatin interneurons have higher input resistances, more depolarized membrane potentials, both early and late after-hyperpolarizing potentials (AHPs), and moderate spike frequency adaptation (Beierlein et al., 2000; Beierlein et al., 2003). Pyramidal neurons were identified through preferential targeting of pyramidal-shaped soma with a diameter greater than 20 μm, in addition to observing their electrophysiological properties. The majority of pyramidal neurons (62%) exhibit a regular spiking (RS) slowly adapting firing pattern, with a moderate sized late after-

hyperpolarizing potential (AHP) and most often no visible early (AHP) or depolarizing afterpotential (DAP) (Chang and Luebke, 2007; Larkman and Mason; 1990). In contrast, SST+ interneurons always display a prominent early AHP and a DAP, making this an important factor for distinguishing between the two cell types. Another less common (5%), but easily distinguished electrophysiological profile of layer 5/6 pyramids was that of intrinsic bursting firing (IB) of 3-6 bursts of APs (Chang and Luebke, 2007; Larkman and Mason; 1990). For recordings, pipettes made of borosilicate capillary glass were pulled to tip resistances of 4-6MΩ and then filled with intracellular solution containing (in mM): 117.0 K-gluconate, 13.0 KCl, 1.0 MgCl2, 0.07 CaCl2, 0.1 EGTA, 10.0 HEPES, 2.0 Na2-ATP, 0.4 Na-GTP, and 0.2% biocytin. Only cells with a membrane potential ≥ -50 mV and overshooting action potentials were included for analysis. Access resistance was monitored throughout the experiments and recordings were not included if the access resistance increased to >20MΩ.

In recordings from layer 5/6 FS and NFS interneurons, excitatory postsynaptic currents (EPSCs) were evoked by electrical stimulation of afferents in layer 2/3 (**Figure 2.1**). For layer 2/3 recordings, a stimulating electrode was placed in layer 4 of the visual neocortex. For EPSC recordings, the chloride channel blocker, 4,4'-dinitrostilbene-2,2'-disulfonic acid (DNDS, 1 mM) was included in the recording pipette to block $GABA_A$–mediated IPSCs, effectively isolating EPSCs in the recorded neurons. Stimuli were delivered at 0.1 Hz, and the peak amplitudes and/or charge of the evoked EPSCs was measured before, during, and after washout of the selective group I and group II mGluR agonists, (RS)-3,5-dihydroxyphenylglycine (DHPG) and (2R,4R)-4-aminopyrrolidine-2,4-dicarboxylate (APDC) respectively. Miniature EPSCs (mEPSCs) were recorded in the presence of tetrodotoxin (1μM). During strontium experiments, the calcium chloride in the physiological saline was replaced with strontium chloride (2 mM).

All compounds used in this study were prepared from stock solutions stored at the appropriate temperature and diluted to the correct concentration with physiological saline prior to administration. All agonists were delivered by bolus injection to the central line of the recording chamber using a syringe pump. Based upon the calculated flow rate of the main line, the delivered drug concentration was estimated to be one-fourth of the initial drug concentration. DNDS was purchased from Life Technologies, while all other compounds were purchased from Tocris and Sigma-Aldrich.

All recordings were acquired using a Multiclamp 700B amplifier (Molecular Devices). Data was filtered at 2.5 kHz and digitized at 10 kHz using pClamp software. For evoked experiments, 12 consecutive sweeps (2 minutes) were averaged to determine the baseline peak amplitude and/or charge of the synaptic response. The drug effect was determined as the average of 3 consecutive sweeps during the maximal drug response. A positive drug response was defined as a change in amplitude or charge that was greater than 2 standard deviations of the baseline response. The frequency and amplitude of mEPSCs or evoked responses in the presence of strontium were analyzed using MiniAnalysis software (Synaptosoft). All data are reported as the mean ± SEM and analyzed using either paired or independent t-test were applicable. Kolmogorov-Smirnoff tests were used to determine if mEPSC frequency and/or amplitude were altered within cells by drug application. A p-value <0.05 was considered statistically significant.

4.3 Results

A. The intrinsic properties of Fmr1 KO layer 5/6 FS interneurons are similar to WT.

After investigating the intrinsic properties of excitatory cells in the layer 5/6, we next questioned whether the intrinsic properties of interneurons in the *Fmr1* KO mouse differ from

those of the wild type. We began our investigation quantifying both input resistance and membrane potential of WT and *Fmr1* KO FS interneurons (**Figure 4.1Ai and ii**), which comprise the major interneuron subtype in the visual neocortex (Markram et al., 2004). In the WT mouse, the average input resistance was 171.7 ± 19.3 MΩ (n=22, **Figure 4.1 Ci**). The *Fmr1* KO FS interneurons had an input resistance similar to that seen in WT FS interneurons. (146.5 ± 21.5 MΩ, n=10) and thus not statistically significant (p>0.05, t-test, **Figure 4.1 Ci**). Next, we quantified membrane potentials of WT and *Fmr1* KO interneurons. WT FS interneurons had an average membrane potential of -73.8 ± 1.2 mV (n=22, **Figure 4.1 Cii**), and *Fmr1* KO cells had a slightly more hyperpolarized potential (-74.1 ± 1.5 mV, n=10, **Figure 4.1 Cii**), however this was not statistically different from WT neurons (p>0.05, t-test, **Figure 4.1Cii**). These results are summarized in the following table **(Table 2.4).**

Table 4.1. Intrinsic properties of layer 5/6 FS interneurons in WT and *Fmr1* KO mice.

	Input Resistance	***Membrane Potential***
Wild Type	171.7 ± 19.3 (n=22)	-73.8 ± 1.2 (n=22)
Fmr1 KO	146.5 ± 21.5 (n=10)	-74.1 ± 1.5 (n=10)
p	0.39 t-test	0.87 t-test

B. Group I mGluRs do not modulate EPSCs in FS interneurons.

Prior to investigating the modulation of FS interneuron EPSCs by group II mGluRs, we first wanted to determine whether group I mGluRs modulate excitatory synaptic transmission in layer 5/6 FS interneurons. To accomplish this task, we obtained whole cell recordings from layer 5/6 FS interneurons in WT and *Fmr1* KO mice. We chose to investigate these interneurons first because they have previously been implicated in neocortical Fragile X pathology (Gibson et al., 2008; Patel et al., 2013), and because they are the most abundant neocortical interneuron

subtype (Rudy et al., 2011). FS interneurons were identified based on their unique physical and electrophysiological properties. Specifically, they are smaller in size, relatively hyperpolarized, exhibit non-accommodating action potential firing to depolarizing current steps, and receive a multitude of spontaneous excitatory inputs visible throughout a series of current steps delivered upon patching the cell (Kawaguchi and Kubota, 2006). Additionally, in some instances FS interneurons were visualized using transgenic mice that express GFP in PV+ interneurons. We evoked EPSCs in WT and *Fmr1* KO FS interneurons by electrical stimulation of layer 2/3 visual neocortex (20-100μA, 0.1Hz, **Figure 4.2 Ai and Bi**). The baseline EPSC amplitude in control animals averaged 520.4 ± 86.6 pA, and application of DHPG (25μM, 30s) had no effect on EPSC amplitude (n=11, DHPG: 491.8 ± 81.4 pA, $p>0.05$, paired t-test, **Figure 4.2 Aii-iii**). In *Fmr1* KO FS interneurons (**Figure 4.2 Bi**), the average pre-drug amplitude of the EPSC was 343.1 ± 46.4 pA, and application of DHPG to these cells also failed to produce significant changes in the amplitude of the response (n=9, DHPG: 348.9 ± 45.9, $p >0.05$, paired t-test, **Figure 4.2 Bii-iii**). The average amplitude of the EPSC response to DHPG in WT FS interneurons was 95.2 ± 1.6 % of control, and the *Fmr1* KO FS interneuron EPSC response was 102.2 ± 2.5% of control (WT=11, *Fmr1* KO=9, **Figure 4.2C**). From this data set, we conclude that group I mGluRs do not modulate glutamatergic transmission in layer 5/6 FS interneurons.

C. Group II mGluRs modulate EPSCs on FS interneurons similarly between WT and Fmr1 KO.

Recall from the previous chapter that we observed an exaggerated group II mGluR-dependent suppression of the IPSC amplitude in pyramidal neurons from *Fmr1* KO mice. We also determined that activating group II mGluRs while simultaneously blocking excitatory drive onto neocortical interneurons leads to IPSC suppression in pyramidal neurons that is similar in

amplitude between *Fmr1* KO and WT. With these results, we are now certain that the change we observe in the IPSC amplitude between WT and *Fmr1* KO pyramidal neurons is due to alterations in group II mGluR-mediated modulation of excitatory drive onto interneurons. Which interneurons are responsible for this effect, however, remains unknown. To that end, we next sought to determine how group II mGluRs modulate excitatory transmission onto specific neocortical interneuron subtypes. We obtained whole cell recordings from layer 5/6 FS interneurons in WT and *Fmr1* KO mice and tested the effects of APDC on the evoked responses of WT and *Fmr1* KO FS interneurons (**Figure 4.3 Ai and Bi**). In WT animals, the average control response was 523.7 ± 89.7 pA, and this was significantly attenuated by APDC (204.4 ± 34.8 pA, n=11, $p<0.05$, paired t-test, **Figure 4.3Aii-iii**). In *Fmr1* KO interneurons, the average response prior to APDC was 319.1 ± 39.1 pA, and this response was also significantly attenuated by the group II agonist (135.0 ±18.7 pA, n=7, $p<0.05$, paired t-test, **Figure 4.3Bii-iii**). Comparison of the change in amplitude between WT and *Fmr1* KO, expressed as % of the control response, determined that the APDC suppression of EPSC amplitude was not different between phenotypes (WT: 40.8 ± 3.3 %, *Fmr1* KO: 43.1 ± 5.5$p>0.05$, t-test, **Figure 4.3C**). These results indicate that group II mGluR-mediated suppression of EPSCs in FS interneurons is intact in the *Fmr1* KO, and that this interneuron subtype is not responsible for the exaggerated suppression of inhibition by APDC that we see in *Fmr1* KO layer 5/6 pyramidal neurons.

D. *Fmr1 KO layer 5/6 NFS interneurons have a decreased input resistance compared to WT.*

NFS interneurons are the second largest subgroup of inhibitory cells in the neocortex (Kawaguchi and Kubota, 1997; Markram et al., 2004). For this reason, we also included them in our analysis of the intrinsic properties of neocortical interneurons. We recorded a series of

current-step injections from both WT and *Fmr1* KO NFS interneurons (**Figure 4.1 Bi and ii**), and compared both input resistance and membrane potential. The average input resistance of wild type layer 5/6 NFS interneurons in the visual neocortex was 359.8 ± 18.1 MΩ (n=39, **Figure 4.1Di**), and this was significantly larger than the input resistance we observed in FS interneurons (**Figure 4.1Ci**), supporting previously published literature (Beierlein, Gibson, & Connors, 200; Kawaguchi and Kubota, 1997). In *Fmr1* KO interneurons, the average input resistance was smaller than that observed in WT NFS interneurons (306.9 ± 17.3 MΩ, n=32, **Figure 4.1Di**), and this difference was statistically significant (p = 0.038, t-test, **Figure 4.1Di**). We also measured membrane potential in both WT and *Fmr1* KO cells (WT: -65.9 ± 0.9 mV, n= 39; Fmr1 KO: -67.1 ± 0.9 mV, n=32, **Figure 4.1Dii**), but found no significant differences between genotypes (p = 0.36, t-test, **4.1Dii**). However, the average membrane potential of NFS interneurons was more depolarized than FS interneurons, and this is what we expected to see based on previous studies (Beierlein, Gibson, & Connors, 2000). The decrease in input resistance of *Fmr1* KO NFS interneurons that we report, indicates that these interneurons are less intrinsically excitable than layer 5/6 wild type NFS interneurons. These results are summarized below (**Table 2.5**)

Table 4.2. Intrinsic properties of layer 5/6 SST+ interneurons in WT and *Fmr1* KO mice.

	Input Resistance	***Membrane Potential***
Wild Type	359.8 ± 18.1 (n=39)	-65.9 ± 0.9 (n=39)
Fmr1 KO	306.9 ± 17.3 (n=32)	-67.1 ± 0.9 (n=47)
p	0.038* t-test	0.928 t-test

E. Fmr1 KO NFS interneurons show an exaggerated response to group II mGluR activation.

After determining that modulation of excitatory drive onto *Fmr1* KO FS interneurons by group II mGluRs is comparable to wild type, we next wondered whether the same would be true of modulated excitatory drive onto NFS interneurons. Do group II mGluRs modulate the excitatory drive of NFS interneurons similarly in WT and *Fmr1* KO mice? For these experiments, we recorded from NFS interneurons in layer 5/6 and electrically evoked EPSCs in these neurons by stimulating layer 2/3 (**Figure 2.1**). In these cells we observed a multi-peaked EPSC response to electrical stimulation (**Figure 4.4 Ai and Bi**), and so we measured the area of the evoked response (charge) in these neurons. In WT animals, the control EPSC averaged 2.9 ± 0.4 pC, and application of APDC led to a significantly attenuated response (APDC: 1.1 ± 0.2 pC, n=13, $p<0.001$, paired t-test, **Figure 4.4 Ai-iii**). In *Fmr1* KO animals, the NFS EPSC was also suppressed by APDC (**Figure 4.4 Bi**), and this was statistically significant (Pre: 3.2 ± 0.6 pC, APDC: 0.7 ± 0.2 pC, n=10, $p<0.001$, paired t-test, **Figure 4.4 Bii-iii**). In the presence of APDC, the average WT EPSC amplitude was 38.2 ± 2.9 % of the control response, while the *Fmr1* KO was 22.7 ± 2.3 % of control, indicating a 15% increase in suppression of glutamatergic transmission by group II mGluRs in the *Fmr1* KO mouse. Statistical analysis determined this difference to be significant ($p<0.001$, t-test, **Figure 4.4 C**). Thus, *Fmr1* KO mice show exaggerated suppression of NFS interneuron excitatory currents, mediated by group II mGluR activation.

F. Group II mGluR-mediated suppression of excitatory transmission onto NFS interneurons is mediated presynaptically.

The suppression of EPSCs onto NFS interneurons could be due to activation of either

pre- or post-synaptic group II mGluRs. To determine the site of action, we next assessed miniature EPSCs (mEPSCs) in the presence of APDC (75μM, 40s). Changes in the frequency of mEPSCs are indicative of a change in release probability, and hence a presynaptic mechanism of origin. Alternatively, changes in mEPSC amplitude reflect a change in pre- and/or post-synaptic mechanisms. We recorded mEPSCs from NFS interneurons in both WT (**4.5 Ai**) and *Fmr1* KO mice (**4.5 Bi**). The average baseline mEPSC amplitude in WT mice was 21.2 ± 0.7 pA, and application of APDC did not alter mEPSC amplitude in 3 of 4 cells tested (APDC: 20.5 ± 1.1 pA, $p > 0.05$, K.S test). For mEPSC frequency, the baseline response was 3.7 ± 1.4 Hz, and application of APDC did not alter frequency in any cells tested (n=4, APDC: 0.8 ± 0.3 Hz, $p > 0.05$, K.S.test). Population averages of mEPSC amplitude and frequency were unaltered by APDC ($p > 0.05$, paired t-test, **Figure 4.5 Aii and iii)**. Activation of group II mGluRs had no effect on mEPSC amplitude in 3 of 4 *Fmr1* KO cells tested (Pre-drug: 26.0 ± 2.8 pA, APDC: 21.7 ± 1.1 pA, $p > 0.05$, K.S test). Similarly, there was no change in KO mEPSC frequency in 3 of 4 cells (Pre-drug: 1.2 ± 0.4 Hz, APDC: 0.8 ± 0.4 Hz, $p > 0.05$, K.S. test). The average population mEPSC response amplitude upon application of APDC, was not statistically significant ($p > 0.05$, paired t-test, **Figure 4.5 Bii**), and this was also true for mEPSC frequency ($p > 0.05$, paired t-test, **Figure 4.5 Biii**). We believe that no significant differences were observed in either mEPSC frequency or amplitude because the baseline number of excitatory events was minimal, indicating that pyramidal neurons are not participating in significant levels of AP-independent neurotransmitter release in a slice preparation. Subsequently, two alternative methods to localize group II mGluRs at the excitatory synapse onto SST+ interneurons were investigated.

We next quantified the paired-pulse ratio (PPR) of two evoked excitatory currents with an interstimulus interval of 30-100ms (**Figure 4.6**). Any changes in paired-pulse ratio have been shown to be indicative of a change in presynaptic release probability. In 3 of 6 wild-type cells tested (50%, **Figure 4.6 C**), application of APDC (15-75μM, 40s) led to a significant change in the paired pulse ratio (Figure **4.6 Ai-iii**). Of these three cells, two showed a decrease in the ratio while one cell showed an increase. The paired pulse ratio was also significantly altered by APDC application in 3 of 5 *Fmr1* KO NFS interneurons (60%, **Figure 4.6 Bi-iii**). In all 3 cells, the paired pulse ratio increased (**Figure 4.6 C**). The mixed effects we see in paired pulse ratio did not allow us to determine the site of action of the group II mGluRs.

Finally, we quantified changes in excitatory events evoked in the presence of modified extracellular solution containing strontium (2mM) in place of calcium (**Figure 4.7**). Strontium prolongs the duration of neurotransmitter release and creates asynchronous release, thereby reducing the temporal summation of events postsynaptically. This occurs due to strontium-binding of voltage gated calcium channels at the axon terminal, effectively prolonging the postsynaptic excitatory response and separating it into smaller "quantal-like" events from which frequency and amplitude measurements can be quantified. In WT NFS interneurons (**Figure 4.7Ai)**, the average baseline number of events was 13.4 ± 1.6, and APDC significantly reduced the number of events to 4.6 ± 1.4 ($n=11$, $p < 0.05$, paired t-test). A similar trend was observed in *Fmr1* KO animals (**Figure 4.7 Bi)**. Prior to drug application, the average baseline number of events in *Fmr1* KO NFS cells was 10.6 ± 4.8, and these events were significantly decreased in the presence of APDC ($n=5$, APDC: 6.0 ± 4.4, $p<0.05$, paired t-test). APDC decreased the number of events in the WT to 31.7 ± 7.7 % of control, while it decreased the *Fmr1* KO number of events to 42.8 ± 15.9 % of control (**Figure 4.7D**). We also assessed changes in amplitude of

the strontium excitatory events to ascertain potential postsynaptic effects. In WT animals (**Figure 4.7 Ai**), 6 of 8 NFS interneurons show no difference in amplitude of the events in response to APDC (K.S. test, $p > 0.05$). The pooled amplitude of all WT NFS neurons in the presence of APDC was 78.2 ± 6.0 % of control (**Figure 4.7 C**). In the *Fmr1* KO mouse (**Figure 4.7 Bi**), 4 of 5 NFS interneurons show no change in amplitude after application of APDC (K.S.test, $p > .05$). The average amplitude for all *Fmr1* KO NFS neurons upon application of group II mGluRs was 92.7 ± 3.5 % of control (**Figure 4.7 C**). Using these results, we conclude that although group II mGluRs are present both pre- and post- synaptically at glutamatergic synapses onto NFS interneurons, the major site of action of group II mGluR-mediated suppression of evoked EPSCs is likely presynaptic.

G. The intrinsic properties of layer 2/3 NFS interneurons are similar between WT and Fmr1 KO mice.

Is the group II mGluR-mediated suppression of excitatory drive onto *Fmr1* KO NFS interneurons specific to layer 5/6? To answer this question, we performed whole cell recordings from NFS interneurons in layer 2/3 of the visual neocortex. We first quantified both input resistance and membrane potential of WT and *Fmr1* KO NFS interneurons (**Figure 4. 8Ai and ii**). WT NFS interneurons had an average input resistance of 321.2 ± 47.7 MΩ (n=16, **Figure 4.8 B**). In *Fmr1* KO mice (**Figure 4.8 Aii**), the input resistance was less than that seen in WT neurons (235.1 ± 17.8 MΩ, n=9), but this decrease was not significant ($p>0.05$, t-test, **Figure 4.8B**). We also measured resting membrane potential, and determined the average value to be -64.6 ± 1.6 mV in wild type mice (n=16, **Figure 4.8C**). The average resting membrane potential in *Fmr1* KO NFS interneurons was -67.1 ± 1.5 mV, and this was not significantly different from

the wild type cells (n=9, p>0.05, independent t-test, **Figure 4.8C**). These results are summarized below (**Table 2.6**).

Table 4.3. Intrinsic properties of layer 2/3 SST+ interneurons in WT and *Fmr1* KO mice.

	Input Resistance (MΩ)	***Membrane Potential (mV)***
Wild Type	321.2 ± 47.7 (n=16)	-64.6 ± 1.6 (n=16)
Fmr1 KO	235.1 ± 17.8 (n=9)	-67.1 ± 1.5 (n=9)
p	0.12 t-test	0.58 t-test

H. Exaggerated group II mGluR-mediated suppression of Fmr1 KO NFS interneuron EPSCs is layer specific.

After quantifying these basic intrinsic properties, a stimulating electrode was placed into layer 4 of the visual neocortex to evoke excitatory currents in layer 2/3 NFS interneurons (**Figure 2.1**). The baseline area response of wild type NFS interneurons was 4.0 ± 0.4 pC and APDC application significantly reduced the area to 0.9 ± 0.2 pC (n=16, p<0.001, paired t-test, **Figure 4.9 Ai-iii**). The area response after APDC application was 21.2 ± 2.8 % of the control response (n=16, **Figure 4.9C**). In *Fmr1* KO superficial NFS interneurons, a similar change was observed (**Figure 4.9 Bi-iii**). The average pre-drug response measured 3.1 ± 0.5 pC, and after APDC application the average EPSC charge was reduced to 0.9 ± 0.2 pC (n=9, p<0.001, paired t-test, Figure **4.9 10Bi-iii**). The *Fmr1* KO response in the presence of APDC, showed a 67.4 ± 2.8% reduction (n=9, **Figure 4.9C**). Comparison of the area response between WT and *Fmr1* KO animals was not significant (p>0.05, t-test, **Figure 4.9 C**). Thus, we determined that the enhanced suppression we see in *Fmr1* KO layer 5/6 NFS interneurons in response to group II mGluR activation is a layer specific dysregulation of the visual neocortex.

4.4 Discussion

In these studies, we investigated the effect of group II mGluR activation on the modulation of excitatory drive onto visual neocortical interneurons in the *Fmr1* KO mouse. Although neocortical hyperexcitability is speculated to be a major contributor of several Fragile X phenotypes, functional neocortical studies remain underrepresented in the Fragile X literature. Here we report that group II mGluR activation leads to suppression of glutamatergic transmission onto NFS interneurons in the layer 5/6 visual neocortex, and this process is exaggerated in the *Fmr1* KO mouse (**Figure 4.11**). We have also shown previously that this leads to disinhibition onto layer 5/6 pyramidal neurons in the *Fmr1* KO, and presumably creates a hyperexcitable layer 5/6 network (**Figure 4.11**).

Perhaps one of the most interesting results of this study, was the observation that group II mGluR signaling is altered in the visual neocortex in the absence of FMRP. This was highly unexpected, as only one study to-date has ever implicated group II mGluRs in FXS pathology. This study found that chronic administration of a group II mGluR antagonist could restore the exaggerated mGluR-LTD phenotype observed in the hippocampus of *Fmr1* KO mice (Choi et al., 2011). It was difficult for the authors to explain these results as no previous studies have experimentally demonstrated the presence of FMRP downstream of the group II mGluR signaling cascade. These authors suggest that the canonical signaling cascades of group I and group II mGluRs crosstalk due to the fact that they are both capable of binding Gq and Gi g-proteins. Thus, the authors suggest that it is actually the loose association of group II mGluRs with Gq signaling that may be responsible for the restoration of LTD in the presence of a group II mGluR antagonist. We do not believe this to be the case in our results. It is now known that FMRP does not interact directly with the canonical Gq signaling pathway (Huber et al., 2001;

Gallagher et al., 2004), so in the event that presynaptic group II mGluRs did loosely associate with Gq binding protein, we would expect this to have no effect when activated in the *Fmr1* KO mouse. Interestingly, two other pathways that are modulated by group II mGluRs include the ERK/MAPK pathway and the PI3K-mTOR pathway (Niswender and Conn, 2010). Both of these pathways lie downstream from group I mGluRs. The PI3K-mTOR pathway interacts with activates FMRP protein to negatively regulate protein translation (Bhakar, Dolen, & Bear., 2012), so it is possible that altered modulation of this pathway by group II mGluRs in the absence of FMRP is causing the changes we observe. Additionally, group II mGluRs bind presynaptic ion channels, the result of which is decreased neurotransmitter release. It has been shown that the Bγ subunit of mGluRs can interact with both K^+ and Ca^{2+} channels, including P/Q Ca^{2+} channels that are abundantly located at the axon terminal (O'Connor et al., 1999). The mRNA targets of FMRP also include regulate the several different potassium channels and most calcium channels (Brager and Johnsten, 2014). Therefore, I suggest that some of the same ion channels modulated by group II mGluRs are upregulated in the absence of FMRP. Finally, Bγ subunits have also been shown in binding assays to associate directly with exocytotic release machinery proteins including isolated binding with syntaxin and/or SNAP-25 as well as combined binding with SNARE complexes comprised of syntaxin, SNAP-25, and VAMP (Blackmer et al., 2001). These proteins are also targets of FMRP. Thus, it is possible that activation of group II mGluRs in the *Fmr1* KO leads to altered inhibition of release machinery by GBγ upon dissociation from the g-protein complex.

Another interesting result of our study was the discovery that the deficits we see in group II mGluR signaling in the *Fmr1* KO are mediated presynaptically. It is widely accepted that group II mGluRs are located abundantly in the extrasynaptic space of presynaptic neurons, where

they can be activated in instances of excess glutamate in the synapse (Scanziani, 1997). However, the axonal or presynaptic role of FMRP remains largely unknown. FMRP targets mRNAs that comprise one-third of the presynaptic proteome (Darnell et. al 2011) and is expressed presynaptically in granules (Antar et al., 2006; Christie et al., 2009; Till et al., 2012, Akins et al., 2009; Akins et al., 2012), indicating that its absence is likely to have drastic consequences on presynaptic function of the synapse. A recent electrophysiological study using *Fmr1* KO mosaic mice, demonstrated that loss of presynaptic FMRP recapitulates the decrease in excitatory drive onto FS interneurons in layer 4 of the somatosensory cortex (Patel et al, 2013). Deletion of postsynaptic FMRP could not recapitulate this deficit. Furthermore, loss of presynaptic FMRP had no effect on excitatory synapses onto excitatory neurons, indicating that the presynaptic function of FMRP at excitatory neurons is target cell specific. This is intriguing when we consider that our data shows defective excitatory drive onto NFS interneurons with no changes in excitatory drive onto pyramidal neurons, and this effect is mediated by presynaptic group II mGluRs. Incidence of this has been observed in a human with a unique point mutation in the *Fmr1* gene that led to loss of function of presynaptic FMRP with intact function of postsynaptic FMRP. The result of this mutation was a child with global developmental delay, intellectual disability, and intractable seizures (Myrick et al., 2015).

What is the consequence for visual processing in the *Fmr1* KO mouse in the presence of exaggerated group II mGluR signaling onto NFS interneurons? This question requires understanding the role of NFS interneurons in the neocortical network. Local glutamatergic inputs from pyramidal neurons onto NFS interneurons are facilitating, unlike those of PV+ interneurons which are depressing. This facilitating capability, allows SST+ interneurons to increase their feedback inhibition as the rate and duration of presynaptic discharge increases. It

is speculated that this unique feature, makes NFS interneurons likely to be preferentially activated during periods of high network activity. Repetitive stimulation during high network activity will elevate glutamate levels in the synapse (Scanziani et al., 1997), and this excess glutamate would likely spillover at the synapse and activate extrasynaptically located group II mGluRs. This activation, in turn, would help limit further cortical excitation by decreasing neurotransmitter release. In the case of the *Fmr1* KO mouse, however, the preferential exaggeration of glutamatergic suppression at pyramidal neuron synapses onto somatostatin interneurons, would be expected to cause an imbalance of the ratio of excitation/inhibition in layer 5/6 neocortical circuitry tending toward hyperexcitability. The majority of layer 5/6 pyramidal neurons in the visual cortex send feedback projections to layer 2/3 neurons that interact with higher order visual centers. So it is likely that these centers will also be inundated with excitatory input, which could cause problems with sensory integration and potentially epileptic activity. Further, some layer 5/6 pyramidal neurons project to subcortical structures such as the pulvinar nucleus of the thalamus and the superior colliculus, suggesting that these structures may also be affected.

One limitation of our study is that we did not investigate the third interneuron subtype found in the layer 5/6, namely the serotonin 5HT3a receptor expressing interneurons. It is, therefore, possible that group II mGluRs modulate excitatory transmission of these interneurons, and that this modulation is altered in the *Fmr1* KO mouse. However, we speculate that because these interneurons comprise no more than 15% of layer 5/6 interneurons (Rudy et al., 2011), it is likely that any potential changes that exist are relatively small compared to the alterations we see in excitation of NFS interneurons. Additionally, methodological limitations do not allow us to precisely identify the source of the glutamatergic inputs onto our NFS interneurons, and so we

cannot say with certainty which excitatory axons are affected in the *Fmr1* KO. However, we hypothesize that the majority of excitatory inputs that we were stimulating originate within V1. In several instances the subcortical area of our slices was removed, and we still observed changes in group II mGluR signaling onto NFS neurons. Furthermore, thalamic afferents are not known to project to layer 5, and have very weak connections to NFS neurons in general (Beierlein and Connors 2000; Beierlein and Connors 2003).

In conclusion, we now add to the body of literature by implicating group II mGluRs in the pathology of the visual system in FXS. Human studies indicate that FMRP is particularly abundant in regions of the magnocellular pathway, and that this pathway may be more susceptible to loss of FMRP. This anatomical study is supported with evidence showing that children with FXS have reduced sensitivity for psychostimuli that probe the M pathway but maintain sensitivity to those stimuli that probe the P pathway (Kogan et al., 2004). Affected individuals with FXS also show marked visual-motor deficits. V1 of the *Fmr1* KO recapitulates the abnormal spine morphology seen in layer 5/6 visual neocortex of humans, and also exhibits a hyperconnected profile in magnetic resonance imaging studies (Haberl et al., 2015). Thus it is our hope, that this discovery leads the way to understanding the circuit mechanisms that give rise to these visual defects, and that restoration of inhibition may potentially serve as a means to rescue these sensory impairments.

APPENDIX

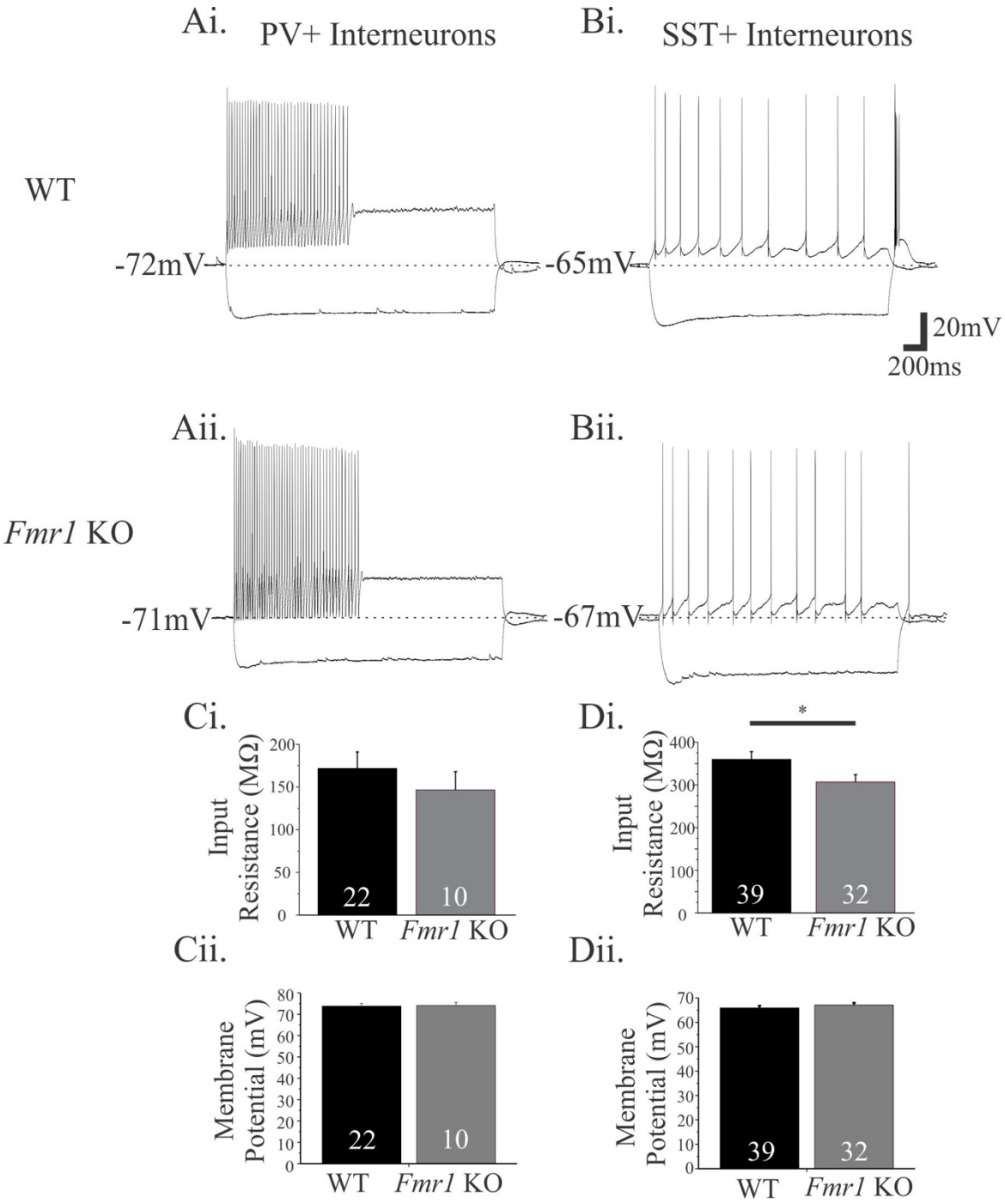

Figure 4.1. Intrinsic excitability is decreased in layer 5/6 *Fmr1* KO visual neocortical NFS interneurons, but not FS interneurons.
Ai. Representative WT trace of a layer 5/6 FS PV+ interneuron obtained from a current-step injection protocol. ii. Same as Ai but for *Fmr1* KO. Bi. Representative WT trace of a layer 5/6 NFS SST+ interneuron obtained from a current-step injection protocol. ii. Same as Bi but for *Fmr1* KO. Ci. Average input resistance of FS PV+ interneurons for both WT (n=22) and *Fmr1* KO (n=10). No significant differences in input resistance or membrane potential were observed in PV+ interneurons between genotypes ($p > 0.05$, t-test). Di. Average input resistance of NFS

Figure 4.1. (cont'd)

SST+ interneurons for both WT (n=39) and *Fmr1* KO (n=32). ii. Average membrane potential of NFS SST+ interneurons for both WT (n=39) and Fmr1 KO (n=22). No significant differences in input resistance or membrane potential were observed in NFS SST+ interneurons between genotypes ($p > 0.05$, t-test).

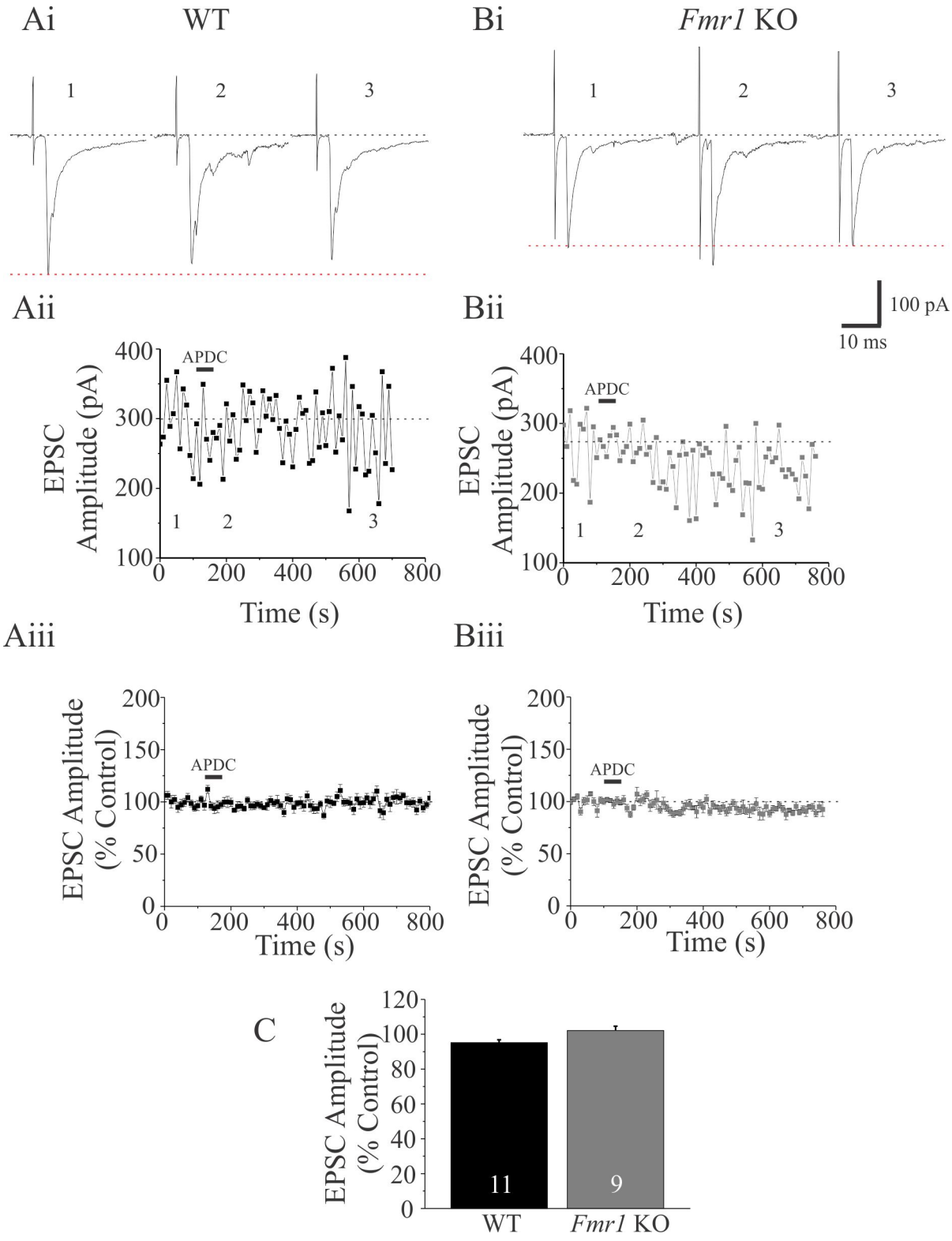

Figure 4.2. Group I mGluRs do not modulate excitatory synaptic transmission onto WT and *Fmr1* KO layer 5/6 FS interneurons.

Figure 4.2. (cont'd)

Ai. Representative trace showing the response of a layer 5/6 wild type FS interneuron EPSC to brief application of group I mGluR agonist DHPG (25μM). Aii. Raw time course of the change in peak amplitude in a single wild type FS cell before, during, and following application of DHPG. Aiii. Wild type normalized time course of the population peak amplitude change to DHPG application (n=11). Bi-iii. Same as Ai-iii, but for *Fmr1* KO. C. Average FS interneuron EPSC amplitude expressed as % of control for all cells tested in both WT and *Fmr1* KO (WT=11, KO=9). No statistical differences were found between genotypes ($p>0.05$, t-test).

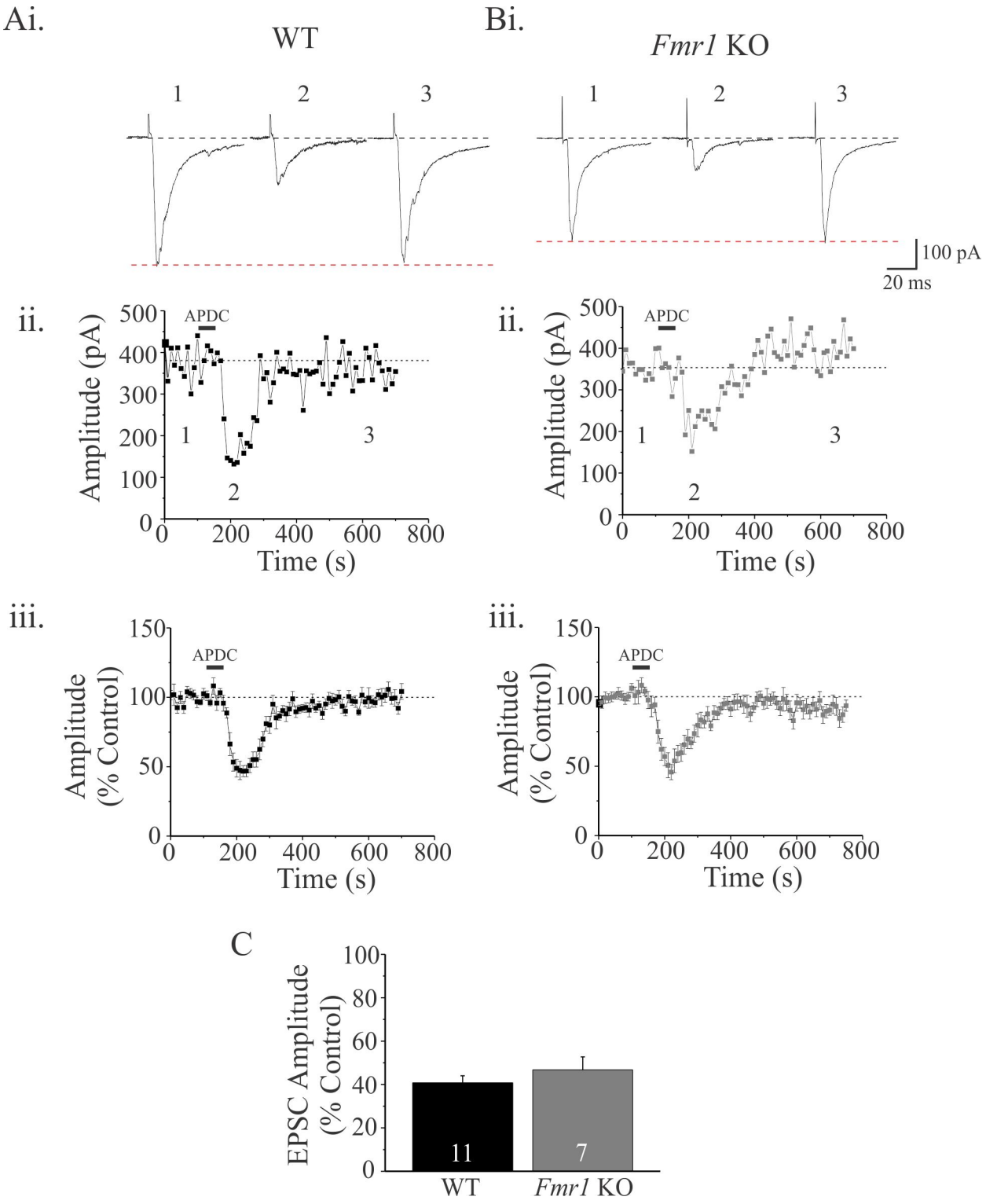

Figure 4.3. Group II mGluR-mediated modulation of excitatory transmission onto FS interneurons is unaltered in the visual neocortex of the *Fmr1* KO mouse.
Ai. Representative trace showing a wild type FS interneuron EPSC evoked by electrical stimulation of layer 2/3. Traces show WT EPSC response before, during, and after brief

Figure 4.3. (cont'd)

application of APDC (75 μM). Aii. Raw time course of the change in WT FS interneuron EPSC amplitude in response to APDC. Aiii. WT population data showing the normalized time course of the change in peak amplitude in response to APDC (n=11). Bi-iii. Same as Ai-iii, but for *Fmr1* KO (n=7). C. Average FS interneuron EPSC amplitude in response to APDC expressed as % of control for both WT and *Fmr1* KO (WT=11, KO=7). No statistical differences were found between peak amplitude of WT and *Fmr1* KO in the presence of APDC ($p > 0.05$, t-test).

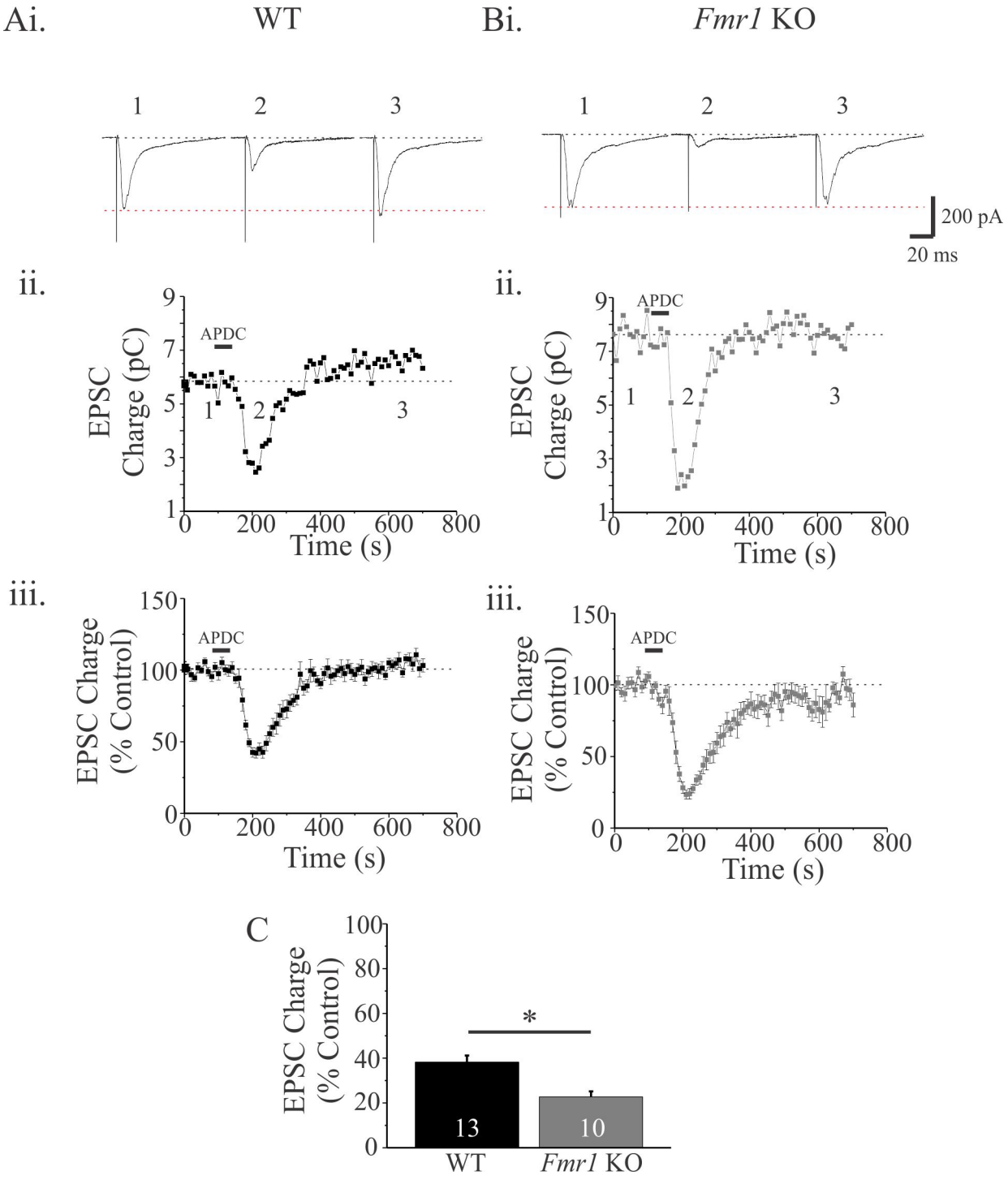

Figure 4.4. Group II mGluR-mediated suppression of excitatory transmission onto NFS interneurons is exaggerated in the visual neocortex of the *Fmr1* KO mouse.
Ai. Representative trace showing a wild type NFS interneuron EPSC evoked by electrical stimulation of layer 2/3. Traces show WT EPSC response before, during, and after brief application of APDC (75 μM). Aii. Raw time course of the change in NFS WT EPSC charge before, during, and after APDC application. Aiii. WT population data showing the normalized

Figure 4.4. (cont'd)

time course of the charge in response to APDC (n=13). Bi-iii. Same as Ai-iii, but for the *Fmr1* KO. C. Average NFS interneuron population EPSC charge in the presence of APDC expressed as % of control for both wild type and *Fmr1* KO (WT=13, KO=10). *Fmr1* KO mice show a statistically significant increase in the group II mGluR-mediated suppression of excitatory drive onto SST+ interneurons compared to WT ($p = 5.3 \times 10^{-4}$, t-test).

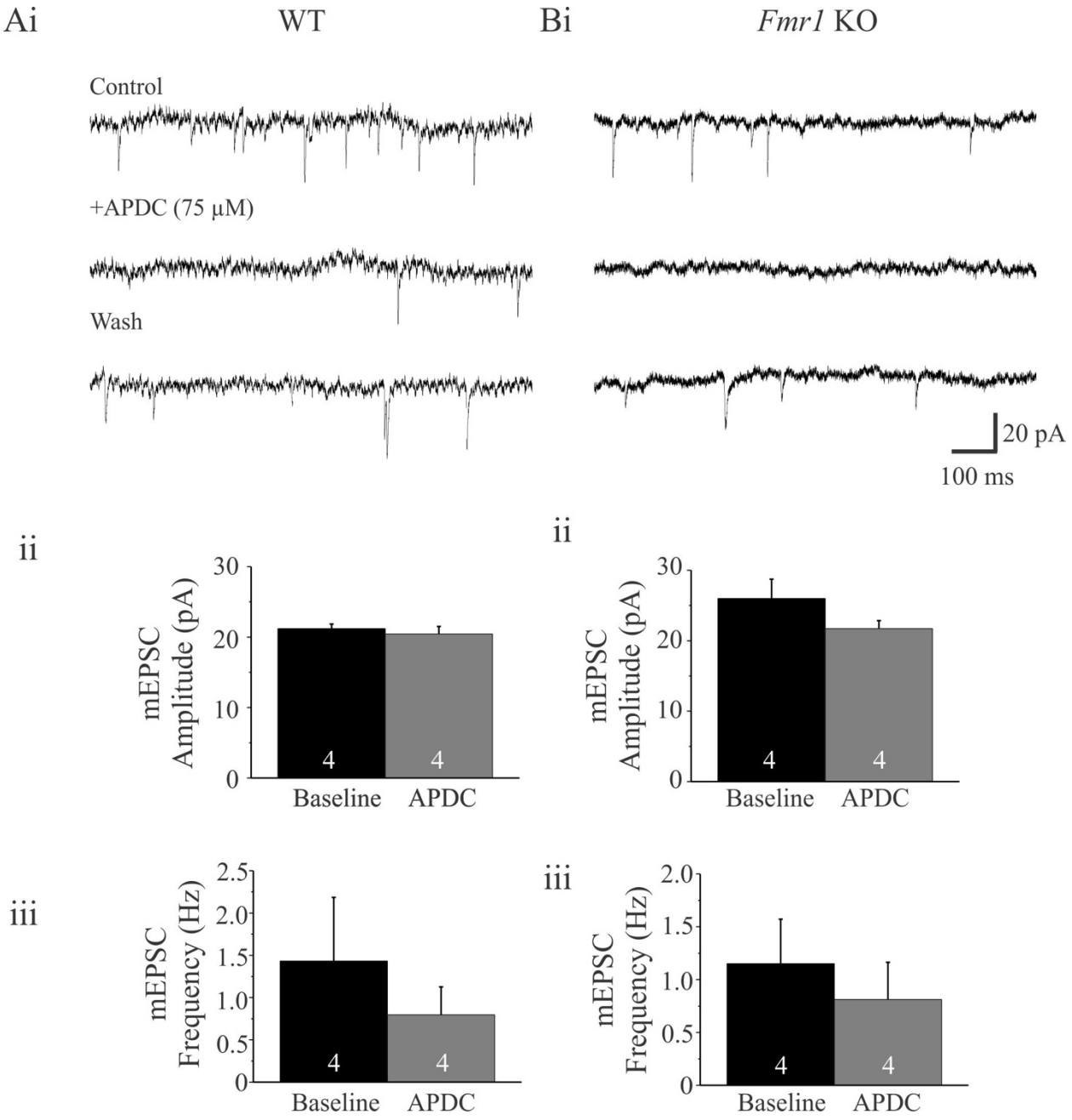

Figure 4.5. Group II mGluR activation does not alter miniature EPSC amplitude or frequency in WT and F*mr1* KO layer 5/6 visual neocortical NFS interneurons.
Ai. Raw data showing a WT miniature EPSC trace before, during, and after recovery from application of group II mGluR agonist APDC (75 µM). Aii. WT population data showing average change in mEPSC amplitude in response to group II mGluR activation (WT=4). Aiii. Population data showing WT mEPSC frequency change in response to APDC (WT=4). Pooled population data show no change in WT amplitude or frequency in response to application of APDC ($p > 0.05$, t-test). Bi-iii. Same as Ai-iii, but for *Fmr1* KO. Statistical analysis reveals no

Figure 4.5. (cont'd)

significant differences in mEPSC amplitude or frequency in response to group II mGluR activation in *Fmr1* KO layer 5/6 NFS interneurons.

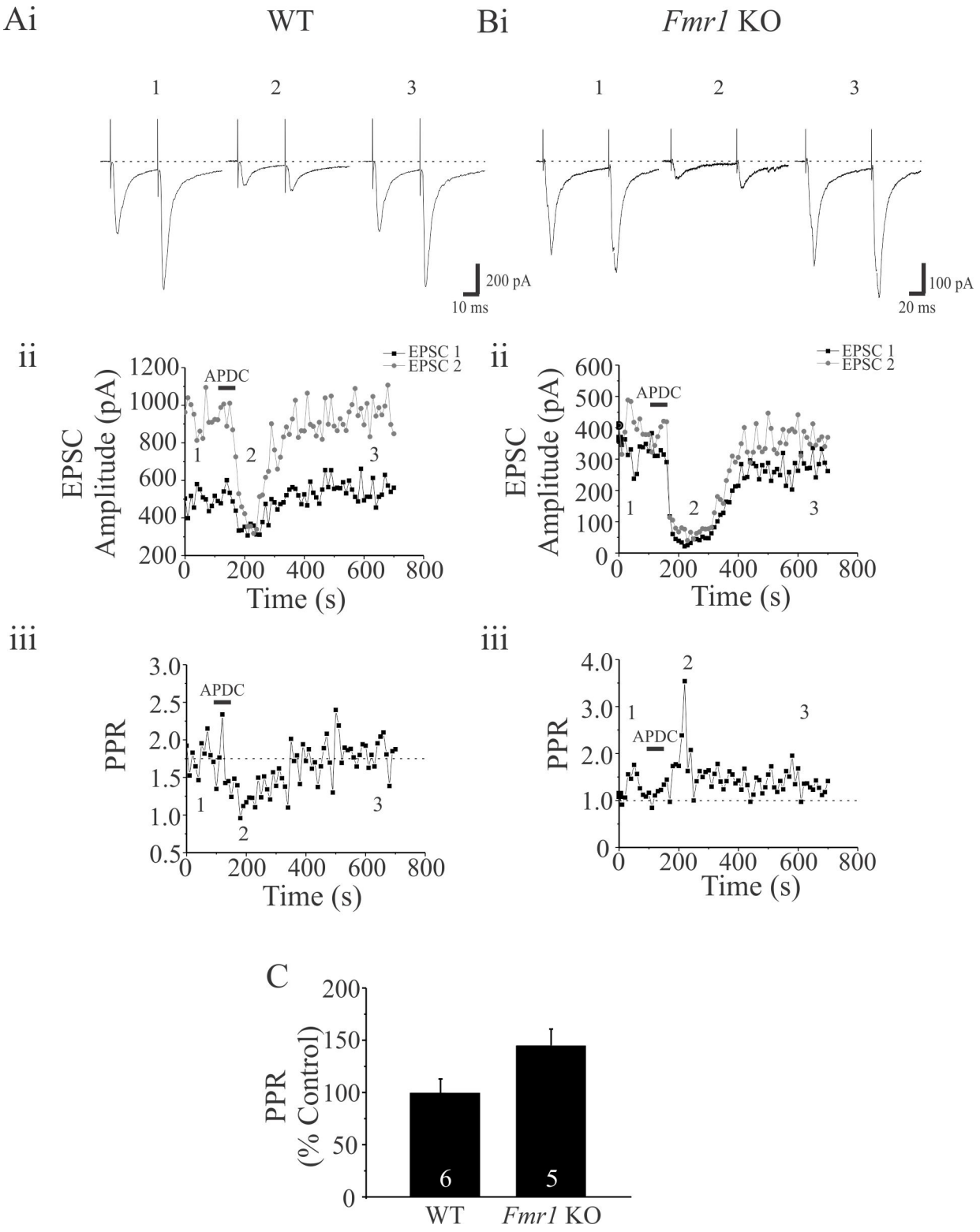

Figure 4.6. Group II mGluR-mediated suppression of EPSCs in layer 5/6 NFS interneurons leads to a change in paired pulse ratio.

Ai. Representative traces showing wild type paired EPSCs before, during, and after application of group II mGluR agonist APDC (75 μM). Aii. Raw time course of the change in amplitude of

Figure 4.6. (cont'd)

EPSC 1 (black) and EPSC 2 (gray) in response to APDC. Aiii. Raw time course of the change in paired pulse ratio (PPR) in response to APDC. Bi-iii. Same as Ai-iii, but in the *Fmr1* KO. C. Average population PPR in the presence of APDC expressed as % of control for both WT and Fmr1 KO (WT=6, KO=5). Pooled data show no statistical difference in PPR between WT and *Fmr1* KO ($p>0.05$, t-test).

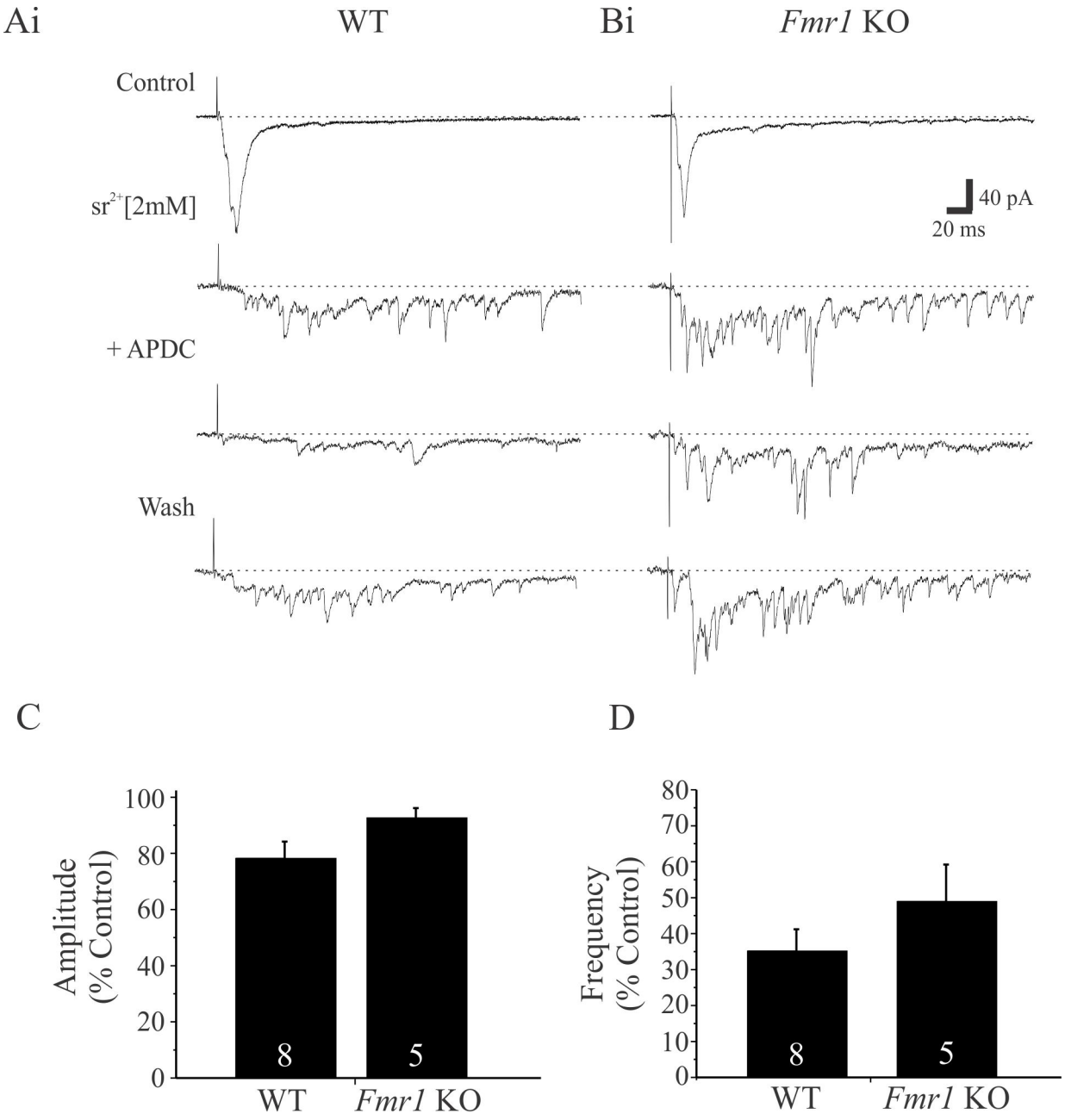

Figure 4.7. EPSCs evoked in strontium show a decrease in frequency in response to application of group II mGluR activation in both WT and *Fmr1* KO layer 5/6 NFS interneurons.

Ai. Raw data showing a WT NFS interneuron EPSC response in standard Ca^{2+} physiological saline, following a substitution with Sr^{2+} saline, during application of group II mGluR agonist APDC (15 μM), and after drug washout. Bi. Same as Ai, but for *Fmr1* KO. C. Population change in mEPSC amplitude in response to application of APDC. D. Population change in mEPSC frequency in response to APDC. For both C and D, black bars indicate the average mEPSC response from the pooled population data. WT and *Fmr1* KO cells show a change in mEPSC frequency without showing a change in mEPSC amplitude (WT=8, KO=5), indicating a predominantly presynaptic effect of group II mGluRs.

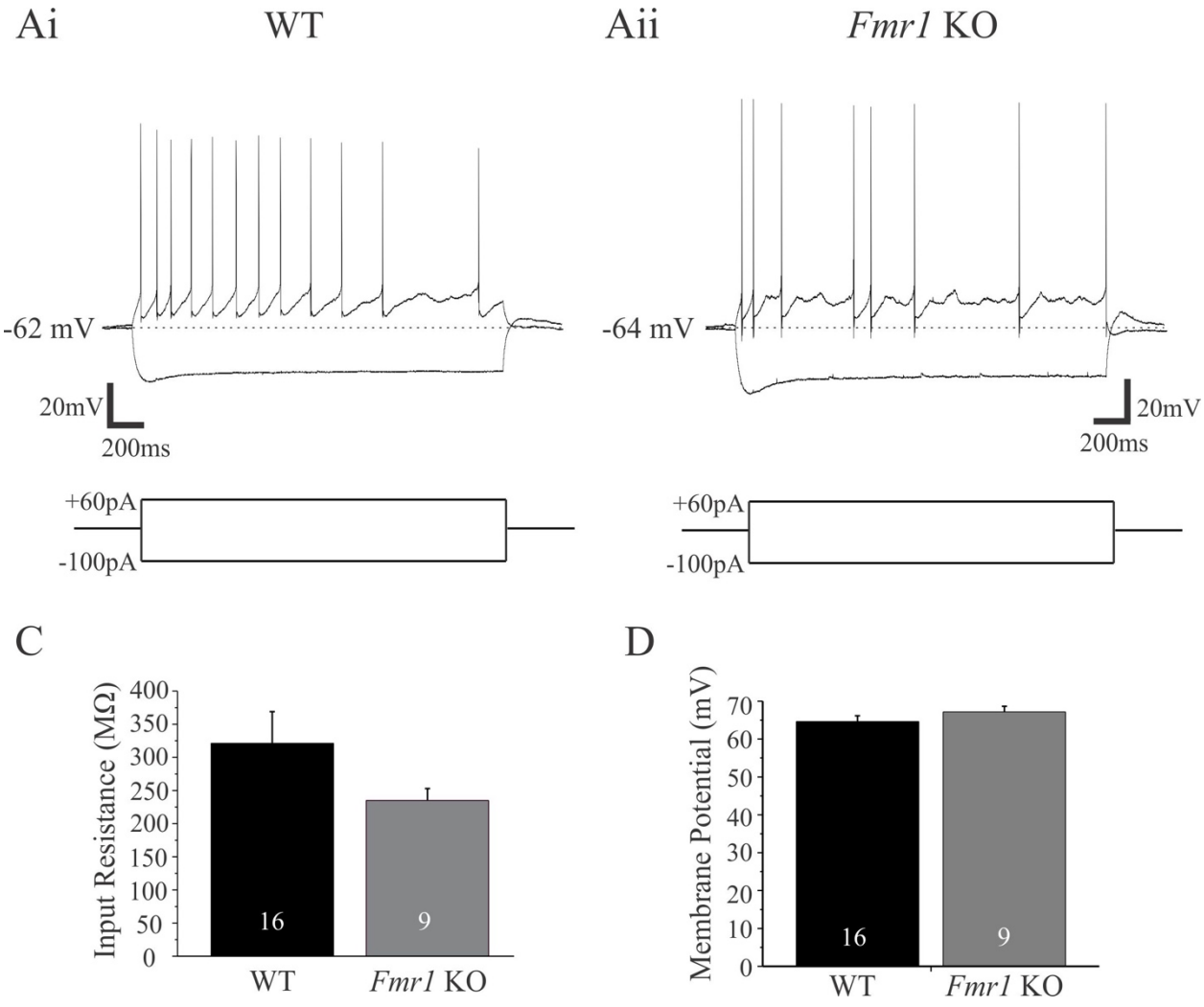

Figure 4.8. The intrinsic properties *Fmr1* KO layer 2/3 NFS interneurons are unaltered. Ai. Representative tracing of a layer 2/3 wild type NFS interneuron during a current-step injection protocol. Aii. Similar to figure Ai but recorded in a layer 2/3 NFS interneuron from the *Fmr1* KO mouse. B. Population data show the average input resistance in wild type and *Fmr1* KO cells (WT=16, KO=9). C. Population data show the average membrane potential of WT and *Fmr1* KO cells (WT=16, KO=9, $p > 0.05$). No statistically significant differences were detected between genotypes for either membrane potential or input resistance ($p > 0.05$, t-test).

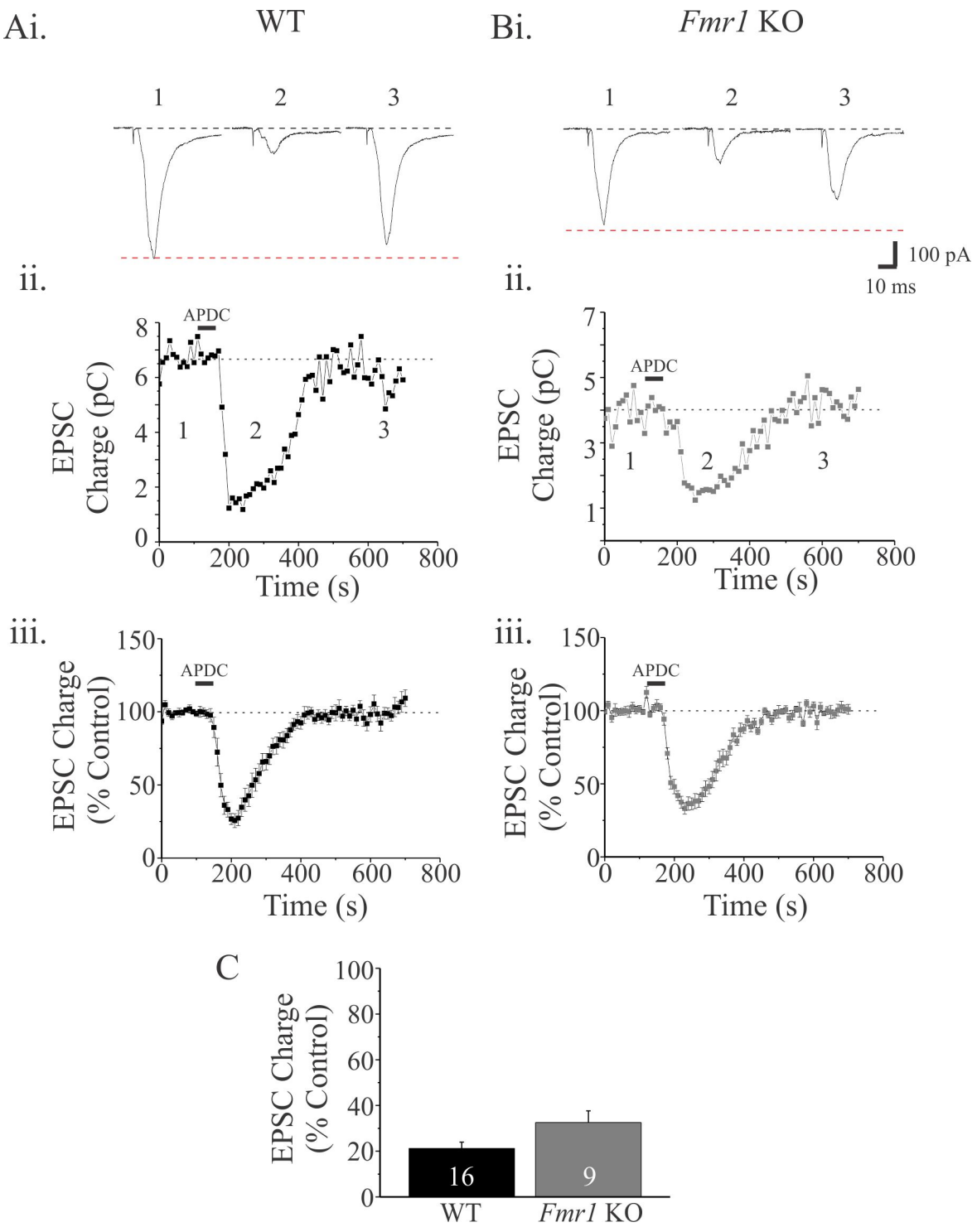

Figure 4.9. Altered group II mGluR-mediated suppression of NFS interneuron EPSCs in the *Fmr1* KO is layer specific.

Ai. Representative trace showing a layer 2/3 wild type NFS interneuron EPSC evoked by electrical stimulation of layer 4. Traces show EPSC response before, during, and after brief application of APDC (75 μM). Aii. Raw time course of the change in WT EPSC charge before, during, and after APDC application. Aiii. WT population data showing the normalized time

Figure 4.9. (cont'd)

course of the change in charge in response to APDC (n=16). Bi-iii. Same as Ai-iii, but for *Fmr1* KO (n=9). C. Average population EPSC charge in the presence of APDC expressed as % of control for both WT and *Fmr1* KO (WT=16, KO=9). No statistical differences were found between the charge of WT and *Fmr1* KO in the presence of APDC ($p > 0.05$, t-test).

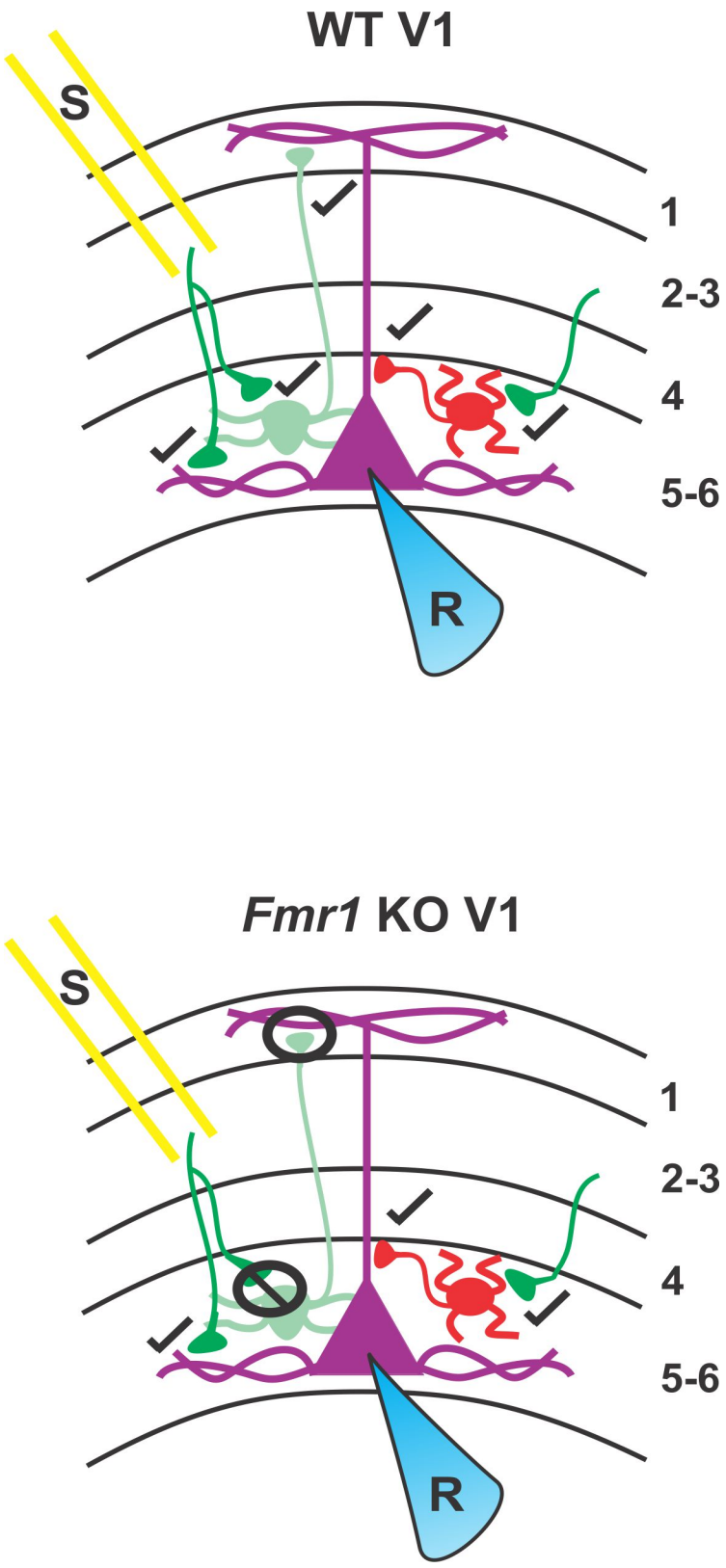

Figure 4.10. Group II mGluR-mediated suppression of EPSCs on NFS interneurons is increased in the *Fmr1* KO mouse.

Figure 4.10. (cont'd)

Top: Circuit diagram for a WT mouse. In chapter 4, excitatory postsynaptic currents (EPSCs) were evoked using a stimulating electrode placed in layer 2/3 (S). We show that activation of group II mGluRs leads to suppression of EPSCs at glutamatergic synapses onto layer 5/6 FS interneurons (red neuron) and NFS interneurons (green neuron) in WT mice. Bottom: Circuit diagram for an *Fmr1* KO mouse. The magnitude of EPSC suppression is similar between WT and *Fmr1* KO mouse on FS interneurons (red neuron, black checkmark). However, the magnitude of suppression of EPSCs on NFS interneurons (black circle, bottom) is enhanced in the *Fmr1* KO.

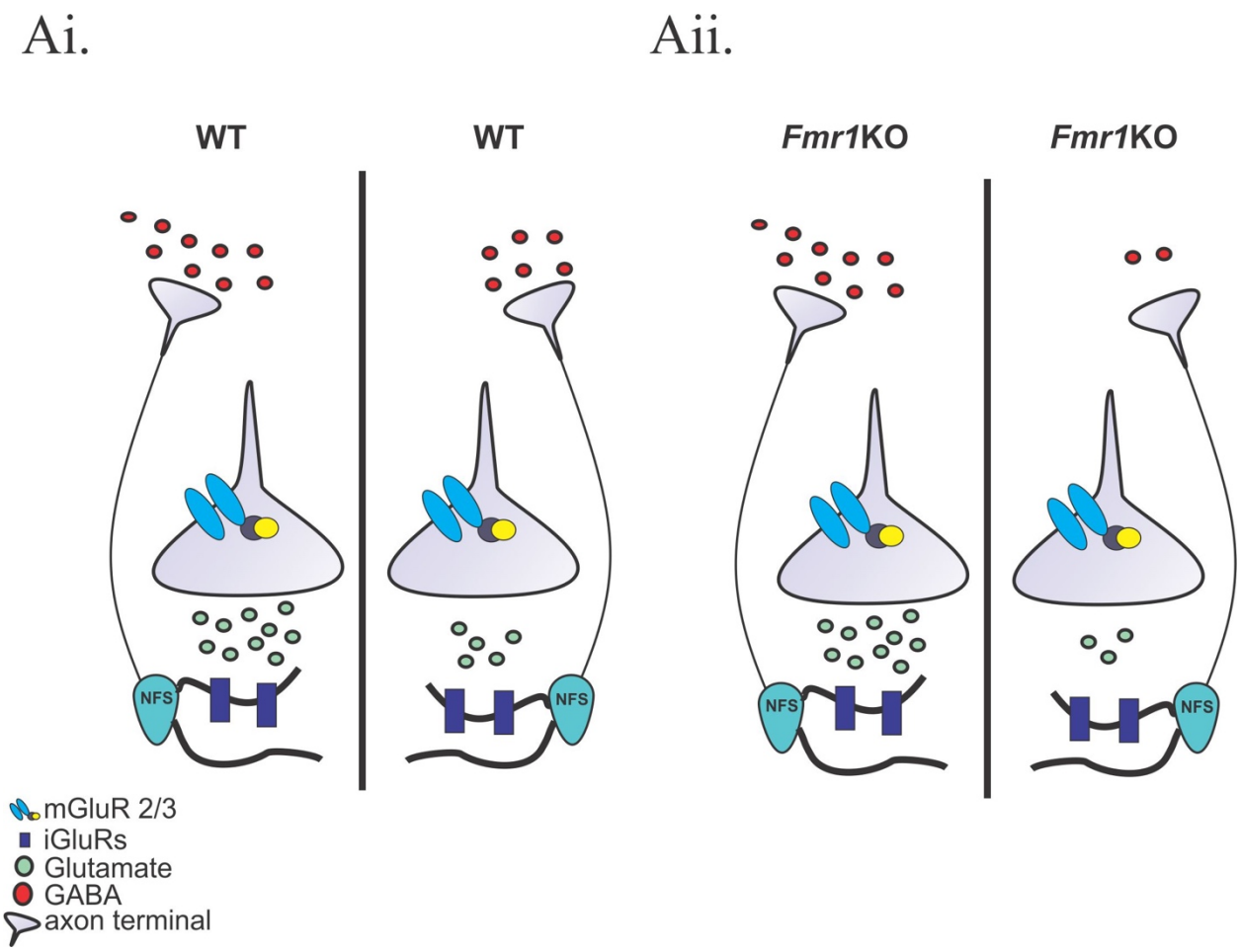

Figure 4.11. Activation of presynaptic group II mGluRs leads to exaggerated suppression of excitatory drive onto NFS interneurons and disinhibition of GABAergic signaling in the visual neocortex of the *Fmr1* KO mouse.
A schematic diagram showing changes in the layer 5/6 microcircuit of the visual neocortex in the *Fmr1* KO mouse. Ai. Activation of presynaptic group II mGluRs in WT mice leads to a decrease in glutamatergic transmission onto NFS interneurons in layer 5/6 of V1. This leads to a decrease in inhibitory transmission at GABA synapses. Aii. Activation of presynaptic group II mGluRs in the *Fmr1* KO mouse, leads to exaggerated decreases in glutamatergic neurotransmission onto NFS interneurons. This exaggeration leads to disinhibition of excitatory pyramidal neurons, and potential hyperexcitability. NFS interneurons predominantly target the dendritic tufts of layer 5 pyramidal neurons, but may also synapse onto the dendrites of neurons in layer 2-4. The net effect of these microcircuit changes is expected to be a disinhibited V1 network. This could affect feed forward signaling to higher order cortical areas connected to V1, as well as feedback signaling to subcortical structures.

REFERENCES

REFERENCES

Akins, M. R., Berk-Rauch, H. E., & Fallon, J. R. (2009). Presynaptic translation: stepping out of the postsynaptic shadow. *Front Neural Circuits, 3*, 17. doi:10.3389/neuro.04.017.2009

Akins, M. R., Leblanc, H. F., Stackpole, E. E., Chyung, E., & Fallon, J. R. (2012). Systematic mapping of fragile X granules in the mouse brain reveals a potential role for presynaptic FMRP in sensorimotor functions. *J Comp Neurol, 520*(16), 3687-3706. doi:10.1002/cne.23123

Antar, L. N., Afroz, R., Dictenberg, J. B., Carroll, R. C., & Bassell, G. J. (2004). Metabotropic glutamate receptor activation regulates fragile x mental retardation protein and FMR1 mRNA localization differentially in dendrites and at synapses. *J Neurosci, 24*(11), 2648-2655. doi:10.1523/JNEUROSCI.0099-04.2004

Antar, L. N., Li, C., Zhang, H., Carroll, R. C., & Bassell, G. J. (2006). Local functions for FMRP in axon growth cone motility and activity-dependent regulation of filopodia and spine synapses. *Mol Cell Neurosci, 32*(1-2), 37-48. doi:10.1016/j.mcn.2006.02.001

Beierlein, M., Gibson, J. R., & Connors, B. W. (2000). A network of electrically coupled interneurons drives synchronized inhibition in neocortex. *Nat Neurosci, 3*(9), 904-910. doi:10.1038/78809

Beierlein, M., Gibson, J. R., & Connors, B. W. (2003). Two dynamically distinct inhibitory networks in layer 4 of the neocortex. *J Neurophysiol, 90*(5), 2987-3000. doi:10.1152/jn.00283.2003

Bhakar, A. L., Dolen, G., & Bear, M. F. (2012). The pathophysiology of fragile X (and what it teaches us about synapses). *Annu Rev Neurosci, 35*, 417-443. doi:10.1146/annurev-neuro-060909-153138

Blackmer, T., Larsen, E. C., Takahashi, M., Martin, T. F., Alford, S., & Hamm, H. E. (2001). G protein betagamma subunit-mediated presynaptic inhibition: regulation of exocytotic fusion downstream of Ca2+ entry. *Science, 292*(5515), 293-297. doi:10.1126/science.1058803

Brager, D. H., & Johnston, D. (2014). Channelopathies and dendritic dysfunction in fragile X syndrome. *Brain Res Bull, 103*, 11-17. doi:10.1016/j.brainresbull.2014.01.002

Chang, Y. M., & Luebke, J. I. (2007). Electrophysiological diversity of layer 5 pyramidal cells in the prefrontal cortex of the rhesus monkey: in vitro slice studies. *J Neurophysiol, 98*(5), 2622-2632. doi:10.1152/jn.00585.2007

Choi, C. H., Schoenfeld, B. P., Bell, A. J., Hinchey, P., Kollaros, M., Gertner, M. J., . . . McBride, S. M. (2011). Pharmacological reversal of synaptic plasticity deficits in the

mouse model of fragile X syndrome by group II mGluR antagonist or lithium treatment. *Brain Res, 1380*, 106-119. doi:10.1016/j.brainres.2010.11.032

Christie, S. B., Akins, M. R., Schwob, J. E., & Fallon, J. R. (2009). The FXG: a presynaptic fragile X granule expressed in a subset of developing brain circuits. *J Neurosci, 29*(5), 1514-1524. doi:10.1523/JNEUROSCI.3937-08.2009

Darnell, J. C. (2011). Defects in translational regulation contributing to human cognitive and behavioral disease. *Curr Opin Genet Dev, 21*(4), 465-473. doi:10.1016/j.gde.2011.05.002

Gibson, J. R., Bartley, A. F., Hays, S. A., & Huber, K. M. (2008). Imbalance of neocortical excitation and inhibition and altered UP states reflect network hyperexcitability in the mouse model of fragile X syndrome. *J Neurophysiol, 100*(5), 2615-2626. doi:10.1152/jn.90752.2008

Haberl, M. G., Zerbi, V., Veltien, A., Ginger, M., Heerschap, A., & Frick, A. (2015). Structural-functional connectivity deficits of neocortical circuits in the Fmr1 (-/y) mouse model of autism. *Sci Adv, 1*(10), e1500775. doi:10.1126/sciadv.1500775

Hagerman, P. J. (2008). The fragile X prevalence paradox. *J Med Genet, 45*(8), 498-499. doi:10.1136/jmg.2008.059055

Hagerman, P. J., & Stafstrom, C. E. (2009). Origins of epilepsy in fragile X syndrome. *Epilepsy Curr, 9*(4), 108-112. doi:10.1111/j.1535-7511.2009.01309.x

Kawaguchi, Y., & Kubota, Y. (1997). GABAergic cell subtypes and their synaptic connections in rat frontal cortex. *Cereb Cortex, 7*(6), 476-486.

Larkman, A., & Mason, A. (1990). Correlations between morphology and electrophysiology of pyramidal neurons in slices of rat visual cortex. I. Establishment of cell classes. *J Neurosci, 10*(5), 1407-1414.

Markram, H., Toledo-Rodriguez, M., Wang, Y., Gupta, A., Silberberg, G., & Wu, C. (2004). Interneurons of the neocortical inhibitory system. *Nat Rev Neurosci, 5*(10), 793-807. doi:10.1038/nrn1519

Myrick, L. K., Deng, P. Y., Hashimoto, H., Oh, Y. M., Cho, Y., Poidevin, M. J., . . . Klyachko, V. A. (2015). Independent role for presynaptic FMRP revealed by an FMR1 missense mutation associated with intellectual disability and seizures. *Proc Natl Acad Sci U S A, 112*(4), 949-956. doi:10.1073/pnas.1423094112

Niswender, C. M., & Conn, P. J. (2010). Metabotropic glutamate receptors: physiology, pharmacology, and disease. *Annu Rev Pharmacol Toxicol, 50*, 295-322. doi:10.1146/annurev.pharmtox.011008.145533

Patel, A. B., Hays, S. A., Bureau, I., Huber, K. M., & Gibson, J. R. (2013). A target cell-specific role for presynaptic Fmr1 in regulating glutamate release onto neocortical fast-spiking inhibitory neurons. *J Neurosci, 33*(6), 2593-2604. doi:10.1523/JNEUROSCI.2447-12.2013

Rudy, B., Fishell, G., Lee, S., & Hjerling-Leffler, J. (2011). Three groups of interneurons account for nearly 100% of neocortical GABAergic neurons. *Dev Neurobiol, 71*(1), 45-61. doi:10.1002/dneu.20853

Scanziani, M., Salin, P. A., Vogt, K. E., Malenka, R. C., & Nicoll, R. A. (1997). Use-dependent increases in glutamate concentration activate presynaptic metabotropic glutamate receptors. *Nature, 385*(6617), 630-634. doi:10.1038/385630a0

Till, S. M., Wijetunge, L. S., Seidel, V. G., Harlow, E., Wright, A. K., Bagni, C., . . . Kind, P. C. (2012). Altered maturation of the primary somatosensory cortex in a mouse model of fragile X syndrome. *Hum Mol Genet, 21*(10), 2143-2156. doi:10.1093/hmg/dds030

CHAPTER V: GENERAL CONCLUSIONS

Fragile X Syndrome affects 1 in 4000 males and 1 in 8000 females (Hagerman, 2008). While this may give the impression that FXS is relatively uncommon, in fact it is the most common genetically inherited disease of intellectual disability (Hagerman, 2009). Additionally, 30% of children with FXS exhibit autism (Gibson et al., 2008) and another 20-25% of children exhibit epilepsy (Stafstrom, 2009), making the pathogenic mechanisms we uncover in the *Fmr1* KO mouse invaluable to our insight about FXS as well as autism spectrum disorders, epilepsy syndromes, and other intellectual disabilities. In my dissertation, I investigated neocortical pathogenesis in the *Fmr1* KO mouse. Electrophysiological studies of neocortical function in the *Fmr1* KO are underrepresented relative to studies that have been done in brain regions such as the hippocampus and amygdala (Sabanov, 2016; Olmos-Serrano et al., 2010), implicating requirement for further investigations of the neocortical pathogenesis in FXS. My decision to investigate the visual neocortex of the *Fmr1* KO was based on previous studies implicating V1 in FXS pathology. Pyramidal neuron dendritic spines in layer 2/3 and 5/6 exhibit immature morphologies in V1 of the *Fmr1* KO mouse (Dolen et al., 2007; Comery et al., 1997), substantiating what has been reported in human studies (Rudelii., 1985; Hinton et al., 1991; Irwin, Galvez, & Greenough, 2000). Additionally, synaptic plasticity in V1 is altered in the *Fmr1* KO. Specifically, our lab previously showed that layer 5/6 visual neocortical LTP is absent in the *Fmr1* KO (Wilson & Cox, 2007). This LTP was mediated in part, by group I mGluRs (Wilson & Cox, 2007). Specifically, it appeared that mGluR5 was the instigating receptor in this defect. These results, led me to hypothesize that other processes mediated by mGluR signaling would be altered in the visual neocortex of *Fmr1* KO mice, leading to circuit hyperexcitability. In Chapter 2, I investigated the effect of mGluRs on the membrane

excitability of layer 5/6 pyramidal neurons, as these neurons are morphologically different in the *Fmr1* KO and would be expected to directly impact cortical hyperexcitability. I determined that both group I and group II mGluRs modulate membrane excitability of pyramidal neurons, but there is no difference between the WT and *Fmr1* KO mouse. Thus, it is evident from these results that not all cellular and synaptic processes modulated by mGluRs will be altered in the *Fmr1* KO mouse. Knowing that group I mGluRs modulate long term changes in synaptic transmission, I next asked whether mGluRs modulate short term dynamics of synaptic transmission differently in the *Fmr1* KO. Previous studies have indicated that mGluRs can reversibly depress excitatory synaptic transmission in the visual neocortex (Sladeczek et al., 1993; Flavin, Jin & Daw, 2000). My studies show that group II mGluRs suppress glutamatergic transmission in layer 5/6 and 2/3 pyramidal neurons. However, I did not observe any significant differences in the magnitude of these changes when comparing WT and *Fmr1* KO animals. How can this be the case when mGluR-LTD is significantly reduced in layer 5/6 of the *Fmr1* KO? It is well known that not all consequences of mGluR activation require protein synthesis. For example, it has been shown that the Bγ subunits of mGluRs can directly activate ion channels independent of protein translation (Niswender & Conn, 2010). Thus, I speculate that the ability of mGluRs to modulate membrane excitability and suppress synaptic transmission in the short term may not require protein synthesis and may therein not be affected by the loss of FMRP. A simple way to test this hypothesis would be to include a protein inhibitor in the bath and/or intracellular electrode to determine whether blockade of protein synthesis would occlude the mGluR effects that I observed. Understanding that mGluR-mediated modulation of excitatory neurons is normal in the *Fmr1* KO, I hypothesized that mGluRs may be altering GABAergic transmission in the *Fmr1* KO visual neocortex, as this could also lead to hyperexcitable

neocortical circuitry. In Chapter 3, I tested this hypothesis by quantifying the changes in evoked IPSC amplitude in layer 5/6 pyramidal neurons in response to a group II mGluR agonist.

Intact GABAergic regulation of pyramidal neurons is required to maintain network excitability within the normal range. Defects in GABAergic transmission are known to cause hyperexcitability and/or epileptiform activity (Olmos-serrano et al., 2010). Additionally, mGluRs have been shown to modulate GABAergic transmission (Doi et al., 2002; Liu, Petrof, and Sherman, 2014). In the visual neocortex, it has specifically been shown that group II mGluRs can act presynaptically to decrease GABAergic transmission by reducing release probability, albeit through a currently unknown mechanism (Liu, Petrof, and Sherman, 2014). This suggests that activation of group II mGluRs in the visual neocortex of the *Fmr1* KO mouse, may lead to alterations in GABAergic transmission onto pyramidal neurons. My results indicate that activation of group II mGluRs leads to suppression of inhibitory transmission that is significantly increased in the *Fmr1* KO. By blocking glutamatergic transmission in the slice, I was then able to effectively isolate GABAergic inputs onto my pyramidal neurons. During this condition I discovered that group II mGluRs continue to suppress evoked IPSCs, but the magnitude of this suppression is similar between WT and *Fmr1* KO pyramidal neurons. I validated these results with experiments looking at the frequency and amplitude of spontaneous and miniature IPSCs. I discovered that although group II mGluRs are present at presynaptic terminals of GABAergic neurons and are capable of decreasing GABAergic transmission, this mechanism of regulation is intact in the *Fmr1* KO. This indicates that the exaggerated suppression of inhibition that I observe in the *Fmr1* KO pyramidal neurons, is due to the effects of group II mGluRs at excitatory synapses onto interneurons. I subsequently hypothesized that group II mGluRs would

suppress excitatory transmission onto inhibitory interneurons, and that this effect would be exaggerated in the *Fmr1* KO mouse. In Chapter 4, I tested that hypothesis.

Interneurons comprise 20-30% of all neocortical subtypes (Markram et al., 2004). The two most abundant subtypes, PV+ and SST+ interneurons, comprise 70% of the interneuron population (Rudy et al., 2011). Furthermore, previous FXS studies have implicated both FS interneurons and SST+ interneurons in the neocortical pathogenesis of the *Fmr1* KO mouse (Gibson et al., 2008; Paluskiewicz et al., 2011). Thus, it seemed likely that these interneuron subtypes may be responsible for mediating the inhibitory changes I see upon activation of group II mGluRs. In chapter 4, I evoked excitatory currents from both FS and NFS interneurons in the layer 5/6 and quantified the change in either charge or amplitude in response to pharmacological activation of group II mGluRs. Activation of group II mGluRs led to suppression of glutamatergic transmission onto both layer 5/6 FS and NFS interneurons. Further, statistical analysis revealed that the suppression of glutamatergic transmission onto SST+ interneurons was exaggerated in the *Fmr1* KO, supporting my hypothesis that decreased excitatory drive onto layer 5/6 visual neocortical interneurons leads to decreased GABAergic activity onto pyramidal neurons in the *Fmr1* KO. In contrast, this exaggeration of group II mGluR-mediated suppression of glutamatergic drive was not seen when FS cells were the postsynaptic targets. Thus, my effect is target-cell specific. To complete my investigation, I asked two final questions: Where are these group II mGluRs located? Is this pathogenic mechanism layer specific or does it occur in more superficial lamina? To answer the first question, I performed a series of experiments that are traditionally used to ascertain whether a synaptic effect is pre- or post- synaptic. I determined that group II mGluRs are present at both excitatory neuron terminals and on the postsynaptic interneuron targets; however, the suppression of EPSCs was

most likely due to a presynaptic mechanism. This was a novel discovery, as the role of FMRP presynaptically remains largely unknown. Finally, by repeating my evoked experiments in layer 2/3, I determined that the alterations observed in layer 5/6 are layer specific. While the specificities of this presynaptic mechanism are unclear, I predict that activation of group II mGluRs in the absence of FMRP is exaggerating one or more of the following processes: activation of K^+ channels, inhibition of Ca^{2+} channels, protein translation downstream of PI3K-mTOR, ERK/MAPK, or Gi signaling cascades, or inhibition of the exocytotic release machinery **(For details see Chapter 4.4)**. For a schematic diagram of these cellular mechanisms, see the appendix (**Figure 5.1**) is Nevertheless, these results provide evidence in favor of a disinhibited deep layer neocortical network. This is likely to have several consequences including aberrant sensory processing in all target neurons of layer 5/6 pyramidal axons. Although my dissertation studies do not permit definitive identification of these target neurons, I can speculate potential defective pathways based on previous studies. Two-thirds of layer 5/6 pyramidal neurons target layer 2/3 (Callaway, 1998), and it is highly likely that some of the targets of these disinhibited neurons are excitatory cells in these superficial layers. These neurons encode information for the dorsal and ventral streams of visual processing, and so both of these pathways may be altered in FXS. Interestingly, individuals with FXS perform poorly on visual-motor tasks compared to both chronological age and mental age-matched controls, implicating potential defects in the M pathway of visual processing (Kogan et al., 2004; Kogan et al., 2004b). Thus, it is equally possible that the disinhibited pyramidal neurons that I recorded from may be targeting layer 2/3 neurons that specifically process M pathway information. Additionally, deep layer pyramidal neurons also project axons to the pulvinar nucleus of the thalamus and the superior colliculus,

both of which are important for visual attention and eye movement. Defects in these pathways would also be expected to lead to severe defects in processing of visual motion.

The research I have provided here is invaluable not only to our understanding of FXS, but potentially to our understanding of autism. FMRP targets the mTOR inhibitors Pten, Nf1, and Tsc2 (Darnell et al., 2011), so it is possible that the mechanisms underlying aberrant behavior in FXS overlap with the mechanisms underlying autism pathology. Theoretically, this should mean that any pharmacological interventions designed to treat FXS may also be clinically beneficial to autism patients. Group II mGluRs are currently being investigated as useful drug targets in a variety of neurological and psychiatric conditions including schizophrenia, addiction, major depression, anxiety, parkinon's, hungtington's, alzheimer's, and epilepsy (Hovelso et al., 2012). Additionally, clinical trials in schizophrenic patients using an oral prodrug for group 2/3 mGluRs have reported significant improvement in both positive and negative symptoms (Patil et al., 2007). It appears that group II mGluRs, predominantly through their presynaptic actions on neurotransmitter release, have the potential to ameliorate a variety of symptoms. However, with the exception of major depression, the majority of the aforementioned studies show benefits of group II mGluR agonism rather than antagonism (Hovelso et al., 2012). On the contrary, my dissertation studies suggest that antagonism of group II mGluRs would be more beneficial in restoring the defects I observe in V1. However, group II mGluRs have a widespread distribution in the CNS and have been shown to exert antiepileptic effects in vitro and in vivo, (Anwyl, 1999) so administration of a group II antagonist could potentially lead to excitotoxicity. Thus, I suggest that my dissertation data provide additional support for the idea of using GABAergic agonists to ameliorate FXS symptoms. Agonizing GABAergic transmission to compensate for a decrease of excitatory drive onto interneurons, may provide a safer alternative to the use of a

group II antagonist. Clinical trials are already underway to investigate the therapeutic potential of GABA agonists in FXS (Davenport et al., 2016). The most promising drug candidate to-date is acamprosate, a compound that is hypothesized to effect $GABA_A$ signaling as well as metabotropic glutamate receptor signaling. An open-label study showed that 75% of patients were "very much improved" or "much improved" on several outcome measures for ADHD, social responsiveness, and other cognitive-behavioral measures (Erickson et al., 2013). As a result, a current Phase II placebo-controlled study is being conducted on the effects of acamprosate. It is my hope that my dissertation provides further mechanistic support in favor of the use of GABAergic agonists for clinical treatment of FXS phenotypes.

While electrophysiology is the gold standard for assessing the functional effects of pathological processes on the synapse, even within the field different techniques present different limitations. My dissertation studies took advantage of the whole-cell patch clamp technique in combination with pharmacology, to begin to determine which neurons and synapses were altered in layer 5/6 of the visual neocortex. While I determined that the glutamatergic excitation of somatostatin neurons was specifically altered, there continues to be questions regarding the synapse under investigation. For example, electrical stimulation is activating several excitatory inputs onto the postsynaptic cell. With this stimulation method it is impossible for me to determine the source of these excitatory inputs. Although I hypothesize that the glutamatergic inputs onto somatostatin interneurons come from pyramidal neurons residing in the neocortex, to quantitatively answer this question it will be advantageous to conditionally express channel rhodopsin (CHR2) in excitatory neurons in either the layer 5/6 or the layer 2/3 of the neocortex. This can be accomplished by injection of CHR2 into transgenic mice selectively expressing CRE in layer 5/6 (Beltramo et al., 2013), or by using a transgenic mouse that is already engineered to

express CHR2 in layer 5/6 pyramidal neurons (Sohal et al., 2009; Arienkiel et al., 2007). Whole cell recordings can then be obtained from somatostatin neurons in layer 5/6, and blue light can be used to activate all glutamatergic neurons expressing channel rhodopsin, which in this case would be layer 5/6 excitatory neurons. This would effectively keep all other excitatory inputs onto the somatostatin neurons silent, with the exception of spontaneous firing. This selective targeting would allow me to determine where my glutamatergic inputs are coming from.

Additionally, although not a limitation per say, the experiments I used to localize my group II mGluR effect presynaptically, could be supported by isolating any potential postsynaptic group II mGluR effects on my somatostatin interneuron. Although group II mGluRs have been shown to hyperpolarize membranes when they are localized to the axo-somatic compartment of the postsynaptic cell, this localization of group II mGluRs is less common. Further, while collecting my data I see almost no change in the holding current of my somatostatin neurons when I apply a group II mGluR agonist to the slice preparation. For these reasons, I strongly suspect that there are minimal, if any, group II mGluRs located upstream from the axon terminal of my SST+ interneurons. Nonetheless, to verify this hypothesis, I could perform glutamate uncaging using a two-photon microscope. Glutamate uncaging in the presence of TTX, could be used to evoke an excitatory postsynaptic potential in the SST+ neuron. I would expect application of APDC to have little or no effect on the amplitude of this response, which would verify my previous results showing that the alterations I see in the *Fmr1* KO mouse are occurring due to presynaptic group II mGluRs.

Finally, it would be advantageous to determine whether restoration of FMRP could rescue the exaggerated group II mGluR-mediated suppression of excitation that I observe in layer 5/6 SST+ interneurons. For this, I would have to use a transgenic mouse that conditionally

restores FMRP function. The group II mGluR effects that I observe may be a direct consequence of the loss of FMRP, or they may be a neurological compensation for alterations in glutamatergic transmission. If restoring FMRP fails to reinstate normal levels of group II mGluR signaling, then I would suspect that my observation is a potentially irreversible compensatory mechanism to offset a potential excess of glutamatergic transmission. Regardless of what direction the research takes from here, my dissertation provides strong evidence in favor of a hyperexcitable visual neocortical network.

APPENDIX

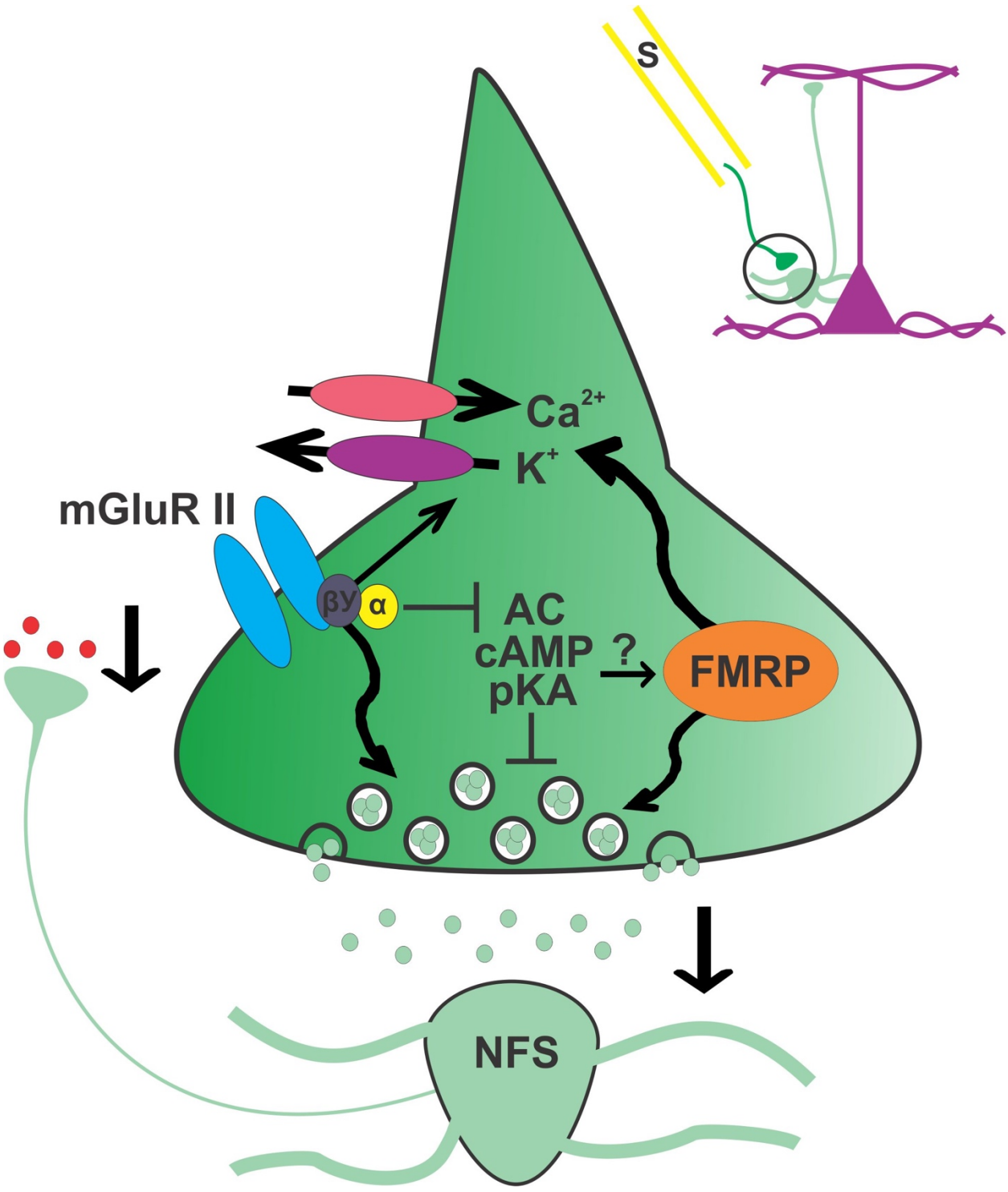

Figure 5.1. Altered presynaptic processes in the *Fmr1* KO mouse upon activation of group II mGluRs.
We demonstrated in previous chapters that activation of group II mGluRs at presynaptic glutamatergic inputs onto NFS interneurons (light green NFS), leads to suppression of evoked excitatory currents (EPSCs). This process is exaggerated in the *Fmr1* KO, leading to

Figure 5.1. (cont'd)

suppression of GABA transmission (red dots). The net effect is disinhibition of downstream excitatory pyramidal neurons. This schematic diagram presents a theoretical model to explain potential changes in cellular mechanisms occurring downstream of group II mGluRs in the *Fmr1* KO mouse. FMRP is a regulator of mRNA translation, and has been shown to modulate the following mRNAs presynaptically: K^+ channels (Deng et al., 2014), Ca^{2+} channels (Brager and Johnston, 2014), and presynaptic vesicular release machinery such as syntaxin 1, SNAP-25, and VAMP (Tang et al., 2015). Activation of group II mGluRs allows α subunit to inhibit adenylyl cyclase (AC), leading to decreases in cAMP, pKA, protein translation, and synaptic transmission (Hovelso et al., 2012). The $B\gamma$ subunit has been shown to directly interact with both K^+ and Ca^{2+} channels at the presynaptic terminal to decrease the excitability of the axon terminal, leading to decreased transmission (Chavis et al., 1994; O'Connor et al., 1999). By can also directly interact with vesicular release machinery to decrease synaptic transmission (Hovelso et al., 2012). I propose that FMRP is either directly downstream of group II mGluR signaling cascades, or it is regulating the translation of the same proteins that are modulated by group II mGluR activation. In the absence of FMRP, we would expect altered levels of protein synthesis of the above mentioned synaptic proteins, which leads to changes in the functional modulation of the synapse upon activation of group II mGluRs.

REFERENCES

REFERENCES

Anwyl, R. (1999). Metabotropic glutamate receptors: electrophysiological properties and role in plasticity. *Brain Res Rev, 29*(1), 83-120.

Arenkiel, B. R., Peca, J., Davison, I. G., Feliciano, C., Deisseroth, K., Augustine, G. J., . . . Feng, G. (2007). In vivo light-induced activation of neural circuitry in transgenic mice expressing channelrhodopsin-2. *Neuron, 54*(2), 205-218. doi:10.1016/j.neuron.2007.03.005

Beltramo, R., D'Urso, G., Dal Maschio, M., Farisello, P., Bovetti, S., Clovis, Y., . . . Fellin, T. (2013). Layer-specific excitatory circuits differentially control recurrent network dynamics in the neocortex. *Nat Neurosci, 16*(2), 227-234. doi:10.1038/nn.3306

Brager, D. H., & Johnston, D. (2014). Channelopathies and dendritic dysfunction in fragile X syndrome. *Brain Res Bull, 103*, 11-17. doi:10.1016/j.brainresbull.2014.01.002

Chavis, P., Shinozaki, H., Bockaert, J., & Fagni, L. (1994). The metabotropic glutamate receptor types 2/3 inhibit L-type calcium channels via a pertussis toxin-sensitive G-protein in cultured cerebellar granule cells. *J Neurosci, 14*(11 Pt 2), 7067-7076.

Comery, T. A., Harris, J. B., Willems, P. J., Oostra, B. A., Irwin, S. A., Weiler, I. J., & Greenough, W. T. (1997). Abnormal dendritic spines in fragile X knockout mice: maturation and pruning deficits. *Proc Natl Acad Sci U S A, 94*(10), 5401-5404.

Darnell, J. C. (2011). Defects in translational regulation contributing to human cognitive and behavioral disease. *Curr Opin Genet Dev, 21*(4), 465-473. doi:10.1016/j.gde.2011.05.002

Davenport, M. H., Schaefer, T. L., Friedmann, K. J., Fitzpatrick, S. E., & Erickson, C. A. (2016). Pharmacotherapy for Fragile X Syndrome: Progress to Date. *Drugs, 76*(4), 431-445. doi:10.1007/s40265-016-0542-y

Deng, P. Y., & Klyachko, V. A. (2016). Genetic upregulation of BK channel activity normalizes multiple synaptic and circuit defects in a mouse model of fragile X syndrome. *J Physiol, 594*(1), 83-97. doi:10.1113/JP271031

Doi, A., Ishibashi, H., Jinno, S., Kosaka, T., & Akaike, N. (2002). Presynaptic inhibition of GABAergic miniature currents by metabotropic glutamate receptor in the rat CNS. *Neuroscience, 109*(2), 299-311.

Erickson, C. A., Davenport, M. H., Schaefer, T. L., Wink, L. K., Pedapati, E. V., Sweeney, J. A., . . . Berry-Kravis, E. (2017). Fragile X targeted pharmacotherapy: lessons learned and future directions. *J Neurodev Disord, 9*, 7. doi:10.1186/s11689-017-9186-9

Flavin, H. J., Jin, X. T., & Daw, N. W. (2000). 2R,4R-4-Aminopyrrolidine-2,4-dicarboxylate (APDC) attenuates cortical EPSPs. *Brain Res, 873*(2), 212-217.

Gibson, J. R., Bartley, A. F., Hays, S. A., & Huber, K. M. (2008). Imbalance of neocortical excitation and inhibition and altered UP states reflect network hyperexcitability in the mouse model of fragile X syndrome. *J Neurophysiol, 100*(5), 2615-2626. doi:10.1152/jn.90752.2008

Hagerman, F. C., Walsh, S. J., Staron, R. S., Hikida, R. S., Gilders, R. M., Murray, T. F., . . . Ragg, K. E. (2000). Effects of high-intensity resistance training on untrained older men. I. Strength, cardiovascular, and metabolic responses. *J Gerontol A Biol Sci Med Sci, 55*(7), B336-346.

Hagerman, P. J. (2008). The fragile X prevalence paradox. *J Med Genet, 45*(8), 498-499. doi:10.1136/jmg.2008.059055

Hayashi, Y., Momiyama, A., Takahashi, T., Ohishi, H., Ogawa-Meguro, R., Shigemoto, R., . . . Nakanishi, S. (1993). Role of a metabotropic glutamate receptor in synaptic modulation in the accessory olfactory bulb. *Nature, 366*(6456), 687-690. doi:10.1038/366687a0

Hinton, V. J., Brown, W. T., Wisniewski, K., & Rudelli, R. D. (1991). Analysis of neocortex in three males with the fragile X syndrome. *Am J Med Genet, 41*(3), 289-294. doi:10.1002/ajmg.1320410306

Hovelso, N., Sotty, F., Montezinho, L. P., Pinheiro, P. S., Herrik, K. F., & Mork, A. (2012). Therapeutic potential of metabotropic glutamate receptor modulators. *Curr Neuropharmacol, 10*(1), 12-48. doi:10.2174/157015912799362805

Irwin, S. A., Galvez, R., & Greenough, W. T. (2000). Dendritic spine structural anomalies in fragile-X mental retardation syndrome. *Cereb Cortex, 10*(10), 1038-1044.

Irwin, S. A., Idupulapati, M., Gilbert, M. E., Harris, J. B., Chakravarti, A. B., Rogers, E. J., . . . Greenough, W. T. (2002). Dendritic spine and dendritic field characteristics of layer V pyramidal neurons in the visual cortex of fragile-X knockout mice. *Am J Med Genet, 111*(2), 140-146. doi:10.1002/ajmg.10500

Liu, B., Li, L., Chen, J., Wang, Z., Li, Z., & Wan, Q. (2013). Regulation of GABAA receptors by fragile X mental retardation protein. *Int J Physiol Pathophysiol Pharmacol, 5*(3), 169-176.

Niswender, C. M., & Conn, P. J. (2010). Metabotropic glutamate receptors: physiology, pharmacology, and disease. *Annu Rev Pharmacol Toxicol, 50*, 295-322. doi:10.1146/annurev.pharmtox.011008.145533

O'Connor, V., El Far, O., Bofill-Cardona, E., Nanoff, C., Freissmuth, M., Karschin, A., . . . Boehm, S. (1999). Calmodulin dependence of presynaptic metabotropic glutamate receptor signaling. *Science, 286*(5442), 1180-1184.

Olmos-Serrano, J. L., Paluszkiewicz, S. M., Martin, B. S., Kaufmann, W. E., Corbin, J. G., & Huntsman, M. M. (2010). Defective GABAergic neurotransmission and pharmacological rescue of neuronal hyperexcitability in the amygdala in a mouse model of fragile X syndrome. *J Neurosci, 30*(29), 9929-9938. doi:10.1523/JNEUROSCI.1714-10.2010

Paluszkiewicz, S. M., Olmos-Serrano, J. L., Corbin, J. G., & Huntsman, M. M. (2011). Impaired inhibitory control of cortical synchronization in fragile X syndrome. *J Neurophysiol, 106*(5), 2264-2272. doi:10.1152/jn.00421.2011

Patel, A. B., Hays, S. A., Bureau, I., Huber, K. M., & Gibson, J. R. (2013). A target cell-specific role for presynaptic Fmr1 in regulating glutamate release onto neocortical fast-spiking inhibitory neurons. *J Neurosci, 33*(6), 2593-2604. doi:10.1523/JNEUROSCI.2447-12.2013

Rudelli, R. D., Brown, W. T., Wisniewski, K., Jenkins, E. C., Laure-Kamionowska, M., Connell, F., & Wisniewski, H. M. (1985). Adult fragile X syndrome. Clinico-neuropathologic findings. *Acta Neuropathol, 67*(3-4), 289-295.

Rudy, B., Fishell, G., Lee, S., & Hjerling-Leffler, J. (2011). Three groups of interneurons account for nearly 100% of neocortical GABAergic neurons. *Dev Neurobiol, 71*(1), 45-61. doi:10.1002/dneu.20853

Sladeczek, F., Momiyama, A., & Takahashi, T. (1993). Presynaptic inhibitory action of a metabotropic glutamate receptor agonist on excitatory transmission in visual cortical neurons. *Proc Biol Sci, 253*(1338), 297-303. doi:10.1098/rspb.1993.0117

Sohal, V. S., Zhang, F., Yizhar, O., & Deisseroth, K. (2009). Parvalbumin neurons and gamma rhythms enhance cortical circuit performance. *Nature, 459*(7247), 698-702. doi:10.1038/nature07991

Stafstrom, C. E. (2009). Severe epilepsy syndromes of early childhood: the link between genetics and pathophysiology with a focus on SCN1A mutations. *J Child Neurol, 24*(8 Suppl), 15S-23S. doi:10.1177/0883073809338152

Tang, B., Wang, T., Wan, H., Han, L., Qin, X., Zhang, Y., . . . Liao, L. (2015). Fmr1 deficiency promotes age-dependent alterations in the cortical synaptic proteome. *Proc Natl Acad Sci U S A, 112*(34), E4697-4706. doi:10.1073/pnas.1502258112

Wilson, B. M., & Cox, C. L. (2007). Absence of metabotropic glutamate receptor-mediated plasticity in the neocortex of fragile X mice. *Proc Natl Acad Sci U S A, 104*(7), 2454-2459. doi:10.1073/pnas.0610875104